

# TRADE AND THE END OF ANTIQUITY\*

Johannes Boehm<sup>†</sup>

Geneva Graduate Institute

Thomas Chaney<sup>‡</sup>

University of Southern California

January 2026

## Abstract

What was the role of trade, and how did economic activity evolve at the End of Antiquity, when political power shifts away from the Mediterranean towards northern Europe and the Middle East? To answer those questions, we assemble a database of hundreds of thousands of ancient coins from the fourth to the tenth century, estimate a dynamic model of trade and money where coins gradually diffuse along trade routes, and recover granular regional trade and real consumption time series. Our estimates suggest that Mediterranean trade was disrupted by the newly formed border between Islam and Christianity; that economic activity shifts away from the Mediterranean starting in the fifth century; that real consumption peaks in the Middle East in the eighth century; and that by the end of the ninth century, Atlantic regions from Islamic Andalusia to Frankish northwestern Europe have become the wealthiest regions of the ancient western world.

**JEL Classification:** F1, O1, N73.

**Keywords:** Gravity Equation, International Trade, Ancient Coins, Diffusion.

---

\*We thank Marek Jankowiak, Reka Juhasz, Chris Meissner, Cathrin Mohr, Ezra Oberfield, Kevin O'Rourke, Pseudoerasmus, Jonathan Vogel, and numerous seminar participants for helpful comments. Malo Cadudal-Illý, Jingshu Chen, Jinpei Tuchel, and in particular Ye Sun provided excellent research assistance. Boehm gratefully acknowledges financial support from the Banque de France/Sciences Po partnership, and Chaney from the European Research Council (ERC grant 884847). All remaining mistakes are our own.

<sup>†</sup>[johannes.boehm@graduateinstitute.ch](mailto:johannes.boehm@graduateinstitute.ch).

<sup>‡</sup>[thomas.chaney@gmail.com](mailto:thomas.chaney@gmail.com).

# Introduction

The transition from classical antiquity to the medieval period marks one of humanity's most profound transformations, altering the intellectual, economic, and political fabric of Europe, the Mediterranean, and the Middle East. This sweeping metamorphosis reshaped entire economic systems and political structures, transforming a world organized around Mediterranean commerce and urban networks into one dominated by new centers of power. We present new data and empirically document this changing economic geography during Late Antiquity. This quantitative analysis sheds new light on the nature and extent of economic change as the Roman civilization in the Mediterranean declines and economic power shifts to western and northwestern Europe, and to the Middle East.

What caused the end of antiquity has been a central question for centuries (see for instance Montesquieu, 1734; Voltaire, 1756; Gibbon, 1789). Most contemporary historians believe that the conquest of Rome by Germanic invaders in the fifth century did not lead to an immediate end of Roman institutions and commerce, as local institutions remained largely in place (Pirenne, 1927, 1939; Findlay and O'Rourke, 2009; McCormick, 2001).<sup>1</sup> The archaeological evidence points to a shift in the economic activity to the north-west of Europe and away from the Mediterranean between the fifth and the eighth century. The timing, extent, and reasons remain debated, but when Charlemagne was crowned as Emperor at the end of the eighth century, the political and economic power in Europe has moved from the Mediterranean to the Frankish lands of northwestern Europe. Famously, historian Henri Pirenne proposes that the expansion of the Arab Caliphate along the southern Mediterranean coast and into the Iberian peninsula disrupted commerce and political ties in the Mediterranean, and turned the emerging Carolingian Empire into a northern European power (“without Mohammed Charlemagne would have been inconceivable,” Pirenne, 1927, p.234). The evidence for these disruptions brought forward by Pirenne is mainly related to the disappearance of certain luxury goods north of the Mediterranean.<sup>2</sup>

In this paper, we study the changing economic geography during Late Antiquity using the tools of modern quantitative trade models and novel data on the circulation of ancient coins. Our aim is not to *explain* the end of antiquity, but to collect novel quantitative evidence *describing* it. Our evidence suggests that the emergence of the Arab Caliphate reshaped Mediterranean

---

<sup>1</sup>Contra: Ward-Perkins (2006).

<sup>2</sup>Pirenne's argument is the near *absence* of mentions of silk and spices in historical texts written north of the Mediterranean, and the disuse of gold for coinage and papyrus for writings. These fragments of evidence, along with new archaeological findings, have been extensively studied and discussed by historians since Pirenne. See Lopez (1943), Ashtor (1970), Hedges and Whitehouse (1983), and, in particular, McCormick (2001)'s monumental work that synthesizes the existing literary and archaeological evidence on changes around the Mediterranean, including patterns of change in the flows of communications, objects, and travelers. The synthesis of Wickham (2006) interprets the evidence through the lens of social structures.

trade, with north-south trade collapsing while south-south trade flourished. But we also show that the relative economic decline of the Mediterranean world started more than a century earlier; and that the Atlantic regions from the Islamic Iberian peninsula to the Frankish lands of northwest Europe became the wealthiest regions of the ancient western world more than seven centuries before the European colonial expansion into the Americas, Africa, and Asia.

We make four main contributions. Our first contribution is to assemble a large database of coin finds from hoards deposited between AD 325 and AD 950, with observations from hundreds of thousands of coins found across Europe, North Africa, and the Middle East. Coins offer rich quantitative information in a data-scarce setting,<sup>3</sup> as numismatists and archaeologists have deciphered, cataloged, and classified ancient coinage for over 200 years. We collect information about where and when coins were minted and buried, and present three stylized facts: (i) bilateral coin flows are disrupted by distance and political borders just like trade flows are, (ii) unlike traded goods, coins are in use over many years and, as a result, coins that are older at the time of deposit tend to have traveled farther, and (iii) the geography of coin flows across the Mediterranean changes abruptly around the time of the Arab conquests of the 7<sup>th</sup> century.

Our second contribution is to build and estimate a dynamic model of trade where agents use coins for transactions. Within each period, trade is governed by comparative advantages as in [Eaton and Kortum \(2002\)](#), and coins flow in opposite direction to trade. After being minted, the same coin can then be saved as a store of value, and re-used for subsequent transactions. We first show that with saving, coin flows within a period inherit the same gravity structure as trade flows, up to a single multiplicative constant. We then characterize the full dynamics of coin flows, as coins are minted, saved, used for multiple transactions, and gradually percolate through the trade network. We show that data solely on coins is sufficient to fully recover the parameters governing coin creation (minting) and trade in goods (trade costs and production efficiency).<sup>4</sup> Our estimates for minting output are in line with known historical evidence, and our estimate for the travel time elasticity of trade is similar to that for Roman trade in ceramics ([Flückiger et al., 2022](#)), and Bronze Age Assyrian trade in textiles and precious metals ([Barjamovic et al., 2019](#)). Our estimates reveal a large cost associated with crossing the newly erected border between Islamic and non-Islamic regions, especially over the Mediterranean.

Our third contribution is to reconstruct granular time series for bilateral trade flows and for real consumption for each 20-year period from the 4<sup>th</sup> to the 10<sup>th</sup> century for each region. We are able to recover real consumption using solely data on coins because coin flows contain information on (nominal) trade flows, which contain information on (relative) prices. Our

---

<sup>3</sup>Due to the fact that no comprehensive data on production, consumption, trade, or demographics exists for the first millennium AD, historians of this period rely to a large extent on qualitative literary sources.

<sup>4</sup>As recognized by numismatists, whether a coin hoard is created (deliberately or accidentally buried), found by archaeologists, and documented by numismatists, depends on a series of endogenous events. To purge our estimation from those endogenous events we use only information on the *shares* of different coins within a hoard.

estimates confirm the thesis proposed by Pirenne (1939) that north-south Mediterranean trade collapsed after the Arab conquests in the 7<sup>th</sup> century, although we also show that south-south trade remained vibrant. Our estimates further reveal that Mediterranean income fell relative to the rest of the ancient western world starting in the 6<sup>th</sup> century, and that the concentration of income fell sharply in the 5<sup>th</sup> century and remained stable thereafter. Our estimates also suggest that real consumption in the heartlands of the Byzantine empire, initially among the highest, gradually collapsed starting in the 7<sup>th</sup> century, in part due to the fall of trade in and out of regions newly conquered by the Arabs, while consumption experienced a spectacular rise in northwest Europe in the 7<sup>th</sup> and 8<sup>th</sup> centuries; consumption in the heart of the western Roman empire regions of Italy, southern France, and Egypt start falling in the 4<sup>th</sup> century, around the time when the institutions of the western Roman empire collapsed; while consumption peaks in Syria under the Umayyad Caliphate of Damascus in the early 8<sup>th</sup> century, in al-Andalus under the Umayyad Caliphate of Cordoba in the late 8<sup>th</sup> century, in al-Iraq under the Abbasid Caliphate of Baghdad, and in the Arabian peninsula in the 8<sup>th</sup> century after the birth of Islam. Aggregate consumption rises in all Atlantic regions from North Africa to northwest Europe starting in the 8<sup>th</sup> century, more than seven centuries before the European colonial expansion.

Our fourth contribution is to confront our estimates to a series of external data. The known exploitation of ancient mineral deposits is positively associated with our estimates of coin minting. Paleo-climatic adverse shocks—severe droughts—have a negative causal impact on real consumption. But military conflicts and the local incidence of the Justinianic plague have no detectable association with consumption. Finally, in the absence of virtually any systematic evidence on ancient production, consumption, or trade, we show that our estimates on real consumption changes from pre- to post-AD 700 are remarkably consistent with measures of European urbanization post-AD 700.

**Related literature.** Our paper relates to the literature on the role of market access in shaping economic outcomes across space, specifically in historical settings. Fogel (1964), Donaldson and Hornbeck (2016) and Hornbeck and Rotemberg (forthcoming) evaluate the impact of the US railroad in the 19th century on economic growth, Donaldson (2018) the impact of railroads in colonial India on relative welfare, and Nagy (2023) the impact of the westward expansion of the US on growth; Pascali (2017) evaluates the impact of steamships on maritime trade and relative development; Redding and Sturm (2008) study the impact of the iron curtain on comparative development in Germany, and Ahlfeldt et al. (2015) the impact of the Berlin wall on the urban structure of Berlin; Juhász et al. (2024) study the impact of knowledge codification on industrial development in Japan, using trade data to infer aggregate productivity; Flückiger et al. (2022) study the impact of the Roman transportation network on trade in ceramics (*terra sigillata*) from the 1st century BC to the 3rd century AD, while Michaels and Rauch (2018) study

changes in the transportation and urban networks after the fall of the Western Roman Empire; Barjamovic et al. (2019) use shipment records from Assyrian merchant archives in Bronze Age Anatolia to estimate the location of ancient lost cities and their size. In contrast to this literature, we do not observe prices, trade costs, or even trade flows. Instead, we use a dynamic model of trade and money to recover trade flows from panel data on the movement of coins. Liu and Tsyvinski (2024) feature a related mechanism where shocks gradually percolate through an input-output network. We follow an approach similar to Donaldson (2018) and Donaldson and Hornbeck (2016) to measure travel time—optimal routing algorithm on a transportation network, but we add substantial historical evidence (Scheidel, 2015; Romanov and Seydi, 2022; Cornu, 1983) including direct evidence from 10<sup>th</sup>-century Arab geographer Al-Muqaddasī (985). Finally our paper speaks to a literature in economic history on the changes in Late Antiquity and early medieval times. This literature frequently uses numismatic evidence, although mostly in a descriptive manner. Two notable exceptions are Noonan (1980)'s study of Islamic coin finds of different vintages and origins in Eastern Europe and Scandinavia, which stops short of using a formal econometric model; and Persson and Sharp (2015) who discuss Pirenne's thesis and economic integration in Europe through the lens of a gravity model.<sup>5</sup>

The remainder of the paper is structured as follows. Section 1 lays out the historical context and describes our data and three stylized facts on ancient coin flows. Section 2 presents our dynamic model of trade and money. Section 3 describes our estimation method and presents our estimates. Section 4 leverages our estimates to uncover novel facts on trade, consumption, and the end of antiquity in the Mediterranean. Section 5 confronts our estimates to external data on ancient mines, climate, urbanization, battles, and plagues. Section 6 concludes.

# 1 Historical context, data, and stylized facts

## 1.1 Historical context

We study the economic and political developments in the Mediterranean between the 4<sup>th</sup> and the 10<sup>th</sup> century AD. At the start of this period the Mediterranean was still entirely under control of the Roman Empire, albeit at times with multiple emperors and conflict between them, and under mounting pressure from Germanic invasions. The death of the eastern emperor Theodosius I in 395 divided the Roman Empire into a western and an eastern half. The fifth century saw increased Germanic incursions in the east and west, culminating with the Ostrogothic king Odoacer deposing the last West Roman emperor Romulus Augustulus in 476 and ending the Western Roman Empire. Italy was ruled by the Ostrogoths until the 550s, then by the Lombards; Spain was taken over by the Visigoths, France by the Merovingian

---

<sup>5</sup>Shatzmiller (2018) qualitatively applies the gravity model to medieval trade in the Middle East.

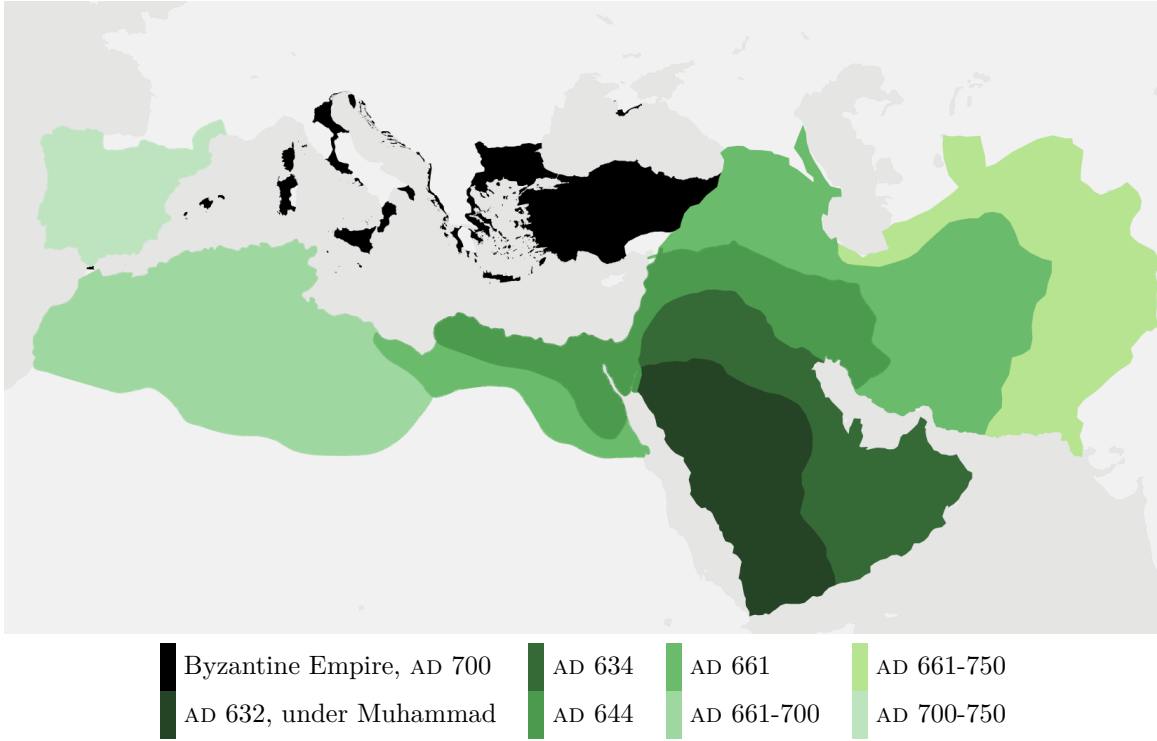


Figure 1: The Arab Conquests, AD 632-750

dynasty of the Franks, and North Africa, Sicily, and Sardinia by the Vandals. The Eastern Roman (Byzantine) Empire at times reconquered parts of the former Western Roman territory, but in the sixth century became increasingly under pressure from the Sasanian Empire in the east. The Byzantine-Sasanian wars of 602–628 depleted the resources of both empires, leaving a vacuum that was filled by the emerging Arab caliphate.

Figure 1 shows the rapid Arab expansion, starting in 632. By 634 the Arabs controlled the entire Arabian Peninsula. The Levant followed in the late 630's and Egypt in the 640's. By the end of the Rashidun Caliphate in 661, the Arabs controlled land from Tripoli in the west to Balkh in the east. The expansion continued under the Umayyad dynasty. In 698 the Arab army razed Carthage and by 709 they had fully conquered the Maghreb. In 711 they crossed the Strait of Gibraltar and defeated the Visigoths at the Battle of Guadalete. In 732 they were stopped by Charles Martel at Tours, and driven back across the Pyrenees. When the Abbasid family overthrew the ruling Umayyads in 750, the Umayyads retained control of most of Iberia (al-Andalus). While the Arab conquest ended Sasanian rule in the east, advances into Byzantine territory in Anatolia did not lead to sustained land border shifts. But the Arabs strengthened their naval capabilities, ended the Byzantine control of the western Mediterranean and contested its control of the east. Arab raids on Mediterranean cities became frequent.

Two other notable and overlapping events have been linked to economic and political changes: the Plague of Justinian (541-549), which, according to contemporary literary sources

led to large declines in population, and the “Late Antique Little Ice Age” temperature anomaly (536-560), likely due to volcanic eruptions, which caused temperatures in the northern hemisphere to drop by about one degree Celsius (Peregrine, 2020). The size and quantitative relevance of these two events is heavily debated among historians. We will think of these events as potentially affecting population and productivity, which our estimation strategy accounts for.

## 1.2 Data

We construct a large dataset on the flows of coins around the Mediterranean between AD 325 and AD 950.<sup>6</sup> For the period from AD 325 to AD 725 we mostly rely on data from the *Framing the Late Antique and Early Medieval Economy* project (FLAME, 2023b),<sup>7</sup> a large-scale effort by historians and numismatists to record harmonized information on the location, dating, and composition of coin finds up to the year 725. FLAME covers hoards<sup>8</sup> from the Mediterranean and beyond, contributed by specialists working on the coinage of their geographical and temporal expertise. We use the most recent release of FLAME (January 2023) which covers 9,831 coin hoards. We remove hoards that fall outside our area of interest, continental western Europe up to the modern-day German-Polish border and including Bohemia, southern Europe up to the line between Vienna and Odessa, and North Africa and the Middle East up to the maximum extent and area of influence of the Umayyad Caliphate (stretching from the Maghreb in the West to the Indus in the east, and up to Bulgar in the north).<sup>9</sup> We also remove all hoards that only consist of incompletely described coins (no mint location or mint date information).

We supplement FLAME’s data, in particular for the period after AD 725, with hand-coded records of 106,371 coins from 830 finds, which we assemble using hoard catalogues from the numismatic literature, similarly to the source documents that underlie FLAME. These additional records include the time period of the Caliphate, so that we can assess the impacts of these changes on the patterns of exchange in the Mediterranean. Together these data cover the vast majority of published information on coin finds in our geographic and temporal scope.

The structure of the coin hoard data is ideally suited for an analysis of dynamic bilateral spatial flows. Each unit of observation—a coin within a hoard—contains the following attributes: (*i*) the location where the coin has been minted, (*ii*) the ruler and/or dynasty under whose authority the coin has been issued, (*iii*) a year interval when the coin was minted, (*iv*)

---

<sup>6</sup>See appendix D for extensive information on the coin data assembly, harmonization and cleaning.

<sup>7</sup><https://coinage.princeton.edu/>

<sup>8</sup>FLAME also includes finds from excavations and single finds. Unless explicitly mentioned, we will treat all records in the same way and just use the word “hoard” to describe deposits of any size.

<sup>9</sup>See figure 6 below for a map of our area of study. We exclude the Viking lands, and therefore do not speak to the discussion on the potential role of the Vikings (and the inflow of Islamic silver through trade via eastern and northern Europe) in the changing economic geography during Late Antiquity (Bolin, 1953). Recent archaeometric studies indicate that Carolingian silver is largely not of Arab origin (Sarah et al., 2008; Kershaw et al., 2024), suggesting a limited role for silver inflows via the Viking route in affecting Carolingian mint output.

No.	MINT	DATE	DIAM.	WEIGHT	NUMB.
51	الأندلس	114	29.	2.93	4
52	"	115	29.5	2.92	1
53	"	116	26.5	2.92	3

Figure 2: Coin hoard data, an example from al 'Ush (1972)

*Notes:* The figure shows an excerpt of an original publication from which we assemble hoard data: al 'Ush (1972) gives the content of the Damascus silver hoard in tabular form. From left to right, for the first row: the record number (51), the mint (al-Andalus), the date (year 114 of the Hijri calendar), diameter (29mm), weight (2.93g), and the number of coins with these attributes (4). The issuing dynasty (Umayyad) is given in the table headings and the material and denomination (silver *dirham*) is stated in the text.

the identifier and the location of the hoard that the coin is part of, (*v*) a year interval when the hoard—and therefore the coin—was deposited. These pieces of information are typically recorded by the author of the original numismatic or archaeological publication. Figure 2 shows an example. Mints are usually inferred from mint marks on the coins.<sup>10</sup> The mint date is often indicated on the coin. When it is not, it can be approximated from the ruler (or dynasty or empire) under whose authority the coin was issued, as well as other information, including the mint mark. Finally, we follow the common approach of historians to estimate the date of deposit of each hoard using the *terminus post quem*, or *tpq* for short, the date of the youngest object in the hoard that can be dated. In our case that is typically the most recent end year of the time intervals of the coins in the hoard.

In coding the mint location and date we typically follow the coding of the author of the original publication which catalogues the hoard.<sup>11</sup> In some cases this information is imprecise: the author may not have been able to inspect the coin or inspected only a fragment. We conduct robustness checks to investigate whether our findings are driven by endogenous selection.

We have data on 5,625 hoards and 494,229 coins that fall into our geographic boundary and have a *tpq* between 325 and 950. After removing from FLAME large hoards found in the 19th century or earlier for which not much besides rough coin counts is known, 270,500 coins are complete with a mint and minting year interval; on average 86% of coins in a hoard are complete. We define the age of coins at time of deposit as the difference between the midpoint of the coin's minting interval and the *tpq* of the hoard. Figure 3a shows the temporal distribution of the number of hoards by *tpq*, and figure 3b the distribution of coin ages within hoards.<sup>12</sup>

Coins are deposited on average 47 years after they are struck. Appendix tables B.1 and B.2

<sup>10</sup>Mint marks have been in use since ancient Greek times to monitor coin weight and metal content.

<sup>11</sup>Sometimes these interpretations are critically evaluated and corrected by subsequent scholars. Appendix D lists the extensive sources we use for each of the hand-coded hoards.

<sup>12</sup>To further validate that our data reflect coin circulation during Late Antiquity, appendix B.1 compares the coin age distribution with the one in twelve Byzantine hoards that Banaji (2016) labels as circulation hoards, i.e. that are known to have originated from coins that were in circulation. Coin age distributions are similar.

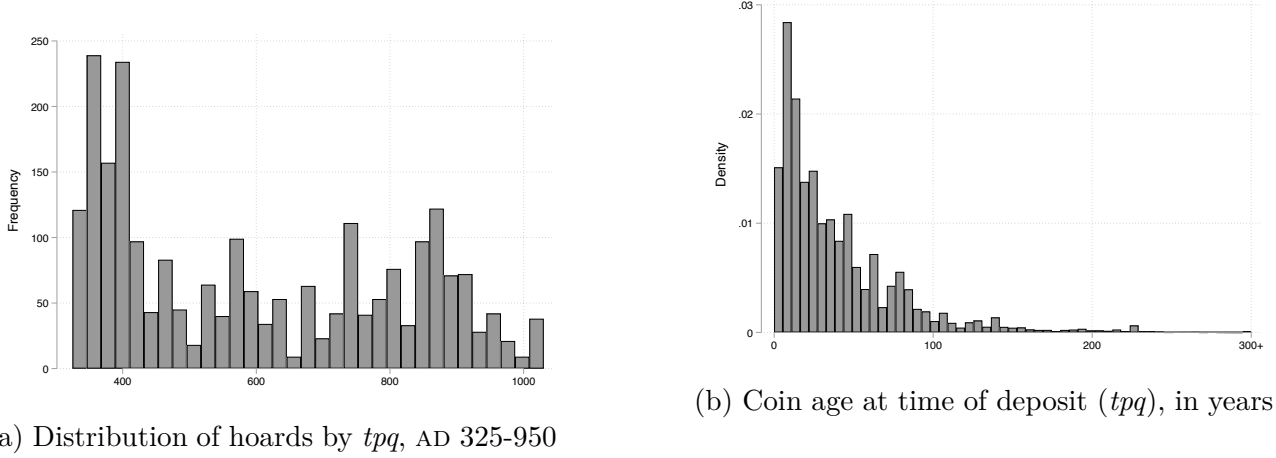


Figure 3: Number of hoards over time and ages of coins within hoards

*Notes:* Panel (a) shows the number of hoards per 20-year period. Panel (b) displays the (annual) density of coins of different ages. Coin age is defined as the difference between the midpoint of the coin's minting interval and the  $tpq$  of the hoard it is found in.

contain additional summary statistics on coins and hoards respectively.

**Discussion.** The interpretation of coin flows as relating to trade, despite having a long tradition among numismatists and historians,<sup>13</sup> deserves some discussion. The Roman and subsequently Byzantine empires were generally fairly monetized economies,<sup>14</sup> with coinage taking a pre-eminent role and credit being very limited (Morrison, 2002). The situation was similar in the caliphate (Bessard, 2020) and in the Carolingian empire (Coupland, 2014). The fact that coins were light, durable, and—because they were made from precious metal, which could be easily reminted—accepted within and across borders made them particularly suitable for long-distance trade.<sup>15</sup> This is particularly the case for gold coins, traded throughout the Mediterranean and valued for their weight in gold (Banaji, 2016).<sup>16</sup> Of course coins did not travel solely because of commerce; theft, gift-exchange, dowry, tribute, ransom and plunder also contribute to coin flows. We acknowledge that while tribute and ransom can be thought of as the price paid for life, theft and plunder may not easily fit into our trade model.<sup>17</sup>

<sup>13</sup>See, in particular, the discussions by Grierson (1959) and, more recently, Naismith (2014).

<sup>14</sup>A possible exception was the eighth century, where Byzantine mint output collapsed.

<sup>15</sup>Examples of coins used in foreign empires abound. Bates (1991) discusses how Byzantine coins kept circulating (and being minted) in Egypt after the Arab takeover in 641. Tribute and ransom payments between the Arabs and Byzantines often included domestic currency. McCormick (2001), chapter 12, discusses the circulation of Arab and Byzantine coins in the west.

<sup>16</sup>We conduct robustness checks of our main results restricting the sample to gold coins.

<sup>17</sup>Other data-driven approaches used by economic historians to measure economic activity include urbanization rates, flows of consumption goods, notably ceramics (Wickham, 2006, Flückiger et al., 2022), communication flows and movements of people (McCormick, 2001), pollen grain measurements (Izdebski et al., 2016), and ice core readings (McConnell et al., 2018). Coin flows bring several econometric advantages and are more directly related to comprehensive patterns of exchange than communications or ceramics. We nonetheless estimate similar distance elasticities from gravity regressions on coins and ceramics (see appendix B.2 and figure B.2).

A potential source of bias comes from the fact that our data do not cover the universe of coin flows, but only hoards that have been created (coins deliberately or accidentally deposited, which may depend on warfare, natural disasters, and property rights protection), found (which may depend on modern-day institutions, such as whether metal detecting is allowed, and on modern-day market prices for historical coins), and documented by experts (which may depend on the local presence of experts, the ‘novelty’ of the hoards’ contents, and the demand for research on these topics).<sup>18</sup> Our estimation in section 3 corrects those biases by using shares of coins *within* hoards, and differs from the more descriptive methods employed by historians.

Finally, in contrast to standard trade data, we do not observe flows at each point in time, but only when and where a coin was minted and eventually deposited into a hoard. Our structural model in section 2 identifies the parameters governing trade flows from data on coin stocks, and reconstructs the possibly numerous successive trips a coin took throughout its life.

### 1.3 Three stylized facts on ancient coins

**Distance and political borders disrupt trade.** The bilateral structure of our dataset allows us to explore the geography of coin flows in reduced form. We aggregate mint-origin ( $m$ ) and hoard-destination ( $h$ ) coordinates to  $1^\circ \times 1^\circ$  cells across all periods, and restrict the sample to coins that were unambiguously issued by the fourteen most important political blocks  $p$ .<sup>19</sup> We then model the number of coins issued by  $p$  in  $m$  and found in  $h$  as a function of distance and a political border dummy,

$$\text{count}_{mhp} = \exp(a_{mp} + a_h + b_1 \log \text{distance}_{mh} + b_2 \text{PoliticalBorder}_{hp} + u_{mhp}). \quad (1)$$

We estimate this model by PPML using data on all triplets  $(m, h, p)$  for mint cell  $m$  in political block  $p$  and hoard cell  $h$ , excluding combinations of mint cells and political blocks that do not produce a single coin. The political border dummy is one if the region where the center of the hoard cell  $h$  is located in has never and to no extent been under the political control of  $p$ .<sup>20</sup>

Table 1 shows that distance and crossing a political border are both negatively correlated with coin flows.<sup>21</sup> Columns 3 and 4 show almost identical results when using only gold coins, only 7% of the coins in our sample, which were universally valued for their metal content and were therefore particularly favored for long-distance trade. Column 5 and 6 also show similar

---

<sup>18</sup>FLAME (2023a) discusses potential sources of biases, which also apply to our combined data.

<sup>19</sup>These are: Eastern Roman Empire, Roman Empire, Umayyads of Spain, Abbasids, Umayyads, Sasanians, Fatimids, Western Roman Empire, Carolingians, Samanids, Visigoths, Ostrogoths, Merovingians, Vandals.

<sup>20</sup>See appendix A for our division of the combined Arab and Mediterranean world into 13 regions.

<sup>21</sup>The distance and border effects are robust to using only the intensive margin of coin flows, see appendix table B.3. An alternative explanation for the border effect could be that coins are redistributed within a political entity before entering circulation. Appendix table B.4 shows similar results for specifications with hoard  $\times$  empire fixed effects, suggesting that this is unlikely.

Table 1: Distance and Border Effects in Coin Flows

	Dependent variable: # Coins <sub>mhp</sub>				Dep. var.: Value <sub>mhp</sub>	
	(1)	(2)	(3)	(4)	(5)	(6)
Log Distance	-1.137*** (0.12)	-1.002*** (0.13)	-1.135*** (0.10)	-0.951*** (0.076)	-1.144*** (0.075)	-0.989*** (0.068)
Political border		-1.945*** (0.62)		-2.073*** (0.47)		-1.516*** (0.27)
Hoard Cell FE	Yes	Yes	Yes	Yes	Yes	Yes
Mint × Empire Cell FE	Yes	Yes	Yes	Yes	Yes	Yes
Sample			Gold only	Gold only	Gold and Silver	Gold and Silver
Pseudo- $R^2$	0.767	0.778	0.808	0.824	0.800	0.810
Observations	217748	217748	57287	57287	146767	146767

*Notes:* This table presents various specifications of equation (1). The dependent variable is the number of coins in a hoard cell  $h$  from a mint cell  $m$  issued by a political entity  $p$  in columns 1-4, and the value of those coins in columns 5-6. The regression drops all  $(m, p)$  combinations that have no emitted coins, and observations only include those that remain after dropping singletons and separated observations. Hoard and mint cells are  $1^\circ \times 1^\circ$ . Political entities here are categorized into fourteen divisions. Columns 1-2 use data on all coins, columns 3-4 gold only, and columns 5-6 value-weighted gold and silver. Standard errors in parentheses, clustered at mint cell  $\times$  empire and hoard cell level. \*  $p < 0.10$ , \*\*  $p < 0.05$ , \*\*\*  $p < 0.01$ .

results when using silver and gold coins and weighing them by their relative value.<sup>22</sup>

While purely descriptive, those results suggest that coin flows contain information related to trade costs (e.g. distance and border effects).<sup>23</sup> Our model in section 2 isolates features of the geography of coin flows that are driven by trade.

**Older coins travel further.** Coins are found, on average, in hoards 800 kilometers from their mint. But within hoards, older coins are also coins that have on average travelled farther. Table 2 shows results from a regression of log distance between a coin’s mint and hoard place on log coin age—the difference between minting and the hoard’s  $tpq$ —with hoard fixed effects to isolate within-hoard variation. The coefficient on coin age is positive and significant, even when including mint  $\times$  mint time fixed effects to control for the average distance traveled and age of coins of a particular mint and issue. This suggests that older coins have been used on average for more transactions, each taking them further away from their mint origin. Our model in

<sup>22</sup>We calculate the equivalent gold weight of silver coins in two steps. First, we code the reference weights of coins of different denominations in our data, noting that coins are often clipped, broken, debased, or abraded (Manas and Velde, 2021). Second, we convert this reference weight into a gold-equivalent weight assuming a constant conversion ratio of 12g of silver for 1g of gold, a rough approximation given the fluctuations of the gold-silver ratio between 1:10 and 1:16 (Bolin, 1953). Gold represents 80% of the resulting value in our data. Since the price of copper/bronze fluctuates heavily during Late Antiquity (see Banaji, 2016, Ch. 5) and copper denominations frequently traded at values different from their intrinsic metal content, we only use silver and gold coins. We also note that FLAME does not record coin weights, resulting in approximate calculations.

<sup>23</sup>To investigate the informativeness of coins for trade flows, appendix figure B.2 compares the distance elasticities for of coins and Roman Terra Sigillata ceramics, the only tradable good from Antiquity on which substantial amounts of data are available (Flückiger et al., 2022). We find similar but slightly higher distance elasticities for Terra Sigillata, possibly due to coins being more frequently re-used (see section 2.2).

Table 2: Coin age and distance traveled

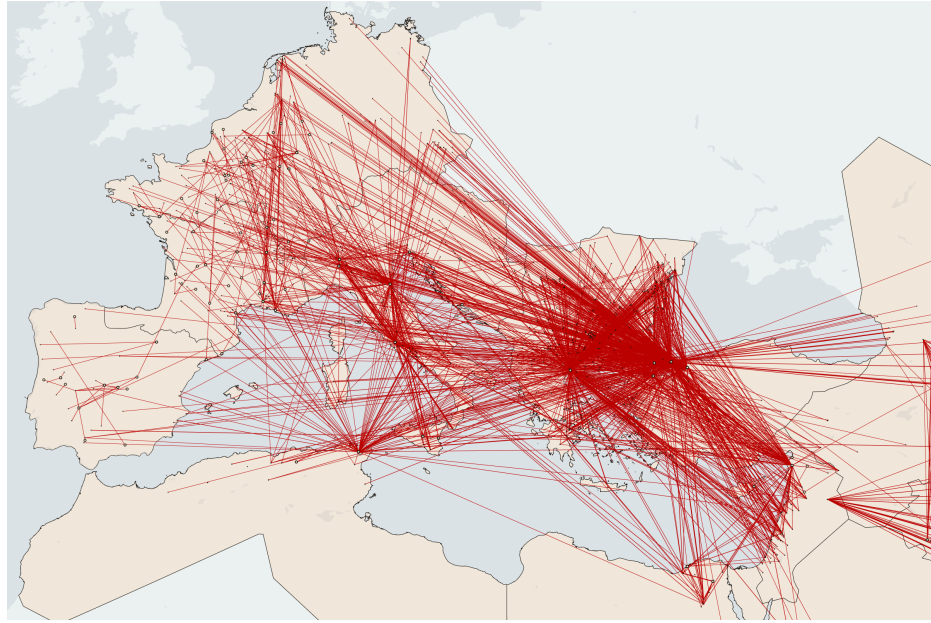
	Dependent variable: Log Distance between Mint and Hoard				
	(1)	(2)	(3)	(4)	(5)
Log Age of Coin	0.146*** (0.044)	0.0831*** (0.026)	0.0749** (0.031)	0.160*** (0.043)	0.0485** (0.020)
Sample			No non-hoards	No non-hoards	
Hoard FE	Yes	Yes	Yes	Yes	Yes
Mint × 50-year-interval FE		Yes			
Mint × 25-year-interval FE			Yes		Yes
$R^2$	0.762	0.863	0.869	0.775	0.898
Observations	287243	287029	286873	250156	249830

*Notes:* The dependent variable is the log distance between the mint and hoard locations. The independent variable is the log age of the coin at the date of the *tpq* of the hoard (where the age is defined as the difference between the midpoint of the minting interval and the maximum of the endpoints of the minting intervals). In the rare cases where this age is zero (the youngest coin in the hoard is dated to a precise year) we set the log age to zero. Mints are identified as all Nomisma or FLAME-recorded entities that have been geocoded to the same  $0.1^\circ \times 0.1^\circ$  cell. Columns 4 and 5 exclude FLAME finds that are tagged as not being hoards. Standard errors in parentheses, clustered at the hoard level. \*  $p < 0.10$ , \*\*  $p < 0.05$ , \*\*\*  $p < 0.01$ .

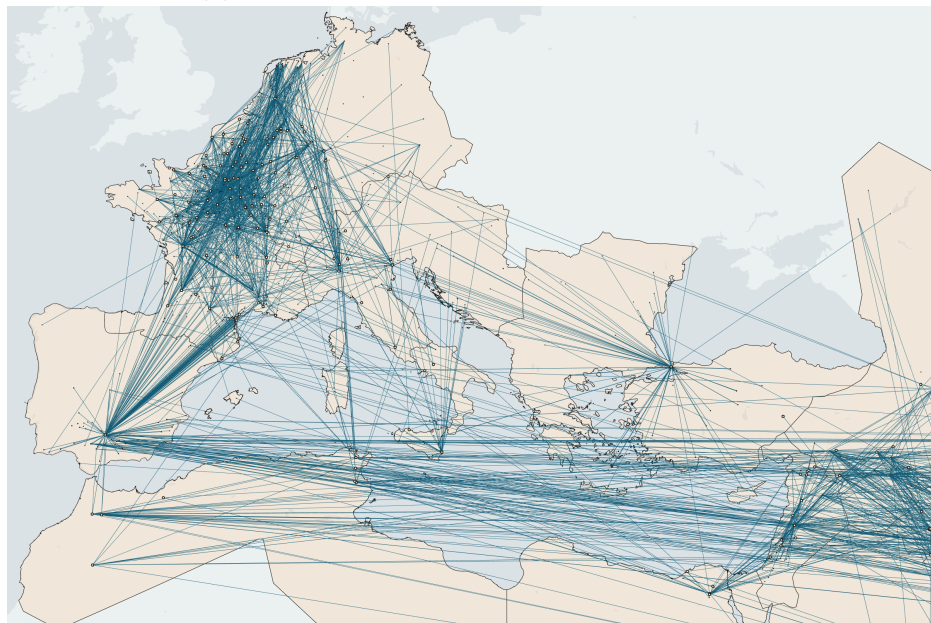
section 2 disentangles the many transactions of older coins from the few of younger coins.

**The geography of coin flows changes sharply around the Arab conquests.** Finally we show descriptives of the movements of coins during Late Antiquity. Figure 4 illustrates the changes in the flow of coins across the Mediterranean before and after the Arab conquests. Panel 4a shows flows from AD 450 to AD 630. Constantinople, Thessalonica, Rome, Ravenna, and Carthage are important mints whose coins flow across the entire Mediterranean. Coins from Carthage cross the sea into Europe, and coins from Rome and Constantinople cross into Africa and the Middle East. Panel 4b shows that the patterns of coin flows are starkly different after 713, by which time the Arabs had conquered the eastern Mediterranean coast (up to and including Antioch), the southern Mediterranean coast, and most of the Iberian peninsula. Most coins now flow east to west within the Islamic Caliphate, within the Arab heartlands of Syria, Mesopotamia, and Egypt, and within the Frankish lands of northern Europe. The coin flows emanating from the remaining Byzantine mints in Constantinople, Syracuse, and Italy are much smaller than in the earlier period.<sup>24</sup> Besides a few coins from the mints of Ifriqiya and al-Abbasiyah that end up in the hoards of Ilanz and Steckborn (McCormick, 2001),

<sup>24</sup>The changes in the magnitude and location of Byzantine coin production has been the topic of a large literature. Kazhdan (1954) was the first to argue for a decline of Byzantine cities in the 8th and 9th century based on archaeological evidence. Several authors (including Kazhdan, Zavagno, 2022, and Pennas, 1996) relate these changes to Arab military pressure. Grierson (1973) notes that the eastern mints of Nicomedia, Cyzicus, Thessalonica, Cyprus, as well as Catania, were closed in 629-630, before the Arab conquests, and production was relocated to Constantinople. Nevertheless, a number of provincial mints, including Syracuse, Ravenna, and Rome, remained active until at least the mid-8th century (in the case of Syracuse until 878 when it fell to the Aghlabids).



(a) Before the Arab conquests: AD 450-630



(b) After the Arab conquests: AD 713-900

Figure 4: Changes in coin flows in the ancient world

*Notes:* The figure shows coin flows, indicated by a straight line, between mints and find spots. The sample consists of all coin groups where both the lower end of the mint interval and the *tpq* of the hoard lie between AD 450 and AD 630 (panel a) and AD 713 and AD 900 (panel b). Hoards from outside the shaded area are excluded.

there are almost no north-south flows across the Mediterranean. Flows that cross the border between Christianity and Islam primarily do so in the the West across the Pyrenees ([Parvérie, 2014](#)). Appendix B.4, figure B.3, and table B.5 present additional evidence that coin flows across the Mediterranean dropped after the Arab conquests, and that Islamic coins crossing

the sea replace Roman coins. Despite the fact that in some historical sources the Arabs called the Mediterranean the “Sea of the Romans” (*Bahr al-Rūm(i)*), after the Arab conquests the Mediterranean became, at least when it comes to coin flows, an Arab-dominated sea.<sup>25</sup>

While only descriptive, figure 4 suggests that the Arab conquest coincided with a substantial change in the economic geography of the ancient world. The structural model in the next section is designed to quantify those changes.

## 2 Model

We now introduce a quantitative model of trade, money, and the diffusion of coins. This model forms the basis for the estimation of trade costs, mint outputs, and technology and labor, from which we quantify changes in the ancient economic geography.

We make two key assumptions. Firstly, we assume that coins are used for transactions. This assumption is necessary for identification: if coins were not used to clear gross bilateral trades, then data on coins would not contain information on bilateral trade flows. The use of coinage was widespread: as historians have noted (e.g. Mayhew, 2019), the presence of millions of coins in present-day collections (only a small fraction of which can be associated to a hoard and included in our sample) indicates that great quantities of coinage must have circulated at the time.<sup>26</sup> The period we study does not yet feature the widespread use of financial contracts for trade. Finally, our finding that coin movements exhibit similar empirical patterns as trade flows also supports this assumption.<sup>27</sup>

Our second key assumption is that coins are fungible. This assumption is natural with coins being valued for their precious metal content, and is supported by historical evidence on the wide circulation of foreign coins and the discovery of precise tools for measuring the weight and fineness of foreign coins (Bates, 1991; McCormick, 2001).<sup>28</sup>

### 2.1 Economic model

**Set up.** There are  $N$  locations. Time is discrete, indexed by  $t$  in square brackets. Each time period is decomposed into three sub-periods: beginning, middle, and end.

---

<sup>25</sup>Paraphrasing Pirenne (1939). We take the Arab conquests as a proximate cause for these changes, and do not attempt to explain why the Arabs were successful. The commonly held view is that the Byzantine-Sasanian war of 602-628 exhausted the forces of both empires and paved the way for Arab military success (Foss, 1975).

<sup>26</sup>Earlier writers, including Polanyi (1977), were yet unaware of the vast amount of coins that would be unearthed from the 1980's onwards through the use of metal detectors.

<sup>27</sup>We present in appendix C a simple extension of our model with both monetized and barter exchanges, inspired by Kiyotaki and Wright (1989). We show in section 4.5 that our estimates with and without endogenous monetization are highly correlated. As we are not aware of systematic records of the degree of monetization in Late Antiquity, we opted to use a simpler model with no barter as our baseline.

<sup>28</sup>Gandal and Sussman (1997) discuss medieval weight and fineness measurement technologies.

At the end of period  $t - 1$ , location  $n$  sets aside  $S_n[t]$  coins for consumption and saving in period  $t$ . At the beginning of period  $t$ , an exogenous fraction  $\lambda_n[t]$  of the coins in this stock  $S_n[t]$  ceases to circulate, either lost or melted into fresh new coins.<sup>29</sup> In addition, some locations own a mint which exogenously generates fresh new coins if it is active in period  $t$ ,  $M_n[t] \geq 0$ . Assuming that minting is exogenous means that we model the *benefit* of minting (seigniorage) but not its *cost*.<sup>30</sup> In the middle of period  $t$ ,  $L_n[t]$  identical workers save a fraction  $s_n[t]$  of their coins, and spend the rest on consumption expenditures,  $X_n[t]$ . Importantly, expenditures contain spending on all goods, possibly including capital goods. What we label saving,  $s_n[t]$ , solely captures saving into nominal financial assets (coins), not investment into physical capital.

Workers face the following budget constraint,

$$X_n[t] = (1 - s_n[t]) \left( (1 - \lambda_n[t]) S_n[t] + M_n[t] \right), \text{ with } s_n[t] \geq 0, \quad (2)$$

where we assume workers cannot borrow ( $s_n[t] \geq 0$ ). In this ‘coin-in-advance’ economy, consumption is financed by currently available coins, and not by promised future income.<sup>31</sup>

At the end of period  $t$ , workers earn a competitive wage  $w_n[t]$  selling goods in exchange for coins. The stock of coins set aside evolves recursively,

$$S_n[t+1] = (1 - \lambda_n[t]) S_n[t] + M_n[t] + w_n[t] L_n[t] - X_n[t]. \quad (3)$$

**Trade.** Within each period trade is modeled as in Eaton and Kortum (2002). Consumers in location  $n$  spend a fraction  $\pi_{ni}[t]$  of their expenditures on imports from location  $i$ ,  $X_{ni}[t]$ ,

$$\pi_{ni}[t] = \frac{X_{ni}[t]}{X_n[t]} = \frac{(w_i[t]/T_i^{1/\theta}[t] d_{ni}[t])^{-\theta}}{\sum_k (w_k[t]/T_k^{1/\theta}[t] d_{nk}[t])^{-\theta}}. \quad (4)$$

Trade shares depends on relative factor prices per efficiency unit (wages,  $w_i[t]$ , relative to productivity,  $T_i^{1/\theta}[t]$ ), relative bilateral trade costs ( $d_{ni}[t]$ ), and the trade elasticity ( $\theta > 0$ ).

**Inter-temporal allocations.** Workers have log-utility over real consumption,

$$U_n[t] = \mathbb{E}_t \left[ \sum_{\tau \geq t} \beta^{\tau-t} \ln \left( \frac{X_n[\tau]}{p_n[\tau]} \right) \right], \text{ with } p_n[t] = \gamma \left( \sum_k \left( \frac{w_k[t]}{T_k^{1/\theta}[t]} d_{nk}[t] \right)^{-\theta} \right)^{-1/\theta}.$$

---

<sup>29</sup>We think of  $\lambda$  primarily as coins melted into bullion for their precious metal, possibly as a seigniorage tax to be re-minted. Only a small fraction is literally lost and becomes part of our data.

<sup>30</sup>We present evidence in section 5.1 that exploitation of ancient mineral deposits is associated with higher minting. This suggests that a lower cost of mining is associated with more minting.

<sup>31</sup>If this assumption were relaxed, labor income (in coins) would buy expenditures in other locations, become income and be used for expenditures again, etc, all within a period. Data on coin stocks would contain no information on trade flows.

$\beta$  is the discount rate,  $p_n[t]$  the ideal price index in  $n$  at  $t$ , and  $\gamma$  is a constant (Eaton and Kortum, 2002). Each location chooses a sequence of coins stocks to maximize utility given wages subject to the no borrowing constraint (2), the budget constraint (3), the optimal within-period allocation across imports (4). A transversality condition prevents holding coins forever.

$$\begin{aligned} \max_{\{S_n[\tau]\}_{\tau \geq t}} & \mathbb{E}_t \left[ \sum_{\tau \geq t} \beta^{\tau-t} \ln \left( \frac{(1 - \lambda_n[\tau]) S_n[\tau] + M_n[\tau] + w_n[\tau] L_n[\tau] - S_n[\tau+1]}{\gamma \left( \sum_k (w_k[\tau]/T_k^{1/\theta}[\tau] d_{nk}[\tau])^{-\theta} \right)^{-1/\theta}} \right) \right] \\ \text{s.t. } & S_n[\tau+1] \geq w_n[\tau] L_n[\tau], \forall (\tau \geq t), \text{ and } \lim_{\tau \rightarrow \infty} \beta^\tau \frac{S_n[\tau+1]}{X_n[\tau]} = 0. \end{aligned} \quad (5)$$

Saving ( $s_n[\tau] > 0 \Leftrightarrow S_n[\tau+1] > w_n[\tau] L_n[\tau]$ ) is used for consumption smoothing.

**Dynamic equilibrium.** Wages are determined by market clearing, given the trade shares,  $\pi_{ni}[t]$  from equation (4), and the coin stock policy function,  $S_n[t]$  from equation (5),

$$w_i[t] L_i[t] = \sum_n \pi_{ni}[t] \left( (1 - \lambda_n[t]) S_n[t] + M_n[t] + w_n[t] L_n[t] - S_n[t+1] \right), \forall (i, t). \quad (6)$$

In a useful benchmark where agents save little to none,  $s_n[t] \approx 0$ , market clearing simplifies to

$$w_i[t] L_i[t] = \sum_n \pi_{ni}[t] \left( (1 - \lambda_n[t]) w_n[t-1] L_n[t-1] + M_n[t] \right), \forall (i, t). \quad (7)$$

**Steady state equilibrium.** A steady state where all variables are constant clarifies the mechanics of the model. If agents correctly anticipate they are in a steady state, there is no consumption smoothing motive for saving,  $s_n = 0$  and  $X_n = (1 - \lambda_n) w_n L_n + M_n$ . If agents incorrectly anticipate shocks and save for precautionary motives, the same equality between expenditure and income holds to a first order,  $X_n = \frac{1-s_n}{1-s_n+\lambda_n s_n} ((1 - \lambda_n) w_n L_n + M_n)$  with  $\frac{1-s_n}{1-s_n+\lambda_n s_n} \approx 1$ .<sup>32</sup> Equilibrium wages jointly clear markets given the trade equilibrium,

$$w_i L_i = \sum_n \pi_{ni} \left( (1 - \lambda_n) w_n L_n + M_n \right), \text{ and } \pi_{ni} = \frac{(w_i/T_i^{1/\theta} d_{ni})^{-\theta}}{\sum_k (w_k/T_k^{1/\theta} d_{nk})^{-\theta}}, \quad (8)$$

and the aggregate stock of coins in circulation is constant,  $\sum_n M_n = \sum_n \lambda_n w_n L_n$ .<sup>33</sup>

---

<sup>32</sup>We estimate  $\lambda = 1.7\%$  p.a. (section 3.1); Scheidel (2015) calculates  $s = 1.5\%$ ; so  $\lambda s = 0.000255 \approx 0$ .

<sup>33</sup>If aggregate minting increases, nominal wages will increase, leading to global inflation.

Our model is analogous to Dekle et al. (2007), with trade deficits and surpluses. Expenditures minus income—the trade deficit of location  $n$ ,  $D_n \equiv X_n - w_n L_n = M_n - \lambda_n w_n L_n$ —is equal to the net creation of coins. Any non-mint location runs a trade surplus ( $D_n < 0$ ), and a mint location runs a trade deficit if minting is large enough, with at least one mint location weakly running a trade deficit each period.

## 2.2 Dynamic accumulation in coin hoards

Our aim is to match the quantities in our model to our data on ancient coins, which contain information on mint/hoard locations and dates. To do so, we explicitly follow the movements of individual coins as they travel through the trade network.

We denote by  $S_{mi}[t, \tau]$  the number of coins minted in location  $m$  at time  $t$  which are part of the coin stock of location  $i$  at time  $\tau$ , with  $S_i[\tau] = \sum_{m=1}^N \sum_{t < \tau} S_{mi}[t, \tau]$ . Coins start their ‘coin life’ when they are minted, so  $S_{mm}[t, t] = M_m[t]$ . Subsequently, they circulate across locations as they are used for transactions or saved,

$$S_{mi}[t, \tau + 1] = \sum_{n=1}^N (1 - s_n[\tau]) (1 - \lambda_n[\tau]) S_{mn}[t, \tau] \pi_{ni}[\tau] + s_i[\tau] (1 - \lambda_i[\tau]) S_{mi}[t, \tau]. \quad (9)$$

At time  $\tau$ , each location  $n$  has a stock of coins set aside. A fraction  $(1 - s_n[\tau])$  is spent on goods (not saved). Of those coins,  $(1 - \lambda_n[\tau]) S_{mn}[t, \tau]$  were minted in location  $m$  at time  $t$ . Consumers in  $n$  send a fraction  $\pi_{ni}[\tau]$  of those coins to  $i$  to pay for imported goods. We assume that coins are fungible so buyers draw coins at random, and  $(1 - s_n[\tau]) (1 - \lambda_n[\tau]) S_{mn}[t, \tau] \pi_{ni}[\tau]$  coins minted in location  $m$  at time  $t$  move from  $n$  to  $i$  at time  $\tau$  in expectation. Summing across all (coin) origins we derive the first term (sum) in equation (9). In addition, a fraction  $s_i[\tau]$  of coins is saved locally and remains in region  $i$ , the second term in equation (9). We can express the dynamic evolution of the composition of coin stocks in a compact matrix form,  $\mathbf{S}[t, t] = \mathbf{M}[t]$  and  $\mathbf{S}[t, \tau + 1] = \mathbf{S}[t, \tau] (\mathbf{I} - \boldsymbol{\lambda}[\tau]) \tilde{\mathbf{\Pi}}[\tau]$ , and solve it forward,

$$\mathbf{S}[t, T] = \mathbf{M}[t] \left( \prod_{\tau=t}^{T-1} (\mathbf{I} - \boldsymbol{\lambda}[\tau]) \tilde{\mathbf{\Pi}}[\tau] \right) \forall T \geq t, \text{ with } \tilde{\mathbf{\Pi}}[\tau] \equiv (\mathbf{I} - \mathbf{s}[\tau]) \mathbf{\Pi}[\tau] + \mathbf{s}[\tau]. \quad (10)$$

$\mathbf{S}[t, T]$  is the square  $N \times N$  matrix of coin stocks with  $(n, i)^{th}$  element  $S_{ni}[t, T]$ .  $\mathbf{M}[t]$  is a diagonal  $N \times N$  matrix of minting with  $n^{th}$  element  $M_n[t]$ .  $\mathbf{I}$  is the  $N \times N$  identity matrix and  $\boldsymbol{\lambda}[\tau]$  is a diagonal  $N \times N$  matrix of coin loss with  $n^{th}$  element  $\lambda_n[\tau]$ .  $\tilde{\mathbf{\Pi}}[\tau]$  is the square  $N \times N$  matrix, which governs bilateral coin flows. This ‘augmented’ trade matrix  $\tilde{\mathbf{\Pi}}[\tau]$  is a function of  $\mathbf{s}[\tau]$ , the diagonal  $N \times N$  matrix of net saving rates with  $n^{th}$  element  $s_n[\tau]$ , and  $\mathbf{\Pi}[\tau]$ , the trade matrix with  $(n, i)^{th}$  element  $\pi_{ni}[\tau]$ . Equation (10) forms the basis of our estimation.

Before describing our estimation strategy, we isolate two original features of our model, which helps gain intuition on how we can extract information about trade from coins, and which clarifies the distinctions between data on coins and data on trade.

**Coins as a medium of exchange versus a store of value.** The stock of coins  $\mathbf{S}$  in equation (10) diffuses across locations not according to the trade matrix  $\mathbf{\Pi}$ , but to the ‘augmented’ trade matrix  $\tilde{\mathbf{\Pi}}$ . Both matrices have almost the same structure, with one distinction: coins,

unlike goods, have an additional tendency to stay locally, because they are also used as a store of value for saving. To make this distinction explicit, we decompose the ‘augmented’ trade share  $\tilde{\pi}_{ni}$  into three multiplicative buyer ( $\tilde{\alpha}_n$ ), seller ( $\tilde{\beta}_i$ ), and bilateral ( $\tilde{\delta}_{ni}$ ) terms,

$$\begin{aligned}\tilde{\pi}_{ni}[\tau] &= \tilde{\alpha}_n[\tau] \tilde{\beta}_i[\tau] \tilde{\delta}_{ni}[\tau], \quad \text{with} \\ \tilde{\alpha}_n[\tau] &= 1 / \sum_k \tilde{\beta}_k[\tau] \tilde{\delta}_{nk}[\tau], \quad \tilde{\beta}_i[\tau] = \left( w_i[\tau] / T_i^{1/\theta}[\tau] \right)^{-\theta}, \quad \text{and} \\ \tilde{\delta}_{ni}[\tau] &= \frac{(d_{ni}[\tau])^{-\theta}}{(d_{nn}[\tau])^{-\theta}} \times \begin{cases} 1 & \text{if } n = i, \\ (1 - s_n[\tau] / \tilde{\pi}_{nn}[\tau]) & \text{if } n \neq i. \end{cases}\end{aligned}\tag{11}$$

The classical [Eaton and Kortum \(2002\)](#) trade matrix  $\boldsymbol{\Pi}$  has almost the exact same structure:  $\pi_{ni} = \alpha_n \beta_i \delta_{ni}$ , where  $\alpha_n = 1 / \sum_k \beta_k \delta_{nk}$ ,  $\beta_i = (w_i / T_i^{1/\theta})^{-\theta}$ , and  $\delta_{ni} = (d_{ni})^{-\theta} / (d_{nn})^{-\theta}$  are buyer, seller, and bilateral terms. In the absence of saving,  $s_n = 0$ , both matrices are identical. But if  $s_n > 0$  the home bias for coins flows is magnified compared to the home bias in trade flows.

Equation (11) shows that coin and trade flows have the same gravity structure up to a constant, so that coin flows and the saving rate are sufficient to recover trade flows.

**Coin flows versus trade flows.** The second key distinction between coin and trade flows is that coins do not travel just once: they may be used for multiple transactions throughout their life. This is made explicit by the product of ‘augmented’ trade matrices in equation (10). Our structural estimation unpacks the different elements of the product of those matrices, leveraging the overlapping yet distinct information contained in young versus old coins—which have traveled through a few versus many iterations of the ‘augmented’ trade matrices.

A naive gravity estimation that combines all coins of different ages, wrongly ignoring the dynamic nature of coin flows, would not identify the parameters of the ‘augmented’ trade matrix. This can be most easily seen in a stationary version of our model, though the result extends to non-stationary cases. In a stationary equilibrium there is no net saving,  $\mathbf{s}[\tau] = 0, \forall \tau$ , and the trade matrix and ‘augmented’ trade matrix are identical and time invariant,  $\tilde{\boldsymbol{\Pi}} = \boldsymbol{\Pi}$ . The dynamics of coin stocks in equation (10) simplify into

$$\mathbf{S}[t, t+a] = \mathbf{S}[a] = \mathbf{M} \left( (\mathbf{I} - \boldsymbol{\lambda}) \boldsymbol{\Pi} \right)^a, \forall (t, a),\tag{12}$$

such that only age,  $a$ , matters. Combining coins of different ages, we get

$$\sum_{a=0}^A \mathbf{S}[a] = \mathbf{M} \left( \sum_{a=0}^A \left( (\mathbf{I} - \boldsymbol{\lambda}) \boldsymbol{\Pi} \right)^a \right) \underset{A \rightarrow +\infty}{=} \mathbf{M} \left( \mathbf{I} - (\mathbf{I} - \boldsymbol{\lambda}) \boldsymbol{\Pi} \right)^{-1}.\tag{13}$$

The share of coins from different mint origins in different destinations depends not on the

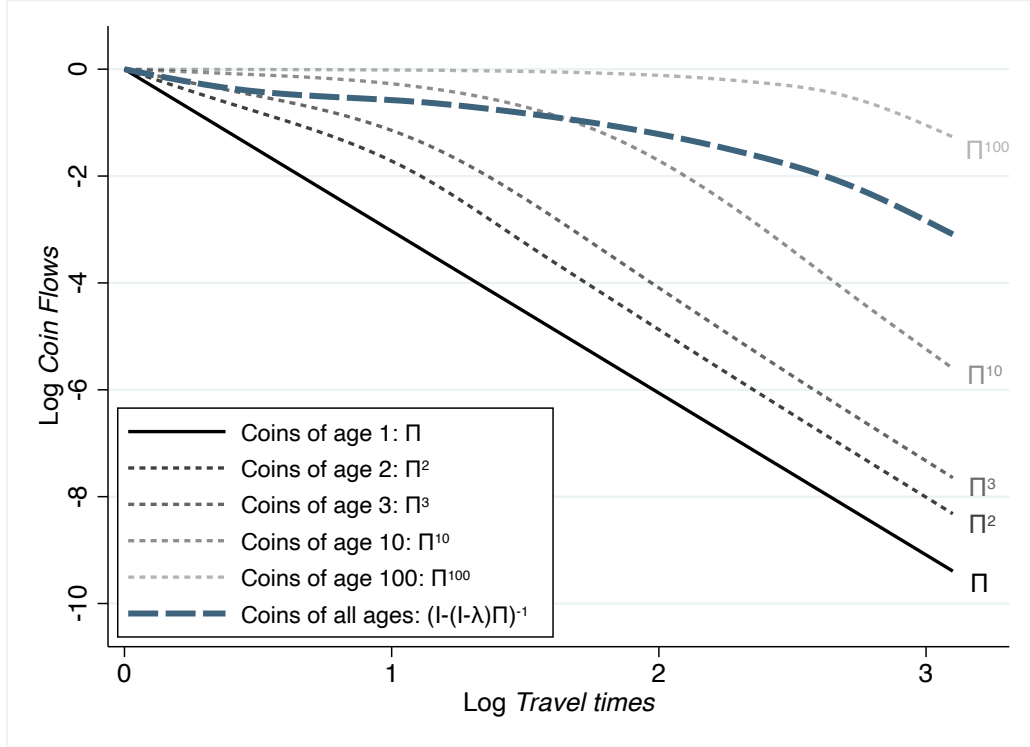


Figure 5: Flows of coins of different ages

*Notes:* This figure presents a numerical illustration of the flow of coins of different ages as a function of trade costs. We use equations (12) and (13), and the trade model (4) to simulate an economy with 50 locations around a regular polygon, with same technology  $T_n = T, \forall n$ , a trade elasticity  $\theta = 4$ , and an annual coin loss rate  $\lambda = 0.017$ . Locations are symmetric so wages are equalized and trade shares simplify to  $\pi_{ni} = (d_{ni})^{-\theta} / \sum_k (d_{nk})^{-\theta}$ . We parameterize  $(d_{ni})^{-\theta} = (\text{TravelTimes}_{ni})^{-\zeta}$  with  $\zeta = 3.03$ —see our structural estimation in table 3. Log travel times are on the x-axis; and log flows of coins of different ages on the y-axis— $\ln(S_{ni}[t, t+a])$  for age  $a$ . To ease comparisons, we normalize the largest log flows and smallest log travel times to zero, so all curves start at  $(0,0)$ . ‘Naively’ combining coins of all ages, i.e. treating the Leontief inverse  $(\mathbf{I} - (\mathbf{I} - \boldsymbol{\lambda}) \boldsymbol{\Pi})^{-1}$  as if it were the trade matrix  $\boldsymbol{\Pi}$ , gives a misspecified travel times elasticity of 1.15 (OLS estimate), substantially below the true  $\zeta = 3.03$ .

trade matrix  $\boldsymbol{\Pi}$ , but on the Leontief inverse of the trade matrix discounted by  $(\mathbf{I} - \boldsymbol{\lambda})$ :  $(\mathbf{I} - (\mathbf{I} - \boldsymbol{\lambda}) \boldsymbol{\Pi})^{-1}$ . The reason is simple: newly minted coins percolate through the trade network, just as value added shocks percolate through the input-output network in the work of Wassily Leontief (Leontief, 1941, 1944). The intensity with which coins flow from one location to another depends on bilateral trade shares, just as the intensity with which one upstream sector affects the production of a downstream sectors depends on bilateral input shares. The same coin will travel multiple times through the trade network (until hit by a Poisson death shock  $\lambda$ ), just as value added travels multiple times through the input-output network. However, unlike in conventional static models of input-output linkages, coins take time to percolate through the system, similar to the dynamic model of Liu and Tsyvinski (2024).

Figure 5 illustrates the potential bias from wrongly interpreting coin flows as trade flows and ignoring coin ages. Within the first period of their life, coin flows mirror trade flows ( $\boldsymbol{\Pi}$  in figure 5). The same elasticity governs coin and trade flows,  $S_{ni}[t, t+1] \propto \pi_{ni} \propto (d_{ni})^{-\theta}$ . In the second period of their life, coins have traveled twice through the trade network ( $\boldsymbol{\Pi}^2$  in

figure 5). The negative impact of trade costs over short distances weakens as coins have started diffusing within nearby destinations. As coins age, their flows gradually escape the negative effect of trade costs; coins diffuse through the trade network and converge towards a uniform distribution (see the flattening slopes of  $\boldsymbol{\Pi}$ ,  $\boldsymbol{\Pi}^2$ ,  $\dots$ ,  $\boldsymbol{\Pi}^{100}$  in figure 5).<sup>34</sup> A naive estimation using coins of all ages combined, i.e. wrongly interpreting the Leontief inverse  $(\mathbf{I} - (\mathbf{I} - \boldsymbol{\lambda}) \boldsymbol{\Pi})^{-1}$  as if it were the trade matrix  $\boldsymbol{\Pi}$ , would infer incorrect parameters. In our numerical example, if we assume that trade depends on travel times,  $(d_{ni})^{-\theta} = (TravelTimes_{ni})^{-\zeta}$ , with a true elasticity  $\zeta = 3.03$ , we would wrongly estimate an elasticity of 1.15. This corresponds approximately to the discrepancy between our reduced-form estimate combining coins of all ages (1.14 in table 1) and our upcoming structural estimate (3.03 in column 2 of table 3).<sup>35</sup> Appendix B.5 and figure B.4 show reduced-form evidence suggestive of this phenomenon in our coin dataset: across separate gravity regressions (as in table 1) for coins of different ages, the elasticity in absolute value falls towards zero as we move from younger to older coins.

## 3 Estimation

### 3.1 Mapping the model to the data

To map the model to the data, we need to define the empirical counterparts to time periods,  $t$ , locations,  $n$ , the coin loss rate,  $\lambda$ , and we parameterize trade costs as a function of observables.

**Definition of time periods.** We aggregate mint and hoard dates ( $tpq$ ) to 20-year intervals, and show robustness for shorter (10-year) and longer (30-year) intervals.

**Definition of locations.** We partition the world into  $N = 13$  regions. In the Islamic world they correspond to aggregates of provinces of the Umayyad caliphate (Cornu, 1983). In the Roman world they are based partly on Roman provincial borders, and partly on 9th-century political borders (see appendix A).

**Assumption: constant loss rate.** With a constant loss rate  $\lambda$ , any collection of coins minted at time  $t$  will gradually disappear from the monetary system. At time  $t + 1$  only a fraction  $(1 - \lambda)$  remains, at time  $t + 2$  a fraction  $(1 - \lambda)^2$ , etc. The same exponential decay holds for any starting date  $t$ , and it holds for the random sample found by archaeologists. We aggregate

---

<sup>34</sup>Our model of gradual diffusion of coins through a trade network is intimately related to the model of diffusion of information through a trade network in Chaney (2018).

<sup>35</sup>Figure 5 is a stylized example with symmetric locations around a regular polygon, meant to build intuition, not to resemble the real ancient world. The proximity between 1.15 in figure 5 and 1.14 in table 1 is coincidental.

all the coins in our dataset, and express the density of coins of age  $a$  as  $f(a) \propto (1 - \lambda)^a$ , corresponding to figure 3b. Taking logs, we estimate  $\lambda$  by OLS,

$$\ln f(a) = \text{constant} + \ln(1 - \lambda) \times a + \varepsilon(a). \quad (14)$$

We estimate a coin loss rate of 1.7% per year, or 30% over 20 years,  $\hat{\lambda}_{\text{20-year}} = 0.3$ .<sup>36</sup>

**Parameterization of trade costs.** We assume that bilateral trade costs scaled by the trade elasticity  $\theta$  are a function of (directed) bilateral travel times, and a possible ad-valorem proportional penalty incurred when crossing political or religious borders,

$$\begin{aligned} \ln((d_{ni}[t])^{-\theta}) &= \kappa_0 - \zeta \ln(\text{TravelTime}_{ni}) \\ &\quad - \kappa_{\text{Pol.}} \cdot \text{PoliticalBorder}_{ni}[t] - \boldsymbol{\kappa}_{\text{Rel.}} \cdot \text{ReligiousBorder}_{ni}[t], \forall(n \neq i, t). \end{aligned} \quad (15)$$

We normalize  $d_{nn}[t] = 1, \forall n, t$ , as in Eaton and Kortum (2002). The constant  $\kappa_0$  adjusts travel time units, and governs the home bias in trade.<sup>37</sup>  $\boldsymbol{\kappa}_{\text{Rel.}}$  is either a scalar or a vector distinguishing the eastern, western, and Mediterranean borders,  $\boldsymbol{\kappa}_{\text{Rel.}} = (\kappa_{\text{Rel.}}^{\text{East}}, \kappa_{\text{Rel.}}^{\text{West}}, \kappa_{\text{Rel.}}^{\text{Med.}})$  in our baseline. From our ‘augmented’ trade model, which describes coin flows driven both by trade and saving, we derive the bilateral determinants of coin flows,  $\tilde{\delta}_{ni}[t]$  in equation (11),

$$\begin{aligned} \ln(\tilde{\delta}_{ni}[t]) &= \tilde{\kappa}_0 - \zeta \ln(\text{TravelTime}_{ni}) \\ &\quad - \kappa_{\text{Pol.}} \cdot \text{PoliticalBorder}_{ni}[t] - \boldsymbol{\kappa}_{\text{Rel.}} \cdot \text{ReligiousBorder}_{ni}[t], \forall(n \neq i, t), \end{aligned} \quad (16)$$

and  $\tilde{\delta}_{nn}[t] = 1, \forall(n, t)$ . The bilateral determinants of external trade flows,  $(d_{ni}[t])^{-\theta}$ , and coin flows,  $\tilde{\delta}_{ni}[t]$ , only differ by a multiplicative scalar,  $e^{\tilde{\kappa}_0 - \kappa_0}$ , due to saving. Given within region coin flows,  $\tilde{\pi}_{nn}[t]$ , this scalar maps into the saving rates,

$$s_n[t] = \tilde{\pi}_{nn}[t] (1 - e^{\tilde{\kappa}_0 - \kappa_0}). \quad (17)$$

---

<sup>36</sup>See appendix B.6 and table B.6 for formal estimation results. Our estimates of an annual coin loss rate of 1.7% are remarkably similar to those estimated by numismatists. For Roman times, the most frequently cited estimates are by Crawford and Hopkins, of 2% per annum (Hopkins, 1980). Patterson (1972) reports estimates of 2% for Roman times (150 AD), and 1% for Islamic times (800 AD). These numbers are based on estimates of mint output from information on the number of dies that were used to mint coins, and multiplying die counts by estimates of the average number of coins that were struck with one die. The comprehensive die studies that are required for this procedure are, however, only available for a small subset of mints and time periods.

<sup>37</sup>Our parameterization for trade costs is potentially inconsistent with the assumption of arbitrage trade because we compute optimal travel routes once, without taking into account the additional costs associated with potentially multiple border crossings. In practice, this does not happen: we manually verify that the estimated costs in equation (15) cannot be lowered by taking a longer route avoiding unnecessary border crossings.

$\tilde{\pi}_{nn}[t]$  controls the home bias in coins, and  $(1 - e^{\tilde{\kappa}_0 - \kappa_0})$  adjusts for the discrepancy (due to saving  $s_n[t]$ ) between the home bias in coins (governed by  $\tilde{\kappa}_0$ ) and the home bias in trade (governed by  $\kappa_0$ ). In the absence of direct evidence on ancient trade, we cannot directly estimate  $\kappa_0$ . Instead, we choose  $\kappa_0$  to match an average ancient saving rate into nominal assets of 1.5% (Scheidel, 2020). This estimated savings rate for Roman times is likely an upper bound for Late Antiquity, where property rights were weaker and conflict more widespread.

**Travel times.** To compute (optimal) travel times given the transportation network and technology we use two geo-spatial models constructed by historians to provide quantitative estimates of (shortest) distances, trade routes, and trade costs. The first is Orbis (Scheidel, 2015), a directed graph of cities and trade routes of the Roman world (i.e. from Britannia in the north-west to Egypt, Palestine, and Syria in the south-east) along with a calibrated model of trade costs, in monetary units and units of time, along the edges to allow for the calculation of shortest paths. The second is al-Turayyā (Romanov and Seydi, 2022), a digitalization of the Atlas of the Islamic World of Cornu (1983), which, similarly, contains the coordinates of cities and trading posts connected by trade routes, but without estimates of travel times. We combine the nodes of al-Turayyā and Orbis and extend Scheidel (2015)'s methodology from Orbis to calculate travel times for the Islamic world (see appendix A for details).

Figure 6 shows the combined graph. We validate the resulting travel times by comparing them to those reported by the 10th-century Arab geographer Al-Muqaddasī (985) (see appendix B.7 and figure B.5). For each region, we calculate the weighted average of mint locations (with the shares of each location in total coin output as weights) and project it to the closest vertex on the graph. The shortest travel time between the central vertices in  $n$  and  $i$  is our time-invariant measure of  $TravelTime_{ni}$ .

**Political and religious borders.** We construct political border and religious border dummies by coding the start and end years of the presence of political entities across regions. We set  $PoliticalBorder_{ni}[t]$  to one if the set of political entities that occupy at least some part of the regions  $n$  and  $i$  for some part of the 20-year time interval is disjoint.  $ReligiousBorder_{ni}[t]$  captures the border between the emerging religion of Islam and the rest of the world. We use two alternative specifications. The first specification is a dummy equal to one if all political entities in region  $n$  are Islamic and none in  $i$  are, or vice versa. The second specification—our baseline—distinguishes the eastern, western, and Mediterranean borders of Islam. The eastern land border is between the Byzantine heartlands and the Caliphate regions east of Egypt, the western land border is between al-Andalus and Aquitaine or Francia/Germania, and the Mediterranean maritime border is between all other region pairs.

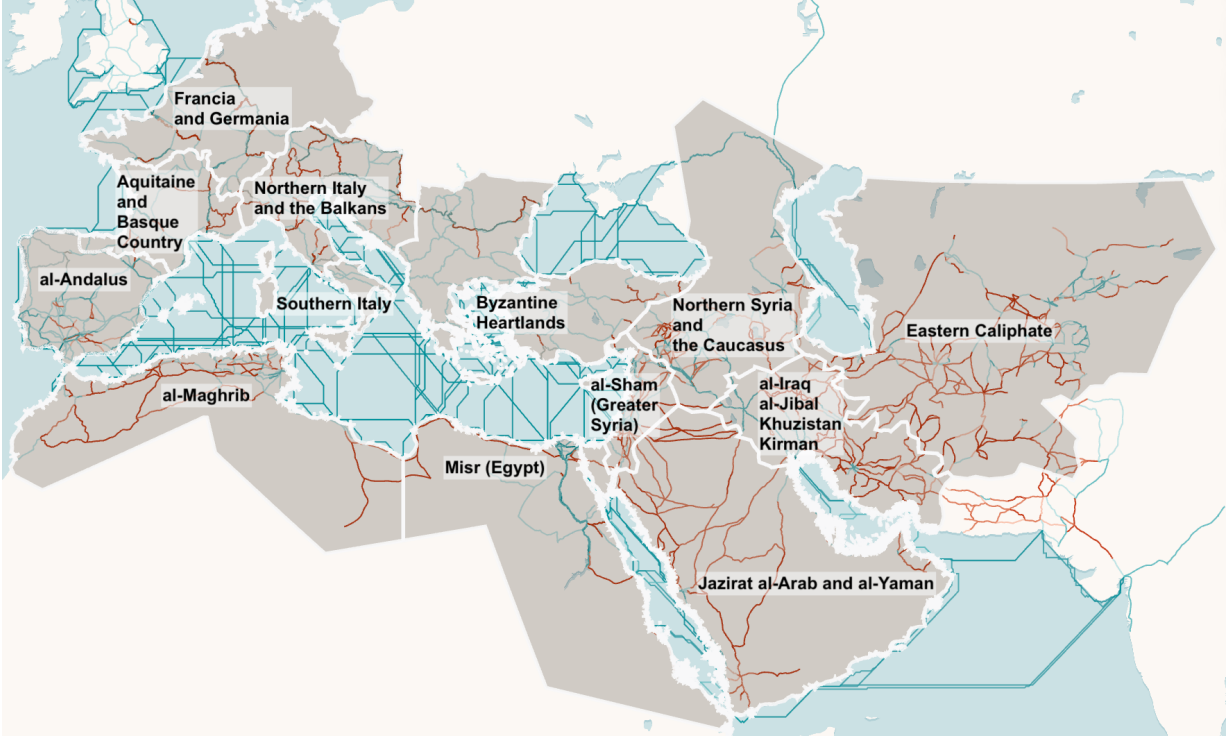


Figure 6: The combined geospatial model

*Notes:* The figure shows the combined geospatial models from Orbis and al-Turayyā, along with our thirteen regions. Edges in blue (red) indicate faster (slower) travel speeds.

**Coin hoard data generating process.** We assume that our hoard dataset  $\mathbf{H}$  is a random sample from the stocks of coins in each region and period. We group all hoards within a region and period, with  $H_h[T]$  the total amount of coins found in region  $h$  and buried at time  $T$  (*tpq*), which we decompose into coin types, with  $H_{m,h}[t,T]$  the amount of coins minted in  $m$  at time  $t$  within that hoard. Our random sampling assumption means that the expected share of coin types within a hoard equals the share of coin types within a coin stock in our model (10),

$$\mathbb{E} \left[ \frac{H_{m,h}[t,T]}{H_h[T]} \right] = \frac{S_{m,h}[t,T]}{S_h[T]}. \quad (18)$$

As we discuss in section 1, we recognize that the probability that a coin ends up in our dataset may vary between regions and periods, depending on whether coins were lost and deposited in the ground, found by archaeologists, and documented by experts. By using only information on the shares of coins *within* hoards, we condition on those events being realized (lost, found, documented), and we purge any variation in the probability of those events.<sup>38</sup>

Appendix B presents suggestive evidence in support of our random sampling assumption.

---

<sup>38</sup>Our assumption of random sampling would be violated if, for example, hoards with certain types of coins were more likely to be described in the literature. This concern is mitigated by the fact that many of the regions we study are covered by catalogues of coin finds that seek to exhaustively describe all finds on a territory.

For eight region  $\times$  periods with the largest number of coins and hoards, we randomly split hoards in two subsets, and confirm that the geographic (domestic vs foreign) and age distributions of coins in each subsample of hoards within a region  $\times$  period are statistically indistinguishable (see table B.7). We further show that for almost all twenty eight pairs of region  $\times$  periods, the geographic (domestic vs foreign) and age distributions of coins in both region  $\times$  periods are statistically different from each other (see table B.8). This suggests that hoards within a region  $\times$  period unit of observation contain similar information about the geography and ages of coins, while hoards in distinct region  $\times$  period units of information contain distinct information.

**Coin accounting.** We use two different accounting methods for the amounts of coins within hoards,  $H_{m,h}[t, T]$ : either the count of coins combining all denominations together, or the value of gold and silver coins accounting for weight, denomination, and metal content as in section 1 (see footnote 22 for details on computing relative gold and silver values), discarding undetermined coins and bronze coins for which relative values fluctuate too much and are poorly documented. Each method has advantages and drawbacks. Using counts minimizes the amount of data we discard, but ignores relative values. Using values is closer to our assumption that coins are fungible, but forces us to discard information on 75% of the coins in our dataset. We use counts as our baseline, and present robustness using values.

### 3.2 Estimation method

We estimate the structural parameters of our model by maximum likelihood. Given our random sampling assumption in equation (18), the probability of observing  $(\dots, H_{m,h}[t, T], \dots)_{m,t}$  coins minted in different regions ( $m$ 's) at different times ( $t$ 's) among the total of  $H_h[T]$  coins within a hoard buried in region  $h$  at time ( $tpq$ )  $T$  is multinomial, and a function of coin stocks,

$$\Pr(\dots, H_{m,h}[t, T], \dots) = \frac{H_h[T]!}{\prod_{m', t' \leq T} H_{m', h}[t', T]!} \prod_{m, t \leq T} \left( \frac{S_{m,h}[t, T]}{S_h[T]} \right)^{H_{m,h}[t, T]}.$$

It depends on the model parameters through the predicted coin shares,  $S_{m,h}[t, T]/S_h[T]$ . They are governed by the coin flow recursive equation (10), the coin flow static equation (11), which depend on the coin loss rate (14), and the bilateral determinants of coin flows (16). We collect all parameters in the vector  $\Theta$ : the saving and trade costs parameters,  $\tilde{\kappa}_0$ ,  $\zeta$ ,  $\kappa_{Po.}$ , and  $\kappa_{Rel.}$  from (16), time-varying minting  $M_n[t]$  from (10), and time-varying seller terms  $\tilde{\beta}_n[t]$  from (11),

$$\Theta = \left( \tilde{\kappa}_0, \zeta, \kappa_{Po.}, \kappa_{Rel.}, (\dots, M_n[t], \dots)_{n \neq n_0, t \neq t_0}, (\dots, \tilde{\beta}_n[t], \dots)_{n \neq n_0, t}, \right).$$

As we target coin shares within hoards, we can never recover the total number of coins minted over 320-950. We normalize mint output  $M_{n_0}[t_0] = 100$  for an arbitrary region  $n_0$  (northern Italy) and period  $t_0$  (320-340). Similarly, only *relative* seller terms matter for coin flow shares within each period, so we normalize  $\tilde{\beta}_{n_0}[t] = 100, \forall t$ , for region  $n_0$ .

To estimate  $\Theta$ , we maximize the likelihood of observing our coin hoards sample,

$$\hat{\Theta} = \arg \max_{\Theta} \sum_{h,T} \sum_{m,t \leq T} H_{m,h}[t,T] \left( \ln S_{mh}[t,T](\Theta) - \ln \sum_{m',t' \leq T} S_{m'h}[t',T](\Theta) \right). \quad (19)$$

Given those structural estimates, we recover the parameter  $\kappa_0$  governing bilateral trade costs (distinct from the parameter  $\tilde{\kappa}_0$  governing bilateral coin flows in the presence of saving), using equation (17) and an average net ancient saving rate into coins of 1.5% (Scheidel, 2020),

$$\kappa_0 \text{ s.t. } (1 - e^{\tilde{\kappa}_0 - \kappa_0}) \mathbb{E}_{n,t} [\tilde{\pi}_{nn}[t]] = 0.015. \quad (20)$$

With those estimates, we can recover all equilibrium variables (see section 4.1).

**Identification.** We present an asymptotic identification proof and explore identification in finite sample using numerical simulations in appendix E. The identification of the trade costs parameters is relatively straightforward: by combining at least two consecutive series of coin hoards, we can isolate both minting and buyer terms into coin origin fixed effects, seller terms into coin destination fixed effects, and estimate the bilateral determinants of coin flows. Intuitively, the relative frequency of coins or different origins across hoards directly informs the bilateral component of coin flows. Separately identifying minting from seller terms is harder, both because by using only coin shares within hoards we do not have direct information on the relative scale of minting from different regions, and because minting affects expenditure in one period but becomes income in the next and therefore gets jumbled up with production, governed by the seller terms. Combining information from hoards in more consecutive periods than regions and the structure of the model allows to break this indeterminacy. A further complication arises with sparse data, where many observations are zeros. Numerical simulations suggest that our estimator recovers known parameters accurately even with sparse data, and that misspecification biases may exist but are unlikely to be large.

### 3.3 Parameter estimates

**Ancient trade costs.** Table 3 shows the estimates of the parameters governing ancient trade costs. Column 2, which distinguishes the religious border in the east (in and out of Byzantium), in the west (in and out of al-Andalus), or over the Mediterranean in and out of its non-Islamic

Table 3: Bilateral determinants of ancient trade

	Log Trade	
	(1)	(2)
Log Travel Time	-2.98 (0.02)	-3.03 (0.02)
Political Border	-0.3 (0.02)	-0.49 (0.02)
Religious Border	-4.05 (0.11)	
Religious Border: East		-1.97 (0.12)
Religious Border: West		-4.59 (0.22)
Religious Border: Mediterranean		-5.2 (0.18)
Sample	All	All
Coin Accounting	Number	Number
Observations	4,413	4,413

*Notes:* The table shows estimates for the trade costs parameters in equation (15). “Political Border” is one if the sets of political entities that occupy at least some part of the regions during the 20-year time period are completely disjoint, and zero otherwise. In column 1 “Religious Border” is one if all political entities in one region are Islamic and all are non-Islamic in the other region, and zero otherwise. In column 2, our baseline, “Religious Border: East” is one iff the religious border dummy is one and the regions are al-Andalus and Aquitaine or Francia/Germania, or vice versa; “Religious Border: West” is one iff the religious border dummy is one and the regions are the Byzantine Heartlands and one of the Caliphate regions east of Egypt, or vice versa; “Religious Border: Mediterranean” is one for all other region pairs where the religious border dummy is one. “Observations” denotes the number of observations  $(m, h, t, T)$  in the log-likelihood equation (19) where  $H_{m,h}[t, T] > 0$ . See appendix table B.9 for the sensitivity of our estimates to alternative coin accounting methods and definitions of period lengths. Asymptotic standard errors in parentheses.

northern shore, is our baseline. We discuss the robustness of our estimates to alternative coin accounting methods and time aggregations in section 4.5.

In our simpler specification (column 1), the travel time elasticity of trade,  $\zeta = 2.98$  (s.e. 0.02), is somewhat larger but close to the 2.05-2.89 range of estimates from Flückiger et al. (2022) using bilateral trade in terra sigillata in ancient Rome and optimal travel times along the Roman transportation network, and to the 1.9 distance elasticity from Barjamovic et al. (2019) using merchant records in Bronze Age Anatolia. This similarity to estimates using actual—though partial—ancient trade data is reassuring, as we do not use any direct information on trade, but only indirect information from coins. This travel time elasticity is robust to alternative specifications for the religion border effect, 3.03 versus 2.98 in column 2 versus 1.

In our simpler specification (column 1), the political ( $\kappa_{Pol.}$ ) and religious ( $\kappa_{Rel.}$ ) border effects are large, but of the same magnitude as estimates for modern border effects. Assuming a trade elasticity  $\theta = 4$  (Simonovska and Waugh, 2014), those correspond to an 8% ad-valorem tax for crossing a political border ( $d_{across}/d_{within} = e^{\kappa_{Pol.}/\theta} \approx 1.08$ ), and a 175% tax for crossing a religious border ( $d_{across}/d_{within} = e^{\kappa_{Rel.}/\theta} \approx 2.75$ ), of the same magnitude as the estimated

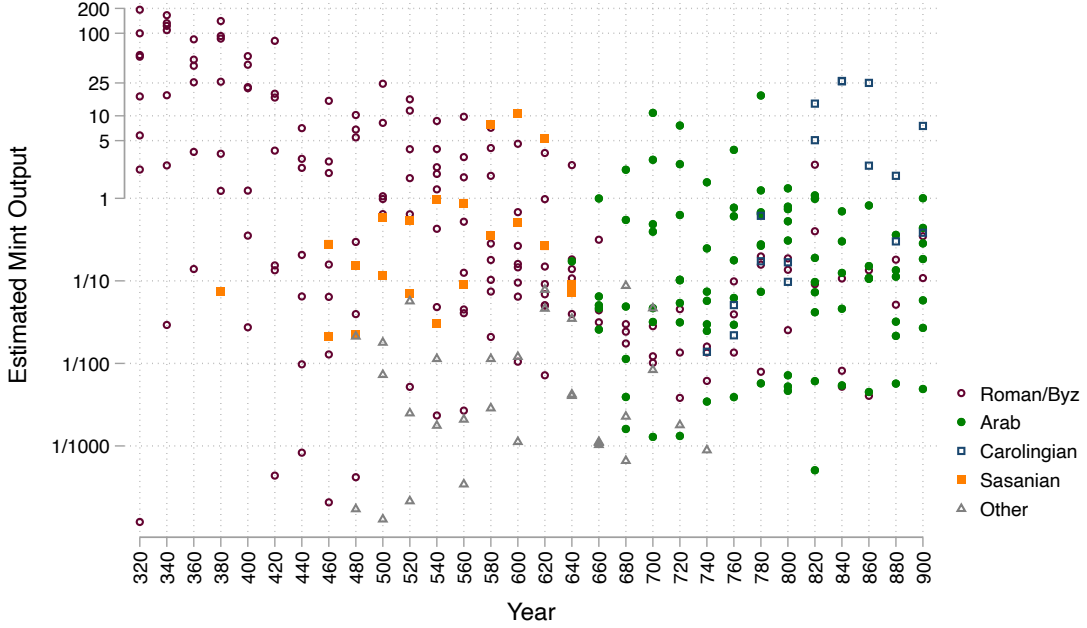


Figure 7: Estimated mint output, AD 320-900

*Notes:* The figure shows the estimated coin output  $M_n[t]$  by time  $t$  (horizontal axis) and region  $n$ , using our baseline specification in column 2 of table 3, and broken down by the political entities that locations are—at that time—primarily associated with. The units are relative to northern Italy in 320-340, which we normalize to have a mint output of 100.

49% cost of crossing the modern US-Canada border (Anderson and van Wincoop, 2003).<sup>39</sup>

Distinguishing the eastern and western land borders from the Mediterranean maritime border (column 2) does not affect our estimate of the political border effect, which remains small (0.3 versus 0.49 in columns 1 versus 2). It does however reveal different estimated penalties associated with crossing from Islamic to non-Islamic regions. The religious border effect is strongest for crossing the Mediterranean ( $\kappa_{Rel.}^{Med.} = 5.20$ ) and for the western border from al-Andalus ( $\kappa_{Rel.}^{West} = 4.59$ ), and lowest for the eastern border into Byzantium ( $\kappa_{Rel.}^{East} = 1.97$ ).

Our structural estimation confirms the reduced form evidence in section 1. The border in and out of Islamic regions becomes costlier to cross *after* the birth of Islam.

**Minting output.** Figure 7 shows estimates of mint output by region and time interval. Our estimates line up with several patterns described in the numismatic literature: (i) the decline of mint output in the western Mediterranean following the demise of the West Roman Empire in the late 5th century; (ii) the large decline of Byzantine mint output in the ‘Byzantine dark ages’ of the 8th century; (iii) the gradual increase in Arab and Frankish mint output starting from the late 7th century. Importantly, we are not merely counting coins; we *estimate* minting output from the relative shares of coins from different mints across hoards, absorbing variation

<sup>39</sup> Anderson and van Wincoop (2003) estimate that trade is  $\exp(1.59) \approx 5$  times larger within than between the US and Canada. For  $\theta = 4$  it corresponds to  $d_{across}/d_{within} = e^{1.59/4} \approx 1.49$ , a 49% ad-valorem border tax.

due for instance to differential hoarding patterns or hoard finding rates across space and time.

**Seller terms.** The last set of estimates, the seller terms, contain combined information about factor prices and technology,  $\tilde{\beta}_n[t] = (w_n[t]/T_n^{1/\theta}[t])^{-\theta}$ . Those terms are not readily interpretable because factor prices ( $w_n[t]$ ) are endogenous and depend on all other parameters. The structure of our dynamic model of trade and coins allows us to separately recover all equilibrium variables from our parameter estimates, including relative prices, which we turn to next.

## 4 Trade and the end of antiquity

In this section, we first explain how we can recover trade and real consumption solely from our parameter estimates. We then present granular evidence on the dynamics of ancient trade and consumption. While those findings are mostly descriptive, they reveal the promise of using ancient coins, and more broadly a quantitative dynamic model of trade, to reveal patterns of a changing economic geography; they also inform and clarify active debates in history.

### 4.1 Recovering trade, nominal income, and real consumption

Even though we only have data on coin hoards, they implicitly contain information about production, trade, and endogenous prices. From those data we can recover all economic variables using solely our parameter estimates, the structure of our model, and a single unknown parameter, the trade elasticity, arbitrarily set to  $\theta = 4$  (Simonovska and Waugh, 2014).<sup>40</sup>

Given the low savings rate (1.5% p.a. computed by Scheidel, 2020), we approximate it to zero to simplify the algebra, but note that our method extends to positive saving with nearly identical results. The inherent sparsity of our ancient coin hoard data introduces noise in our estimates for seller terms and minting. To smooth out some of this noise, we use a simple moving average: for  $t \in [380, 880]$ , we use  $\frac{1}{3} \sum_{\tau=t-1}^{t+1} \tilde{\beta}_n[\tau]$  instead of  $\tilde{\beta}_n[t]$ , and  $\frac{1}{3} \sum_{\tau=t-1}^{t+1} M_n[\tau]$  instead of  $M_n[t]$ . We do not smooth our precisely estimated parameters for bilateral trade costs.

**Trade.** We recover trade shares from estimated seller terms,  $\tilde{\beta}_i[t]$ , and the determinants of bilateral trade,  $(\kappa_0, \kappa_{Pol.}, \kappa_{Rel.}^{East}, \kappa_{Rel.}^{West}, \kappa_{Rel.}^{Med.})$  from which we compute  $d_{ni}^{-\theta}[t]$  using (15),

$$\pi_{ni}[t] = \frac{\tilde{\beta}_i[t] d_{ni}^{-\theta}[t]}{\sum_k \tilde{\beta}_k[t] d_{nk}^{-\theta}[t]}, \forall (n, i, t). \quad (21)$$

---

<sup>40</sup>This unknown elasticity  $\theta$  has no impact on our estimation strategy, which is identical for *any* choice of  $\theta$ . It also has no impact on the computation of trade flows and nominal incomes. It is solely required to distinguish nominal from real consumption. In practice however, even tripling  $\theta$  from 4 to 12 has a barely noticeable impact on estimated consumption (see table 4).

Estimated trade shares are invariant to any normalization of  $\tilde{\beta}_i[t]$  and  $M_n[t]$ , and hold for any  $\theta$ .

**Nominal income.** Market clearing imposes a relationship between nominal income in one region, income and minting in other regions, and trade shares. Information on estimated trade shares  $\pi_{ni}[t]$ , minting  $M_n[t]$ , and the coin loss rate  $\lambda$ , is sufficient to recover incomes. Markets clear dynamically so we need to make an assumption for period  $t_0 - 1$  before our sample starts. Absent any data, we simply assume that aggregate incomes in  $t_0 - 1$  are the same as in  $t_0$  and use the steady state market clear condition (8). For every subsequent periods we recover incomes by recursively solving the dynamic market clearing conditions (7).

$$(w_i[t_0]L_i[t_0]) = \sum_n \pi_{ni}[t_0] \left( (1 - \lambda) (w_n[t_0]L_n[t_0]) + M_n[t_0] \right), \forall i,$$

$$\text{and } (w_i[t]L_i[t]) = \sum_n \pi_{ni}[t] \left( (1 - \lambda) (w_n[t-1]L_n[t-1]) + M_n[t] \right), \forall (i, t > t_0). \quad (22)$$

Estimated nominal incomes inherit our (single) minting normalization and hold for any  $\theta$ .

**Real consumption.** Real consumption is defined as nominal consumption normalized by the price index,  $X_n[t] = (1 - \lambda) w_n[t-1]L_n[t-1] + M_n[t]$  over  $p_n[t] = \gamma (\sum_k (w_k[t]/T_k^{1/\theta}[t]d_{nk}[t])^{-\theta})^{-1/\theta}$ , where  $\gamma$  is a constant. Simple manipulations yield,

$$\frac{X_n[t]}{p_n[t]} = \gamma^{-1} (\pi_{nn}[t])^{-1/\theta} (T_n^{1/\theta}[t]L_n[t]) \left( \frac{(1 - \lambda) w_n[t-1]L_n[t-1] + M_n[t]}{w_n[t]L_n[t]} \right). \quad (23)$$

The first and last terms are directly computed from estimates for trade shares, nominal incomes, minting, the coin loss rate, and  $\theta$ . Using  $\tilde{\beta}_n[t] = (w_n[t]/T_n^{1/\theta}[t])^{-\theta}$  in (11), the middle term is recovered from nominal incomes, seller terms, and  $\theta$ :  $T_n^{1/\theta}[t]L_n[t] = (w_n[t]L_n[t])(\tilde{\beta}_n[t])^{1/\theta}$ .

The intuition for the components of real consumption in (23) is as follows. A higher production capacity ( $T_n^{1/\theta}L_n$ ) allows to produce more goods and improves real consumption. As in Eaton and Kortum (2002), trade openness ( $\pi_{nn}^{-1/\theta}$ ) further increases real consumption, leveraging the gains from trade. As in Dekle et al. (2007), trade deficits (surpluses) financed by net coin creation allow a region to consume more (less) than it produces ( $\frac{X_n[t]}{w_n L_n[t]} = \frac{(1-\lambda)w_n[t-1]L_n[t-1]+M_n[t]}{w_n L_n[t]}$ ).

Our normalizations for the seller terms and for minting do not affect the first and last terms, both unit-free ratios, but they affect the middle term. We arbitrarily choose units for technology such that  $\sum_n X_n[t]/p_n[t] \equiv 1, \forall t$ , so regional consumption within each period is always defined as a share of aggregate consumption. This normalization is an important limitation of our structural estimation: data on nominal trade flows can reveal *relative* aggregate production and consumption, but can never reveal *absolute* levels. This means that our estimates cannot identify any one-period shock affecting all regions from the Indus to the Atlantic.

## 4.2 The geography of Mediterranean trade and the Pirenne thesis

Our granular estimates for trade and income allows us to paint a detailed picture of the evolution of Mediterranean trade. We partition the Mediterranean into southern—al-Andalus, al-Sham (Greater Syria), Misr (Egypt), al-Maghrib—and northern regions—Aquitaine and Basque Country, Northern Italy, Southern Italy, Byzantine Heartlands—and decompose Mediterranean trade to and from northern and southern regions. Figure 8 shows the geographic evolution of Mediterranean trade,<sup>41</sup> partitioned into north-south crossings (panel 8a), south-south crossings (panel 8b), and north-south crossings (panel 8c).

We confirm in panel 8a the hypothesis formulated by Pirenne (1939) that north-south Mediterranean trade fell sharply after the Arab conquests of the near east, northern Africa, and the Iberian peninsula. North-south crossings collapse from around 4% of the total income of Mediterranean regions until the late 6<sup>th</sup> century to below 1% after the late 7<sup>th</sup> century. This is to be expected given our estimate of a large Mediterranean border effect discouraging trade in and out of Islamic regions. This structural evidence also confirms the reduced form evidence on counts of coins crossing the Mediterranean in section 1.3 (see appendix figure B.3).

However, our estimates also reveal that while north-south crossings fell sharply after the Arab conquests, overall Mediterranean trade remained flourishing throughout Late Antiquity, as south-south crossings compensate the collapse of north-south trade. Panel 8b shows that south-south crossings represented between 5% and 10% of aggregate Mediterranean income, both before and after the Arab conquests. Following the rapid economic expansion of Islamic regions in the early 8<sup>th</sup> century, south-south crossings actually increase after the Arab conquests, although our estimates are less precise. Panel 8c shows that north-north crossings on the other hand remain small—below 1% of Mediterranean income—until the very end of our sample period when they start increasing following the economic rise of Carolingian Aquitaine.

Taken together, our evidence that north-south Mediterranean trade collapsed in the 7<sup>th</sup> century after the Arab conquests, while south-south trade remained stable and even rose, offers both support and nuance to the Pirenne (1939) thesis and to our descriptive evidence.

## 4.3 The economic decline of the Mediterranean

The collapse of north-south Mediterranean trade is mirrored in the overall economic decline of Mediterranean regions. Figure 9a displays time series estimates of the average size of Mediter-

<sup>41</sup>We define any predicted trade flow from one Mediterranean region to another as Mediterranean, but exclude trade flows within regions. This means, for instance, that we count a shipment from Northern Italy to al-Andalus as Mediterranean, even though it may travel overland through the Alps and the Pyrenees; and we do not count a shipment within Northern Italy as Mediterranean, even though it may travel by sea.

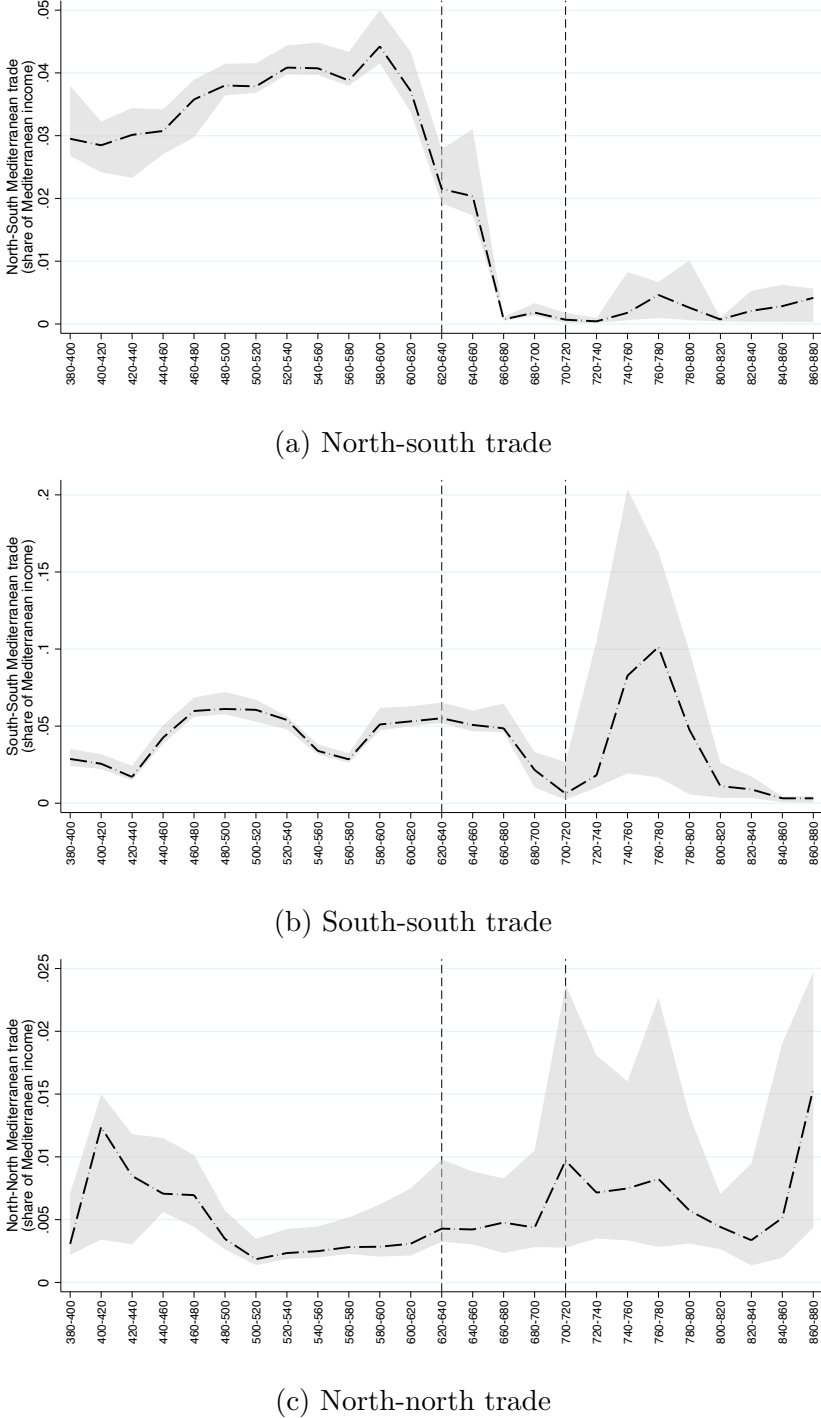


Figure 8: The geography of Mediterranean trade, AD 380-880

*Notes:* We partition the Mediterranean into southern—al-Andalus, al-Sham (Greater Syria), Misr (Egypt), al-Maghrib—and northern regions—Aquitaine and Basque Country, Northern Italy, Southern Italy, Byzantine Heartlands. We compute exports from origin  $i$  to destination  $n$  as the product of trade share and importer's income,  $\pi_{ni}[t] \times w_n[t]L_n[t]$ . Mediterranean trade is partitioned into north-south, south-south, and north-north flows. Each panel shows the time series of one component of Mediterranean trade as a share of total Mediterranean income: north-south for panel 8a, south-south for panel 8b, and north-north for panel 8c. 95% confidence intervals (shaded areas) are computed from re-estimating our model on 100 bootstrapped samples from our coin hoard data. The vertical lines correspond to the Arab conquests, starting in 622 under Muhammad and ending in 713 with the conquest of Iberia.

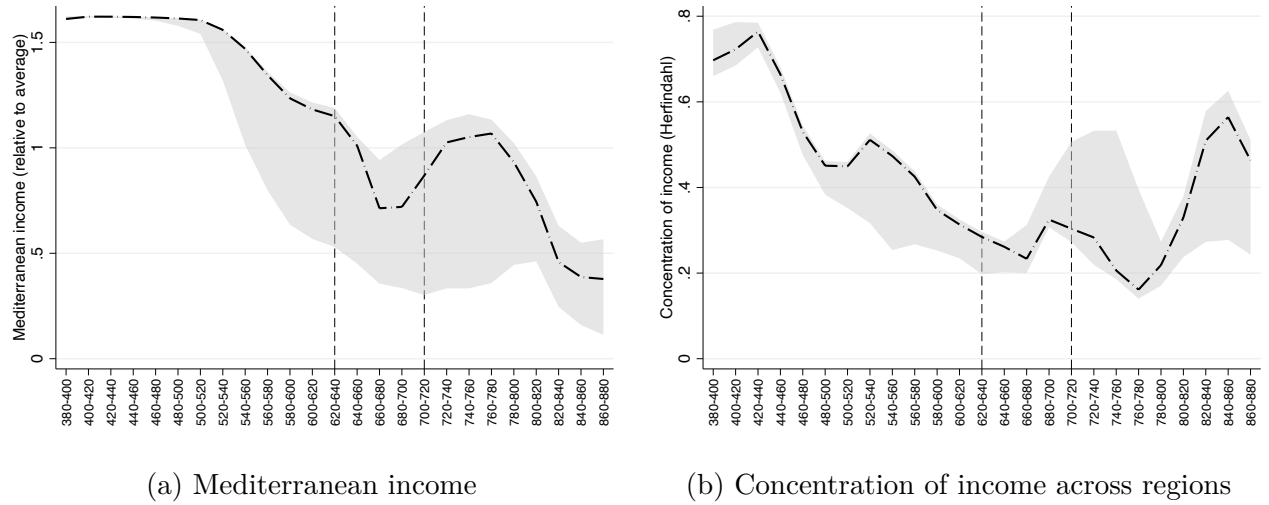


Figure 9: Mediterranean decline and falling economic concentration, AD 380-880

*Notes:* Panel (a) presents the time series of average nominal incomes of the eight Mediterranean regions relative to the average nominal income of all thirteen regions. Panel (b) presents the time series of Herfindahl indices of income concentration, defined for each period as the sum across all thirteen regions of the squared share of regional income over aggregate income. 95% confidence intervals (shaded areas) are computed from re-estimating our model on 100 bootstrapped samples from our coin hoard data. The vertical lines correspond to the Arab conquests, starting in 622 under Muhammad and ending in 713 with the conquest of Iberia.

ranean regions relative to the average size of all regions in our sample.<sup>42</sup> It shows a gradual decline starting in the early 6<sup>th</sup> century and continuing at least until the late 9<sup>th</sup> century. Over four centuries, Mediterranean regions went from being 50% larger to 50% smaller than the average region of the ancient western world. This relative economic decline of the Mediterranean starts more than a century before the birth of Islam, and therefore cannot be attributed to a newly formed religious border. It is initially driven by the relative rise of eastern regions—both before and after the birth of Islam—and subsequently by the relative rise of northern Europe—starting in the 6<sup>th</sup> century and accelerating in the 8<sup>th</sup> century.

Our granular estimates also reveal that the relative economic decline of the Mediterranean conceals a substantial reallocation of economic activity not just away from the Mediterranean, but also within the Mediterranean. Figure 9b shows the evolution of economic concentration from the 4<sup>th</sup> to the 9<sup>th</sup> century. Starting as early as the end of the 4<sup>th</sup> century, which corresponds to the split of the Roman empire between western and eastern provinces, the concentration of economic activity in the entire ancient western world falls. This fall pre-dates both the birth of Islam and the collapse of north-south Mediterranean trade, and the economic decline of the Mediterranean by more than a century. It is initially driven by a relative decline of the regions at the core of the Roman empire, northern Italy, western Europe, and Egypt, and subsequently by a relative rise of middle-eastern and eastern regions. Interestingly, while we document almost continuous shifts in relative economic activity throughout our sample period,

<sup>42</sup>We use nominal incomes to compute relative sizes. Since those estimated income series contain endogenous relative prices, relative nominal incomes are identical to relative real incomes using a single global price index.

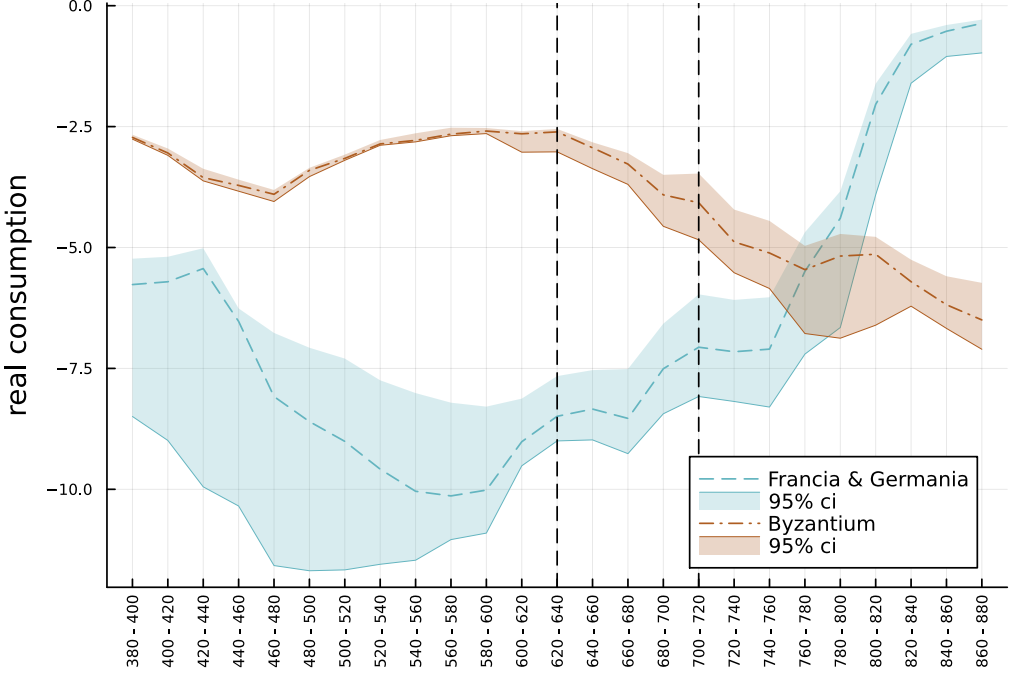


Figure 10: Byzantine Heartlands versus Francia & Germania, AD 380-880

*Notes:* This figure shows time-series of (log) real consumption as a share of aggregate consumption from AD 380 to AD 880 for the Byzantine Heartlands and for Francia and Germania. See section 4.1 for details on the computation of real consumption using estimates from the specification in column 2 of table 3. 95% confidence intervals (shaded areas) are computed from re-estimating our model on 100 bootstrapped samples from our coin hoard data. The vertical lines correspond to the Arab conquests, starting in 622 under Muhammad and ending in 713 with the conquest of Iberia. Time series for all 13 regions are in appendix figure B.6.

concentration remains relatively stable from the 6<sup>th</sup> to the 9<sup>th</sup> century.

Our evidence suggests that (regional) inequality may not fall solely following catastrophic violent events (Scheidel, 2017), and that the ancient western world remained (economically) multi-polar throughout Late Antiquity (Wickham, 2006; McCormick, 2001).

#### 4.4 Reversal of fortunes: Byzantium versus northern Europe

To showcase the promise of our structural estimates of granular real consumption time series, figure 10 displays the evolution of real consumption, for each 20-year period over AD 380-880, for Byzantium and for Francia and Germania. We highlight those two regions because they undergo some of the most striking reversals of fortune over our sample period. We briefly discuss the other regions at the end of this section.

For over two centuries, from the late 4<sup>th</sup> to the early 7<sup>th</sup> century, the heartlands of the Byzantine empire are stable and one of the wealthiest region of the ancient western world. Byzantium is also unique in that its real consumption is in part sustained by a very large openness to trade—the term  $\pi_{nn}^{-1/\theta}$  in equation (23)—and by a large trade deficit financed by excess minting—the term  $(1 - \lambda)w_n[t-1]L_n[t-1] + M_n[t]/w_nL_n[t]$ . By contrast, the northwest European region of Francia and Germania experiences a steep decline, at a time which coincides with the

fall of the western Roman empire.

Starting in the early 7<sup>th</sup> century, the fortunes of those two regions are radically altered. Byzantium undergoes a gradual economic collapse, the timing of which corresponds approximately to the Arab conquests of the lands to its east and south. This collapse is in part driven by a collapse of Byzantium’s access to international trade following the rapid decline of Mediterranean trade (see section 4.2), in part by a decline in trade deficits financed by excess minting, and in part by a fall in measured production capacity. The northwest European Frankish lands of Francia and Germania on the other hand experience a spectacular and accelerating growth in real consumption relative to other regions, becoming one of the wealthiest regions of the ancient western world over the course of the 8<sup>th</sup> century. While our estimates are solely descriptive and we do not claim any causal link, we note that the economic rise of northwest Europe happens to accelerate after Islam has reached half of the Mediterranean, in line with the thesis by Pirenne (1927) that “(...) without Mohammed Charlemagne would have been inconceivable.”

We briefly note that our estimates of economic activity for all 13 regions (see appendix figure B.6) have a detectable correlation with known historical events. For instance, real consumption starts falling in the 4<sup>th</sup> century in the regions at the heart of the western Roman empire, northern Italy and Aquitaine, under pressure from political instability and Germanic incursions. Egypt gradually declines as it loses its central role in the Roman economic system. By contrast, real consumption reaches a peak in al-Sham, greater Syria, under the Umayyad caliphate of Damascus in the early 8<sup>th</sup> century; in al-Andalus under the Umayyad Caliphate of Cordoba in the late 8<sup>th</sup> century; in al-Iraq under the Abbasid caliphate of Baghdad in the late 8<sup>th</sup> century; and in the Arabian peninsula, the birthplace of Islam, in the 8<sup>th</sup> century.

We also note, starting in the 8<sup>th</sup> century, the rapid and spectacular economic rise of Atlantic regions—al-Maghrib, al-Andalus, Aquitaine and Basque country, and Francia and Germania. This evidence suggests that the rise of western Europe may have been initiated more than seven centuries before the European colonial expansion into the Americas, Africa, and Asia.

## 4.5 Sensitivity analysis

We conclude this section with an exploration of the sensitivity of our real consumption estimates. We consider both alternative treatments of our data, and alternative modeling assumptions. In order to more easily compare different series of estimates across alternatives, we solve for steady state real consumption for the AD 460-620 and the AD 700-900 periods, and present regional log changes for each alternative. The results are presented in table 4.

Column 1 presents our baseline estimates. We use the trade costs specification from column 2 in table 3; we average our estimates for bilateral and seller terms ( $d_{ni}^{-\theta}[t]$  and  $\tilde{\beta}_i[t]$ ) and for minting ( $M_i[t]$ ) separately for AD 460-620 and for AD 700-900, and we follow the steps in

Table 4: Real consumption from AD 460-620 to AD 700-900: sensitivity analysis

	Real consumption change: $\Delta \log(X_n/p_n)$					
	(1)	(2)	(3)	(4)	(5)	(6)
al-Andalus	3.54	1.95	3.08	4.31	3.19	0.53
Aquitaine and Basque Country	6.67	4.70	7.32	4.74	6.22	1.27
Francia and Germania	10.13	8.25	11.20	9.68	9.31	1.99
Northern Italy and Balkans	-1.15	-3.37	-1.45	-1.67	-0.99	-0.36
Southern Italy	-2.58	-2.58	-3.94	-0.31	-2.31	-0.48
Byzantine Heartlands	-4.12	-3.05	-4.17	-4.54	-3.80	-1.56
al-Sham (Greater Syria)	-0.30	2.11	-1.59	-5.76	-0.46	-0.28
Northern Syria and Caucasus	0.26	0.53	3.97	-0.48	0.15	-0.04
al-Iraq, al-Jibal, Khuzistan, Kirman	0.42	-0.24	-0.34	1.10	0.32	0.02
Eastern Caliphate	0.66	-0.55	-1.04	0.37	0.53	0.05
Jazirat al-arab and al-Yaman	5.46	-1.77	-0.46	12.53	4.78	1.12
Misr (Egypt)	-3.98	-2.03	-1.22	-3.14	-3.68	-0.05
al-Maghrib	-0.59	1.53	1.74	1.65	-0.30	0.29
<i>Pearson correlation with baseline</i>	0.80	0.84	0.85	1.00	0.93	
[95% CI]	[ 0.71 , 0.88 ]	[ 0.76 , 0.91 ]	[ 0.71 , 0.87 ]	[ 0.94 , 1.00 ]	[ 0.82 , 0.95 ]	
<i>Spearman rank correlation</i>	0.72	0.79	0.82	0.99	0.91	
[95% CI]	[ 0.62 , 0.75 ]	[ 0.68 , 0.87 ]	[ 0.77 , 0.91 ]	[ 0.94 , 0.99 ]	[ 0.84 , 0.96 ]	
Period length	20 years	20 years	10 years	30 years	20 years	20 years
Coin Accounting	Number	Value	Number	Number	Number	Number
Sample	All	Gold/Silver	All	All	All	All
Model	Standard	Standard	Standard	Standard	$\theta = 12$	w. Barter

*Notes:* This table shows alternative estimates of relative changes in real consumption between AD 460-620 and 700-900. Column 1 uses our baseline specification corresponding to column 2 of table 3; we compute regional real consumption in two steady state equilibria from parameters averaged over AD 460-620 and 700-900, and report log changes. Column 2 uses gold and silver coin values instead of counts (in equivalent grams of gold, assuming a constant exchange rate of 12g of silver for 1g of gold). Columns 3 and 4 use our baseline specification but aggregates our data into 10-year or 30-year intervals, adjusting the coin loss rate to the period length (always 1.7% p.a.). Column 5 uses our baseline estimates but sets the trade elasticity to  $\theta = 12$ . Column 6 uses an extension of our baseline model with both monetized and barter transactions inspired by Kiyotaki and Wright (1989)—see appendix C for details. 95% confidence intervals, in square brackets, are computed from re-estimating our model on 100 bootstrapped samples from our coin hoard data.

section 4.1 to compute steady state real consumption relative to aggregate consumption for each region and period. For each region, we compute the log change in relative real consumption from AD 460-620 to AD 700-900. A positive number means that a region is getting larger as a share of the ancient western world.<sup>43</sup> Column 1 confirms the stylized facts discussed in section 4.4, for instance the reversal of fortune between Byzantium versus Francia and Germania, the rise of Islamic al-Andalus, or the decline of Italy and Egypt.

Columns 2, 3, and 4 use different treatments of our coin data. Column 2 uses solely gold and silver coins—about 25% of our dataset—and computes coin values in equivalent grams of gold instead of counts, using known exchange rates and denominations. Columns 3 and 4 aggregate

<sup>43</sup>If the world is shrinking, a positive number means this region is either growing or shrinking at a slower pace than the rest. The values reported in table 4 are similar to log consumption series projected on region and period fixed effects: expressing regional consumption relative to global consumption removes period fixed effects (in logs), and computing (log) differences between periods removes time-invariant region fixed effects.

our coin dataset into shorter 10-year intervals (column 3) or longer 30-year intervals (column 3) than our 20-year intervals baseline. Using newly estimated parameters from the specification of column 2 in table 3 for each dataset, we recover real consumption series from the same model as in column 1. Columns 5 and 6 instead use the same parameters as column 1, but a different model. In column 5, we set the trade elasticity  $\theta$  to 12 instead of 4 as in our baseline. In column 6, we assume a simple model with endogenous monetization of exchanges.<sup>44</sup>

Across all specifications, while the levels of consumption changes vary, they are highly correlated with our baseline, and the qualitative patterns of relative changes are nearly identical. The correlations with our column 1 baseline for both log changes and the ranks of log changes are high, ranging from 72% to 99.95%. We systematically confirm the reversal of fortunes between the heartlands of the Byzantine empire and the Frankish northern European region of Francia and Germania, or the rise of al-Andalus and decline of Italy and Egypt.

Interestingly, our estimates for real consumption are stable despite the fact that the estimated trade cost parameters vary as we modify our dataset across columns 1-4 (see appendix table B.9): the estimated travel time elasticity of trade costs is lower when using value-weighted gold and silver coins, and when aggregating our data into longer time intervals, as expected from the discussion in section 2.2. We also note that even tripling the trade elasticity  $\theta$  from 4 to 12 in column 5 barely affects our estimates for real consumption changes.

Finally, we observe that allowing for an endogenous level of monetization in column 6, where wealthier regions rely proportionately more on monetized exchanges, does affect the *absolute* levels of real consumption changes, but it preserves their *relative* levels. This specification relies on the plausible assumption that as regions develop, more transactions become monetized. While we are not aware of any systematic information on the degree of monetization which would allow us to precisely parameterize our simple model of endogenous monetization, we believe the estimates reported in column 6 are our most credible.

## 5 Ancient mines, climate, and cities

In this section, we confront our estimates with several external data sources. Our minting estimates are strongly correlated with the known exploitation of ancient mineral deposits (section 5.1). Our real consumption estimates are strongly correlated with paleo-climatic shocks (section 5.2) and with urbanization (section 5.3), but not with military conflicts or the Justinianic plague of the 6<sup>th</sup> century (section 5.4). The evidence in this section is not meant to capture causal effects—except for paleo-climate. Instead, it serves both as a validation of our

---

<sup>44</sup>We present in appendix C a simple extension of our model with barter and monetized transactions inspired by Kiyotaki and Wright (1989). We explain how to estimate this extended model from coin data, in practice simply replacing the term  $T_n^{1/\theta} L_n$  in equation (23) by  $(T_n^{1/\theta} L_n)^{1/(1+\theta)}$  to account for endogenous monetization.

Table 5: Active mines and mint output

	Dep. var.: Log Mint Output		
	(1)	(2)	(3)
(Active Mine) <sub>it</sub>	1.266*** (0.37)	1.722*** (0.34)	1.401*** (0.45)
20-year time period FE	No	Yes	Yes
Region FE	No	No	Yes
$R^2$	0.0438	0.318	0.427
Observations	344	344	344

*Notes:* The dependent variable is logged minting,  $\log(M_i[t])$ , estimated in section 3.3. The independent variable is a dummy equal 1 iff region  $i$  has a documented active mine at the start of a 20-year period  $t$ . Data on ancient mines is from: Stöllner and Weisgerber (2004); Merkel et al. (2023); Merkel (2016); Morony (2019); Strabo (1917); Rhoby (2019); Mundell Mango (2009); Sarah (2010). Standard errors in parentheses, clustered at the 20-year time interval level. \*  $p < 0.10$ , \*\*  $p < 0.05$ , \*\*\*  $p < 0.01$ .

estimates and as an informal test of the determinants of ancient economic activity.

## 5.1 Ancient mines and minting output

We collect information on 37 known ancient mines, their geographic location, approximate dates of operation, and the metal being mined—gold, silver, and copper—from the scholarly literature in history and archaeology. We regress (logged) minting output on a dummy variable equal to one if and only if region  $i$  has a documented active mine at the start of a 20-year period  $t$ .

The results are presented in table 5. It shows a large and statistically significant association between ancient mining activity and our minting estimates, robust to controlling for region and period fixed effects. The presence of an active mine is associated with a four-fold increase in minting output ( $e^{1.4} \approx 4$  in column 3).

This association is not causal, as the decision to exploit a mine is endogenous and may be driven by the desire of local rulers to increase minting output. However, to the extent that the presence of accessible mineral deposits is exogenous to local monetary policy, it suggests that a lower cost of minting leads to a higher minting output. This is consistent with our model, where an increase in minting in one region, everything else equal, increases real consumption. Minting in one region generates inflation, but since inflation is partly exported, the private (regional) gain from minting is always strictly positive. The equilibrium of a minting game—which we do not explicitly model—is such that the gain from minting equals its cost; with an increasing and convex cost, an easier access to mineral deposits induces more minting.

Table 6: Climate shocks and real consumption

	Dep. var.: Log Real Consumption			
	(1)	(2)	(3)	(4)
# Years with medium drought	-0.209** (0.091)			
# Pairs of consecutive years with medium drought		-0.375** (0.16)		
# Years with severe drought			-0.530** (0.24)	
# Pairs of consecutive years with severe drought				-1.433*** (0.46)
20-year time period FE	Yes	Yes	Yes	Yes
Region FE	Yes	Yes	Yes	Yes
$R^2$	0.290	0.292	0.294	0.296
Observations	399	399	399	399

*Notes:* The dependent variable is logged real consumption,  $\log(X_i[t]/p_i[t])$ , estimated in section 4.1. The independent variables are measures of drought. For each region and each year, we average the values of the Palmer Drought Severity Index (PDSI) over a four-by-four degree rectangle centered on the location of the largest regional mint (a single for each region). The PDSI is a normalized index of wet/dry conditions, taking values between -10 and +10, with negative values corresponding to dry conditions. Our drought measures are: in column 1, the number of years of moderate drought (index below -2) for region  $i$  and 20-year period  $t$ ; in column 2 the number of pairs of consecutive years of moderate drought; in column 3 the number of years of severe drought (index below -3); in column 4 the number of pairs of consecutive years of severe drought. Standard errors in parentheses, clustered at the 20-year time interval level. \*  $p < 0.10$ , \*\*  $p < 0.05$ , \*\*\*  $p < 0.01$ .

## 5.2 Paleo-climate and real consumption

We show evidence that real consumption is strongly affected by adverse climate shocks. We collect granular data on summer—June to August—drought severity indices reconstructed from tree-rings chronologies from the Great Eurasian Drought Atlas (Burnette, 2021).<sup>45</sup> We define four variables: the number of years of moderate or severe drought for region  $n$  and 20-year period  $t$ , and the number of pairs of consecutive years with moderate or severe droughts. Importantly, those measures of adverse climate shocks vary both over time and space, allowing us to isolate their impact on our real consumption series controlling for region and period fixed effects.

Table 6 shows the results of regressions of (logged) real consumption on droughts. We find a large and significant association between droughts and real consumption. To the extent that severe drought events are plausibly exogenous, we can interpret those coefficients as causal. Column 3 suggests that one year of severe drought reduces real consumption by 41% ( $1 - e^{-0.53} \approx 0.41$ ). Using the estimates from a model with endogenous monetization, one year of severe drought causes a 10% reduction in real consumption (treatment  $\approx 1 - e^{-0.53/5} \approx 0.10$ ).

<sup>45</sup>See <http://drought.memphis.edu/GEDA>.

Those results show that weather is an important determinants of aggregate productivity, production, and ultimately real consumption. Since our estimates for real consumption are derived from coin and trade flow data, those results also suggest either that agricultural products—directly affected by droughts—were traded, and/or that non-farm industrial productivity was also negatively affected by droughts. Our results extend by more than one millennium the finding from Dell et al. (2012) that adverse climate shocks negatively affect both agricultural and industrial productivity among poor countries in the late 20<sup>th</sup> century.

### 5.3 Urbanization in ancient Europe

We confront our estimates for changes in real consumption to realized changes in urbanization in Europe. While our model does not feature any explicit notion of urbanization, we conjecture that a higher real consumption allows to sustain a larger urban population. This exercise is illustrative, meant to verify that our estimates for real consumption derived solely from information on coin flows are consistent with independent evidence on economic growth.

Figure 11 shows our estimates for changes in real consumption (top panel, 11a) together with urban population growth north of the Mediterranean over AD 700-900, aggregated from city size data (bottom panel, 11b).<sup>46</sup> Comparing both maps suggests that our estimates for real consumption are qualitatively in line with independent evidence on urbanization. Our estimated drop in real consumption in the heartlands of the Byzantine empire, and substantial increase in western and northern Europe are consistent with urban population declines in Asia Minor and Cyprus, low urban growth in Greece, Thracia, and Dacia, medium urban growth in the Balkans, and Italy, and strong urban growth in Iberia, Aquitaine, and Francia/Germania.

### 5.4 Additional results

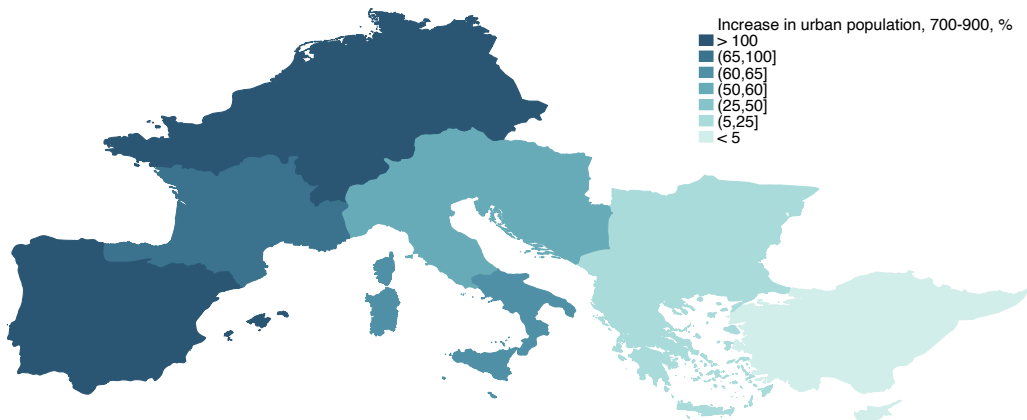
**Real consumption is not correlated with military conflicts.** We find no systematic association between instances of military conflict and our estimates for real consumption (see appendix table B.10). We collect data on 297 major battles and sieges for AD 300-950 as covered by Jaques (2006). Real consumption in region  $n$  and period  $t$  is correlated neither with the number of battles in the region-period, nor with having at least one recorded battle, even controlling for region and period fixed effects. This non-result may reflect countervailing forces, where on the one hand wealthier regions are better able to mount military campaigns, while on the other violence disrupts production and trade. It may also be due to the selective and biased recording of violent confrontations in the literature.

---

<sup>46</sup>While ancient city size estimates are naturally imprecise, panel 11b is in line with the consensus view of increased urbanization in northwestern Europe, and stagnation or decline in the eastern Mediterranean.



(a) Relative real consumption changes: pre- to post-conquests



(b) Urban Population Growth in European Regions, AD 700-900

Figure 11: Real consumption and urbanization

*Notes:* Panel (a) shows the logged relative real consumption change from the pre-conquest period to the post-conquest period, column 1 of Table 4. Panel (b) shows the percentage growth of the urban population post-conquest, between AD 700 and AD 900. City size data from Buringh (2021), except for Byzantine Anatolia, which is not covered. We construct measures of urban decline in Anatolia (calculations available upon request) based on the shrinking surface area of cities described in Brandes (1989). The resulting figure of a 10% decline in urban population over this time interval seems to be a conservative estimate in light of the fact that many coastal cities saw large amounts of destruction and depopulation as a consequence of Arab raids.

**Real consumption is not correlated with the Justinianic plague.** We do not find any systematic association between the local incidence of the Justinianic plague (Stathakopoulos, 2004) and real consumption (see appendix table B.11). This non-result may be due to the fact that the Justinianic plague was truly a global event and had a uniform impact across regions, which our estimates are unable to detect since we can only recover relative consumption each period. The documented differences in lethality across regions may only reflect differences in the availability or quality of literary sources. Or it may be consistent with the hypothesis that the Justinianic plague was after all an ‘inconsequential pandemic’ (Mordechai et al., 2019).

## 6 Conclusion

In this paper we study the patterns of change in economic geography around the Mediterranean during Late Antiquity through the lens of coin flows. We propose a dynamic model of trade where coins are used for transactions, so that they gradually diffuse over space and time in proportion to trade flows. We estimate this model using data on the composition of coin finds. We then use these parameters to recover granular time series for trade and relative real consumption from the fourth to the tenth century. Our estimates for changes in real consumption are consistent with measures of relative urbanization across European regions. They also suggest that climate shocks were key drivers of real consumption, while military conflicts were not.

Our evidence from coin finds indicate that north-south Mediterranean trade flows declined following the Arab conquests. This can be explained by a newly formed trade barrier between the emerging Arab Caliphate and the Christian West. These changes in trade patterns are in line with the claims of a trade disruption in the Mediterranean by Pirenne (1939). Our results show, however, that intra-caliphal trade in the Mediterranean remained vibrant. Moreover, Pirenne believed that trade disruptions also led to a vast reduction in economic activity and exchange within the Frankish lands. We find instead that Frankish regions experienced a spectacular economic rise over that period, contrasting the relative economic decline of the Byzantine empire. Our estimates also reveal that the start of the relative decline of the Mediterranean predates the birth of Islam, contradicting mono-causal theories of change during Late Antiquity that attribute the entirety of the shift in economic activity to the Arab conquests.

## References

- AHLFELDT, G. M., S. J. REDDING, D. M. STURM, AND N. WOLF (2015): “The Economics of Density: Evidence From the Berlin Wall,” *Econometrica*, 83, 2127–2189.
- AL-MUQADDASI (985): *Ahsan al-taqāsim fi ma’arfat al-aqalīm* (*The Best Divisions for Knowledge of the Regions*), Garnet Publishing (transl. B.A. Collins, 1994).
- AL ’USH, A.-F. (1972): *The silver hoard of Damascus: Sasanian, Arab-Sasanian, Khuwarizmian, and Umayyad kept in the National Museum of Damascus*, Damascus: Direction General of Antiquities and Museums.
- ANDERSON, J. E. AND E. VAN WINCOOP (2003): “Gravity with Gravitas: A Solution to the Border Puzzle,” *American Economic Review*, 93, 170–192.
- ASHTOR, E. (1970): “Quelques observations d’un orientaliste sur la thèse de Pirenne,” *Journal of the Economic and Social History of the Orient*, 13, 166–194.
- BANAJI, J. (2016): *Exploring the Economy of Late Antiquity: Selected Essays*, Cambridge University Press.

- BARJAMOVIC, G., T. CHANEY, K. COŞAR, AND A. HORTAÇSU (2019): “Trade, merchants, and the lost cities of the bronze age,” *The Quarterly Journal of Economics*, 134, 1455–1503.
- BATES, M. (1991): “Coins and money in the Arabic Papyri,” *Documents de l’Islam Medieval*, 43–643.
- BESSARD, F. (2020): “Money Supply and Currency,” in *Caliphs and Merchants: Cities and Economies of Power in the Near East (700-950)*, Oxford University Press.
- BOLIN, S. (1953): “Mohammed, Charlemagne and Ruric,” *Scandinavian Economic History Review*, 1, 5–39.
- BRANDES, W. (1989): *Die Städte Kleinasiens im 7. und 8. Jahrhundert*, De Gruyter.
- BURINGH, E. (2021): “The population of European cities from 700 to 2000: Social and economic history,” *Research Data Journal for the Humanities and Social Sciences*, 6, 1–18.
- BURNETTE, D. J. (2021): “The Tree-Ring Drought Atlas Portal: gridded drought reconstructions for the past 500-2000 years,” *Bulletin of the American Meteorological Society*, 102, 953–956.
- CHANEY, T. (2018): “The Gravity Equation in International Trade: An Explanation,” *Journal of Political Economy*, 126, 150–177.
- CORNU, G. (1983): *Atlas du monde Arabo-Islamique à l’époque classique: IX.-X. siècles*, Brill.
- COUPLAND, S. (2014): “The use of coin in the Carolingian Empire in the ninth century,” *Early Medieval Monetary History: Studies in Memory of Mark Blackburn*, Farnham, 257–93.
- DEKLE, R., J. EATON, AND S. KORTUM (2007): “Unbalanced Trade,” *American Economic Review, Papers and Proceedings*, 97, 351–355.
- DELL, M., B. F. JONES, AND B. A. OLKEN (2012): “Temperature Shocks and Economic Growth: Evidence from the Last Half Century,” *American Economic Journal: Macroeconomics*, 4, 66–95.
- DONALDSON, D. (2018): “Railroads of the Raj: Estimating the impact of transportation infrastructure,” *American Economic Review*, 108, 899–934.
- DONALDSON, D. AND R. HORNBECK (2016): “Railroads and American economic growth: A “market access” approach,” *The Quarterly Journal of Economics*, 131, 799–858.
- EATON, J. AND S. KORTUM (2002): “Technology, Geography, and Trade,” *Econometrica*, 70, 1741–1779.
- FINDLAY, R. AND K. H. O’ROURKE (2009): *Power and Plenty: Trade, War, and the World Economy in the Second Millennium*, Princeton University Press.
- FLAME (2023a): “Biases in FLAME’s data,” <https://coinage.princeton.edu/biases-in-flames-data/>.

- (2023b): “Framing the Late Antique and early Medieval Economy,” <https://coinage.princeton.edu/>, accessed: 2023-07-01.
- FLÜCKIGER, M., E. HORNUNG, M. LARCH, M. LUDWIG, AND A. MEES (2022): “Roman transport network connectivity and economic integration,” *The Review of Economic Studies*, 89, 774–810.
- FOGEL, R. W. (1964): *Railroads and American economic growth*, Johns Hopkins Press Baltimore.
- Foss, C. (1975): “The Persians in Asia Minor and the end of Antiquity,” *The English Historical Review*, 90, 721–747.
- GANDAL, N. AND N. SUSSMAN (1997): “Asymmetric information and commodity money: tickling the tolerance in medieval France,” *Journal of Money, Credit, and Banking*, 440–457.
- GIBBON, E. (1789): *The history of the decline and fall of the Roman Empire*, vol. I-VI, London: Strahan & Cadell.
- GRIERSON, P. (1959): “Commerce in the Dark Ages: a critique of the evidence,” *Transactions of the Royal Historical Society*, 9, 123–140.
- (1973): *Catalogue of the Byzantine Coins in the Dumbarton Oaks Collection and in the Whittemore Collection, 3: Leo III to Nicephorus III, 717-1081*, Dumbarton Oaks.
- HODGES, R. AND D. WHITEHOUSE (1983): *Mohammed, Charlemagne & the origins of Europe: archaeology and the Pirenne thesis*, Cornell University Press.
- HOPKINS, K. (1980): “Taxes and trade in the Roman Empire (200 BC–AD 400),” *The Journal of Roman Studies*, 70, 101–125.
- HORNBECK, R. AND M. ROTEMBERG (forthcoming): “Growth Off the Rails: Aggregate Productivity Growth in Distorted Economies,” *Journal of Political Economy*.
- IZDEBSKI, A., G. KOLOCH, T. SŁOCZYŃSKI, AND M. TYCNER (2016): “On the use of palynological data in economic history: new methods and an application to agricultural output in Central Europe, 0–2000 AD,” *Explorations in Economic History*, 59, 17–39.
- JAQUES, T. (2006): *Dictionary of Battles and Sieges: A Guide to 8,500 Battles from Antiquity through the Twenty-first Century*, Greenwood.
- JUHÁSZ, R., S. SAKABE, AND D. WEINSTEIN (2024): “Codification, Technology Absorption, and the Globalization of the Industrial Revolution,” Working Paper 32667, National Bureau of Economic Research.
- KAZHDAN, A. (1954): “Vizantijskie goroda v VII-IX vv,” *Sovetskaja arkheologija*, 21, 164–188.
- KERSHAW, J., S. W. MERKEL, P. D’IMPORZANO, AND R. NAISMITH (2024): “Byzantine plate and Frankish mines: the provenance of silver in north-west European coinage during the Long Eighth Century (c. 660–820),” *Antiquity*, 98, 502–517.

- KIYOTAKI, N. AND R. WRIGHT (1989): “On Money as a Medium of Exchange,” *Journal of Political Economy*, 97, 927–954.
- LEONTIEF, W. W. (1941): *The Structure of the American Economy, 1919–1929*, Cambridge, MA: Harvard University Press.
- (1944): “Output, Employment, Consumption, and Investment,” *The Quarterly Journal of Economics*, 58, 290–314.
- LIU, E. AND A. TSYVINSKI (2024): “A Dynamic Model of Input–Output Networks,” *The Review of Economic Studies*.
- LOPEZ, R. S. (1943): “Mohammed and Charlemagne: a revision,” *Speculum*, 18, 14–38.
- MANAS, A. AND F. R. VELDE (2021): “Coin wear: a power law for small shocks,” *Physica A: Statistical Mechanics and its Applications*, 574, 125948.
- MAYHEW, N. (2019): “Money and the Economy,” in *Money and Coinage in the Middle Ages*, ed. by R. Naismith, Brill, 203–230.
- MCCONNELL, J. R., A. I. WILSON, A. STOHL, M. M. ARIENZO, N. J. CHELLMAN, S. ECKHARDT, E. M. THOMPSON, A. M. POLLARD, AND J. P. STEFFENSEN (2018): “Lead pollution recorded in Greenland ice indicates European emissions tracked plagues, wars, and imperial expansion during antiquity,” *Proceedings of the National Academy of Sciences*, 115, 5726–5731.
- MCCORMICK, M. (2001): *Origins of the European economy: communications and commerce AD 300-900*, Cambridge University Press.
- MERKEL, S. (2016): “Analysis of Slag and Ore from the Tashkent and Samarqand Areas,” in *Silver and the silver economy at Hedeby*.
- MERKEL, S. W., J. ORAVISJÄRVI, AND J. KERSHAW (2023): “Sources of early Islamic silver: lead isotope analysis of dirhams,” *Antiquity*, 97, 1564–1580.
- MICHAELS, G. AND F. RAUCH (2018): “Resetting the Urban Network: 117–2012,” *The Economic Journal*, 128, 378–412.
- MONTESQUIEU, C. (1734): *Considérations sur les causes de la grandeur des Romains et de leur décadence*.
- MORDECHAI, L., M. EISENBERG, T. P. NEWFIELD, A. IZDEBSKI, J. E. KAY, AND H. POINAR (2019): “The Justinianic Plague: An inconsequential pandemic?” *Proceedings of the National Academy of Sciences*, 116, 25546–25554.
- MORONY, M. (2019): “The early Islamic mining boom,” *Journal of the Economic and Social History of the Orient*, 62, 166–221.
- MORRISSON, C. (2002): “Byzantine money: its production and circulation,” *The Economic History of Byzantium*, 3, 909–966.

- MUNDELL MANGO, M. (2009): *Byzantine Trade: Local, Regional, Interregional and International*, Society for the Promotion of Byzantine Studies. Ashgate Publishing Great Britain.
- NAGY, D. K. (2023): “Hinterlands, City Formation and Growth: Evidence from the U.S. Westward Expansion,” *The Review of Economic Studies*, 90, 3238–3281.
- NAISMITH, R. (2014): “The Social Significance of Monetization in the Early Middle Ages\*,” *Past & Present*, 223, 3–39.
- NOONAN, T. S. (1980): “When and how dirhams first reached Russia: a numismatic critique of the Pirenne theory,” *Cahiers du monde russe et soviétique*, 401–469.
- PARVÉRIE, M. (2014): “Corpus des monnaies arabo-musulmanes des VIII et IX siècles découvertes dans le Sud de la France,” *Revista Numismática OMNI*, 79–100.
- PASCALI, L. (2017): “The wind of change: Maritime technology, trade, and economic development,” *American Economic Review*, 107, 2821–2854.
- PATTERSON, C. C. (1972): “Silver stocks and losses in ancient and medieval times,” *The Economic History Review*, 25, 205–235.
- PENNAS, V. (1996): “Life in Byzantine Cities of Peloponnesos: The Numismatic Evidence (8th-12th Century),” in *Mneme Martin Jessop Price*, Hellenic Numismatic Society.
- PEREGRINE, P. N. (2020): “Climate and social change at the start of the Late Antique Little Ice Age,” *The Holocene*, 30, 1643–1648.
- PERSSON, K. G. AND P. SHARP (2015): *An economic history of Europe*, Cambridge University Press.
- PIRENNE, H. (1927): *Medieval Cities: Their Origins and the Revival of Trade*, Princeton University Press.
- (1939): *Mohammed and Charlemagne*, London: G. Allen & Unwin.
- POLANYI, K. (1977): *The Livelihood of Man*, Studies in Social Discontinuity, Academic Press.
- REDDING, S. J. AND D. M. STURM (2008): “The Costs of Remoteness: Evidence from German Division and Reunification,” *American Economic Review*, 98, 1766–97.
- RHOBY, A. (2019): *Gold, Goldsmiths and Goldsmithing in Byzantium*, 9–19.
- ROMANOV, M. AND M. SEYDI (2022): “al-Thurayyā,” <https://althurayya.github.io/> [Accessed: (1 July 2023)].
- SARAH, G. (2010): *L'avènement de l'argent. Activité minière, frappe monétaire et commerce dans les mondes franc et islamiques du haut Moyen Age*, vol. 25 of *Byzantina Sorbonensis*, Paris: Éditions de la Sorbonne.
- SARAH, G., M. BOMPAIRE, M. MCCORMICK, A. ROVELLI, AND C. GUERROT (2008): “Analyses élémentaires de monnaies de Charlemagne et Louis le Pieux du Cabinet des Médailles: l’Italie carolingienne et Venise,” *Revue numismatique*, 164, 355–406.

- SCHEIDEL, W. (2015): “ORBIS: The Stanford geospatial network model of the Roman world,” *Tech. rep.*
- (2017): *The Great Leveler: Violence and the History of Inequality from the Stone Age to the Twenty-First Century*, Princeton, NJ: Princeton University Press.
- (2020): “Roman wealth and wealth inequality in comparative perspective,” *Journal of Roman Archaeology*, 33, 341–353.
- SHATZMILLER, M. (2018): “At the origins of Middle Eastern trade, 700-1000 AD: An application of the gravity theory of trade,” in *Economic integration and social change in the Islamic world system*, ed. by H. Kennedy and F. Bessard, 800–1000.
- SIMONOVSKA, I. AND M. E. WAUGH (2014): “The elasticity of trade: Estimates and evidence,” *Journal of International Economics*, 92, 34–50.
- STATHAKOPOULOS, D. C. (2004): *Famine and Pestilence in the Late Roman and Early Byzantine Empire: A Systematic Survey of Subsistence Crises and Epidemics*, Routledge.
- STÖLLNER, T. AND G. WEISGERBER (2004): “Die Blei-/Silbergruben von Nakhlak und ihre Bedeutung im Altertum: Zum Neufund eines Förderkörbchens im Alten Mann,” *Der Anschnitt*, 56, 76–97.
- STRABO (1917): *Geography*, Loeb Classical Library, Cambridge, MA: Harvard University Press.
- VOLTAIRE (1756): *Essai sur les mœurs et l'esprit des nations*, Geneva: Frères Cramer.
- WARD-PERKINS, B. (2006): *The fall of Rome: and the end of civilization*, Oxford University Press.
- WICKHAM, C. (2006): *Framing the early middle ages: Europe and the Mediterranean, 400-800*, Oxford University Press.
- ZAVAGNO, L. (2022): “A Lost World That Never Died,” *Dumbarton Oaks Papers*, 76, 281–310.

# Supplemental Appendix for

# Trade and the End of Antiquity

by Johannes Boehm and Thomas Chaney

<b>A Data description</b>	<b>1</b>
A.1 Area of interest . . . . .	1
A.2 Coin Data . . . . .	1
A.3 Regions . . . . .	1
A.4 Constructing the geospatial model . . . . .	2
<b>B Additional empirical results</b>	<b>3</b>
B.1 Comparison to circulation hoards in Banaji (2016). . . . .	3
B.2 Comparison to the flows of West Roman Terra Sigillata. . . . .	3
B.3 Within-empire coin redistribution . . . . .	4
B.4 Arab conquests and the Mediterranean. . . . .	4
B.5 Coin flows and coin ages . . . . .	5
B.6 Estimation of the coin loss rate $\lambda$ . . . . .	6
B.7 Validating the geospatial model . . . . .	6
B.8 Alternative accounting method and period lengths . . . . .	6
B.9 Tables and figures . . . . .	8
<b>C Additional theoretical derivations</b>	<b>20</b>
<b>D Coin hoard data (NOT FOR PUBLICATION)</b>	<b>23</b>
D.1 Hand-collected data . . . . .	23
D.2 FLAME . . . . .	26
D.3 Locating mints . . . . .	27
D.4 Political entities and the geography of hoards and mints . . . . .	27
D.5 Tables and references . . . . .	31
<b>E Identification (NOT FOR PUBLICATION)</b>	<b>66</b>
E.1 Asymptotic identification proof . . . . .	66
E.2 Numerical identification with sparse data and finite sample . . . . .	74
E.3 Numerical identification with misspecified model . . . . .	77

# A Data description

## A.1 Area of interest

We define the boundaries of our region of interest in Europe by taking the union of the AD 200 Roman provincial boundaries with the 814 boundaries of the Frankish empire and the area of the West Slavs. The resulting border is roughly the modern-day German-Polish border, plus Bohemia, but follows otherwise roughly the AD 200 Roman Empire boundary. We obtain shapefiles from the *Digital Atlas of the Roman and Medieval Civilizations* (DARMC) hosted at Harvard University (McCormick et al., 2007). In the Arab world, the border is delineated roughly by the convex hull of the spatial extent of administrative district boundaries of the extent of the Umayyad caliphate, as given in al-Turayyā (Romanov and Seydi, 2022).

## A.2 Coin Data

See Appendix D for a detailed description of the construction of the coin data. Tables B.1 and B.2 shows summary statistics for coins and hoards, respectively.

For the structural analysis, we use the same sample of coins as for the reduced-form analysis in section 1, with the following exceptions: (i) we exclude coins where the mint date interval exceeds 150 years; (ii) we exclude non-hoard coin finds from excavations (because the  $tpq$  for these finds is meaningless).

## A.3 Regions

We define the regions of the ancient world based on political delineations from the 814 political boundaries map of the *Digital Atlas of the Roman and Medieval Civilizations*, and the district boundaries of the caliphate in al-Turayyā. The latter originally contains just district affiliation for each city; we construct regions by assigning space to the district affiliation of its nearest city (Voronoi tessellation).

**al-Andalus.** Iberian Peninsula, maximum extent of the Umayyad Caliphate 661-750 (DARMC), minus the areas of the Carolingian Kingdom of Aquitaine under Louis in ca. 814 (DARMC).

**Aquitaine and Basque Country.** Territory of the Iberian Peninsula that is not part of the above definition of *al-Andalus* (i.e. Basque lands), plus the area of the Carolingian Kingdom of Aquitaine under Louis in ca. 814 (DARMC).

**Francia and Germania.** Kingdom of Charlemagne, ca. 814, plus the area of East Frankish influence (West Slavs), and Brittany (all from DARMC's 814 layer).

**Northern Italy and Balkans.** Kingdom of Pippin (including Corsica), Papal States, Avar and Croat area, as well as modern-day Bosnia and the Byzantine areas on the Balkans and in modern-day Italy (all from DARMC's 814 layer).

**Southern Italy.** All regions of modern-day Italy that are not part of *Northern Italy and the Balkans* above, including Sardinia, the Duchy of Benevento, and Sicily.

**Byzantine Heartlands.** Byzantine territory in modern-day Greece, Turkey (according to DARMC's 814 map), and Cyprus.

**al-Sham (Greater Syria).** Area of al-Sham (Greater Syria), in al-Turayyā.

**Northern Syria and Caucasus.** Areas of Aqur (al-Jazirat), al-Rihab (Caucasus), al-Khazar from al-Turayyā.

**al-Iraq, al-Jibal, Khuzistan, Kirman.** Areas from al-Iraq, al-Jibal, Khuzistan, Kirman, and Fars, from al-Turayyā.

**Eastern Caliphate.** Areas of al-Mafazat, al-Daylam, Hurasan, Sijistan, al-Sind, and Ma-wara-l-nahr (Transoxiana), all from al-Turayyā.

**Jazirat al-Arab and al-Yaman.** Areas of Jazirat al-Arab, al-Yaman, and most of the Badiyyat al-Arab, all from al-Turayyā.

**Misr (Egypt).** Area of Misr, and the area of Barqat (Lybia) east of al-Uqaylah, both from al-Turayyā.

**al-Maghrib.** Areas of al-Maghrib and the area of Barqat (Lybia) west of al-Uqaylah, both from al-Turayyā.

## A.4 Constructing the geospatial model

We build our geospatial model by combining two geospatial models constructed by historians to model travel distances and routes. The first one, ORBIS ([Scheidel, 2015](#)), is a geospatial model of the Roman world and spans roughly the maximum extent of Roman conquests. The

second, al-Turayyā (Romanov and Seydi, 2022) is a digitization of Cornu (1983)'s atlas of the Islamic world in the 9th and 10th century. Both geospatial models take the form of undirected graphs; in the case of ORBIS this is augmented by measures of travel costs on each edge. ORBIS also contains sea routes; for the Arab world we augment al-Turayyā with a number of known sea routes. For al-Turayyā we also construct bilateral travel distances by applying the methodology from ORBIS, taking into account the topography of the terrain, and wind directions and speeds for sea routes. Details are available from the authors. We validate these choices by comparing the shortest paths that the model generates to known routes in the Arab world, and by comparing travel times to the ones reported by 10th century Arab geographer Al-Muqaddasī (985) in section B.7 below.

## B Additional empirical results

### B.1 Comparison to circulation hoards in Banaji (2016).

To support the argument that the coins in our hoards are broadly reflective of coin circulation during Late Antiquity, we compare the age distribution of the hoards in our data with a sample of Byzantine circulation hoards described by Banaji (2016), Chapter 6. These are twelve hoards containing between 12 and 751 Byzantine solidi. Figure B.1 shows the average fraction of coins in each 10-year age bin in these hoards, and the distribution of coin ages in Figure 3b, showing a similar age profile. Banaji (2016) also reports that 44% of the coins in these hoards are older than 33 years at time of deposit, compared to 38% in our data (for hoards with more than ten coins).

### B.2 Comparison to the flows of West Roman Terra Sigillata.

Figure B.2 compares the relationship between distance and coin flows in our data with the relationship between distance and flows of Terra Sigillata in the data of Flückiger et al. (2022).<sup>1</sup> The distance elasticity is similar but slightly lower for coins, which is potentially due to the fact that naive gravity regressions using coin stocks will exhibit a distance elasticity that is biased

---

<sup>1</sup>Comparing the pairwise flows in the two datasets directly does not make sense since Terra Sigillata are produced in different locations than mints (see Figure 4 in their paper).

towards zero (see Section 2).

### B.3 Within-empire coin redistribution

One potential explanation for the high coin flows within relative to between empires (political border effect) is that coins could be redistributed across mints before entering circulation, so that the distance from mint to hoard would be less relevant for within-empire flows. Table B.4 shows that distance has the same impact of coin flows with and without hoard cell  $\times$  empire (that mints the coin) fixed effects in equation (1), suggesting that redistribution within empires was not quantitatively important.

### B.4 Arab conquests and the Mediterranean.

Figure B.3 shows the number of coins crossing the Mediterranean, and their composition. The Arab conquests (dashed vertical lines) correspond to a decline of north-south flows and an increase in east-west flows, with Islamic coins replacing Roman/Byzantine coins. To further decompose these changes, we estimate by PPML

$$\text{count}_{mhpt} = \exp \left( a_{mh} + a_{mp} + b_1 \text{Mediterranean}_{mh} \times \text{After}_t + b_2 \text{Mediterranean}_{mh} \times \text{After}_t \times \text{Islamic}_p + u_{mhpt} \right). \quad (\text{B.1})$$

We aggregate all hoard ( $h$ ) and mint ( $m$ ) locations to  $1^\circ \times 1^\circ$  cells, separately for each time period ( $t$ ), and note for each coin which one of fourteen aggregate political blocks  $p$  had issued it.<sup>2</sup> Count <sub>$mhpt$</sub>  is the number of coins issued in cell  $m$  under empire/dynasty  $p$  and found in a cell  $h$ , both within time period  $t$ . Mediterranean <sub>$mh$</sub>  is a dummy that is one if the geodetic line between cells  $m$  and  $h$  intersects the Mediterranean; After <sub>$t$</sub>  is a dummy equal to one if  $t$  is between 713 and 900, and zero if between 400 and 630; Islamic <sub>$p$</sub>  is one if the coin is of Islamic issue (any dynasty);  $a_{mh}$  and  $a_{mp}$  denote mint cell  $\times$  hoard cell and mint-cell  $\times$  dynasty/empire fixed effects, respectively. The objective is to investigate whether the Mediterranean acts differentially

---

<sup>2</sup>These political blocks are: Eastern Roman Empire, Western Roman Empire, Roman Empire (pre-division), Sasanians, Umayyads, Spanish Umayyads, Abbasids, Fatimids, Samanids, Visigoths, Ostrogoths, Vandals, Merovingians, and Carolingians. See Appendix Figure D.1 for a breakdown of these and more aggregate political entities.

as a barrier to coin flows after the Arab conquests, and if so, for coins of which issue. Table B.5 presents the results. We drop all mint cell  $\times$  empire/dynasty combinations that did not produce coins. Column (1) shows a negative coefficient on the interaction of the Mediterranean and post-conquest dummies, so that after the Arab conquests coin flows declined in cell pairs across the sea. Column (2) shows a positive coefficient on the triple interaction: Islamic coins were facing disproportionately lower barriers on sea routes in the post-conquest world, conditional on origin and destination characteristics. Column (3) contrasts this with Roman/Byzantine coins, which experience disproportionately higher barriers. Column (4) shows similar estimates with hoard cell  $\times$  time and mint cell  $\times$  time fixed effects, neutralizing potential location-time-specific confounders. All specifications point to the same facts highlighted by Figure 4: there are fewer coins flowing across the Mediterranean in the 8th and 9th century than before; the drop is particularly strong for Roman coins, and the emergence of flows of Islamic coins partly make up for this drop.

## B.5 Coin flows and coin ages

Figure B.4 uses our data to empirically explore the hypothesis that gravity regressions with flows of durables over longer horizons bias the distance elasticity towards zero. It shows a coefficient plot of the following regression:

$$\text{count}_{mth\tau} = \exp \left\{ \sum_{\tau' \in T} \beta_{\tau'} \log \text{distance}_{mh} \times 1(t - \tau = \tau') + \alpha_{mt} + \alpha_{h\tau} + \varepsilon_{mth\tau} \right\} \quad (\text{B.2})$$

where  $T = \{0, 20, 40, 60, 80, 100\}$  and mint and hoard  $tpq$  dates are rounded to 20-year intervals. Coins with longer timespans between mint and hoard  $tpq$  dates are omitted. We estimate the coefficients using PPML.

The results confirm that the distance elasticity for coins that have travelled for longer is lower (i.e. closer to zero) than for coins that have travelled for shorter periods. Section 2.2 and Figure 5 provide the intuition for this result.

## B.6 Estimation of the coin loss rate $\lambda$ .

To estimate  $\lambda$ , we divide coins by their age of deposit (using the  $tpq$  as the date of deposit) into  $n$ -year bins (for  $n = 10$  and  $n = 20$ ). We calculate the fraction  $f^{(n)}(k)$  of coins in bin  $[k, k + n]$ , and estimate the parameter of exponential decay from

$$\log f^{(n)}(k) = \tilde{\lambda}^{(n)} \frac{k}{n} + \varepsilon_k.$$

Table B.6 shows the OLS estimation results using 10-year and 20-year bins.  $\lambda$  can be recovered from  $\lambda = 1 - \exp(\tilde{\lambda})$ , yielding, respectively,  $\hat{\lambda}_{10} = 0.15$  and  $\hat{\lambda}_{20} = 0.3$ .

## B.7 Validating the geospatial model

We compare the implied travel times from our geospatial model (section A.4) to those reported by the 10th-century Arab geographer al-Maqdīsī in his work *The Best Divisions for the Knowledge of the Regions* (Al-Muqaddasī, 985).<sup>3</sup> Figure B.5 shows the comparison. Our model generates travel times that are slightly larger for shorter distances, and on average similar for longer routes.

## B.8 Alternative accounting method and period lengths

Table B.9 shows estimates of the trade cost function parameters for alternative accounting methods and time aggregations. Those robustness checks correspond to changes in data processing. In column 1, we reproduce our baseline estimates, using simple coin counts and 20-year time intervals. In column 2, we use 20-year time intervals, and use only gold and silver coins aggregated according to their relative values (12g of silver for 1g of gold). In column 3, we use counts of coins and 10-year time intervals. In column 4, we use counts of coins and 30-year time intervals.

---

<sup>3</sup> Al-Maqdīsī reports cities and (unsystematically) distances (in travel stages, post stages, and *farsakhs*) or travel times (in days, or nights in the desert) between cities in different parts of the Islamic lands. Historians note that it is unlikely that al-Maqdīsī did indeed travel to all these regions, and some distances and travel times are unrealistic. We exclude the most egregious outliers. See the notes of Figure B.5 for details.

## References

- AL-MUQADDASĪ (985): *Ahsan al-taqāṣīm fi ma³arfat al-aqalīm* (*The Best Divisions for Knowledge of the Regions*), Garnet Publishing (transl. B.A. Collins, 1994).
- BANAJI, J. (2016): *Exploring the Economy of Late Antiquity: Selected Essays*, Cambridge University Press.
- CORNU, G. (1983): *Atlas du monde Arabo-Islamique à l'époque classique: IX.-X. siècles*, Brill.
- FLÜCKIGER, M., E. HORNUNG, M. LARCH, M. LUDWIG, AND A. MEES (2022): “Roman transport network connectivity and economic integration,” *The Review of Economic Studies*, 89, 774–810.
- MCCORMICK, M., G. HUANG, AND K. GIBSON (2007): *Digital atlas of Roman and medieval civilizations*, Harvard University.
- ROMANOV, M. AND M. SEYDI (2022): “al-Thurayyā,” <https://althurayya.github.io/> [Accessed: (1 July 2023)].
- SCHEIDEL, W. (2015): “ORBIS: The Stanford geospatial network model of the Roman world,” Tech. rep.

## B.9 Tables and figures

### Tables

Appendix Table B.1: Summary statistics: Coins

	count	mean	sd	min	p10	p50	p90	max
Has mint date interval	494,229	0.85	0.36	0	0	1	1	1
Has mint location	494,229	0.55	0.50	0	0	1	1	1
Has mint location and date interval	494,229	0.55	0.50	0	0	1	1	1
Mint date interval, years	418,927	29.48	41.66	-19	1	20	58	432
Mint date interval, start year	418,927	465.46	186.71	34	306	375	815	949
Mint date interval, end year	418,927	494.94	184.49	79	333	395	840	950
Age at tpq	418,927	58.74	81.37	0	6	29	154	805
Has material	494,229	0.98	0.15	0	1	1	1	1
Coin is gold	494,229	0.07	0.25	0	0	0	0	1
Coin is silver	494,229	0.18	0.38	0	0	0	1	1
Coin is copper/bronze	494,229	0.74	0.44	0	0	1	1	1
Has denomination	494,229	0.99	0.10	0	1	1	1	1
Has some empire/dynasty information	494,229	0.69	0.46	0	0	1	1	1
Geodesic distance mint to hoard, km	273,342	769.72	783.97	0	59	503	1,631	6,302

*Notes:* Sample consists of all coins from hoards with tpq between 325 and 950. “Age at tpq” is defined as tpq of the hoard minus the midpoint of the mint date interval.

Appendix Table B.2: Summary statistics: Hoards

	count	mean	sd	min	p10	p50	p90	max
Hoard tpq	5,519	591.05	148.14	325	375	578	782	950
Number of coins in hoard	5,519	89.55	822.74	1	1	1	81	43,867
Fraction of coins with mint date interval	5,519	0.98	0.12	0	1	1	1	1
Fraction of coins with mint location	5,519	0.87	0.27	0	0	1	1	1
Fraction of coins with mint date interval and mint location	5,519	0.86	0.27	0	0	1	1	1
Average mint date interval	5,519	23.20	32.62	0	1	11	80	377
Average age of coins at tpq	5,519	25.38	41.72	0	0	10	50	522
Fraction of coins with material	5,519	0.99	0.08	0	1	1	1	1
Fraction of coins that are gold	5,519	0.29	0.45	0	0	0	1	1
Fraction of coins that are silver	5,519	0.15	0.35	0	0	0	1	1
Fraction of coins that are bronze	5,519	0.55	0.49	0	0	1	1	1
Fraction of coins with denomination	5,519	0.99	0.08	0	1	1	1	1
Fraction of coins with empire/dynasty information	5,519	0.80	0.38	0	0	1	1	1
Average distance of coins from mint, km	5,417	685.10	612.07	0	88	533	1,462	6,124

*Notes:* Sample consists of all coins from hoards with tpq between 325 and 950. “Age at tpq” is defined as tpq of the hoard minus the average coins’ midpoint of the mint date interval.

Appendix Table B.3: Gravity and border effects: # coins vs values of coins

	Dep. var.: # Coins <sub>mdh</sub>		Dep. var.: Value <sub>mdh</sub>	
	(1)	(2)	(3)	(4)
Log Distance	-1.137*** (0.12)	-1.002*** (0.13)	-1.144*** (0.075)	-0.989*** (0.068)
Political border		-1.945*** (0.62)		-1.516*** (0.27)
Hoard Cell FE	Yes	Yes	Yes	Yes
Mint × Empire Cell FE	Yes	Yes	Yes	Yes
Sample			Gold and Silver	Gold and Silver
Estimator	PPML	PPML	PPML	PPML
Pseudo- <i>R</i> <sup>2</sup>	0.767	0.778	0.800	0.810
Observations	217748	217748	146767	146767

Standard errors in parentheses, clustered at mint cell × empire and hoard cell level.

+  $p < 0.10$ , \*  $p < 0.05$ , \*\*  $p < 0.01$

*Notes:* This table presents variations of equation (1). The dependent variable is the number of coins in a hoard cell  $h$  from a mint cell  $m$  issued by a political entity  $p$ . Columns 1 and 2 reproduce columns 1 and 2 from table 1, while columns 3 and 4 exploits only the intensive margin of coin flows (restricting the sample to  $m \times h$  pairs where some coins from mint cell  $m$  were found in hoard cell  $h$ ).

Appendix Table B.4: Do coins get redistributed within empires before entering circulation?

	Dependent variable: # Coins <sub>mdh</sub>			
	(1)	(2)	(3)	(4)
Log Distance	-0.709*** (0.092)	-0.923*** (0.17)	-0.669*** (0.11)	-0.839*** (0.068)
Empire × Hoard Cell FE	Yes	Yes	Yes	Yes
Mint × Empire Cell FE		Yes		Yes
Sample			Gold only	Gold only
Estimator	PPML	PPML	PPML	PPML
<i>R</i> <sup>2</sup>				
Observations	41443	41443	11363	11344

Standard errors in parentheses, clustered at mint cell × empire and hoard cell level.

+  $p < 0.10$ , \*  $p < 0.05$ , \*\*  $p < 0.01$

*Notes:* This table presents variations of equation (1). The dependent variable is the number of coins in a hoard cell  $h$  from a mint cell  $m$  issued by a political entity  $p$ . The regression drops all  $(m, h)$  combinations that have no emitted coins. Hoard and mint cells are  $1^\circ \times 1^\circ$ . Observations only include those that remain after dropping singletons and separated observations. Political entities are categorized into fourteen divisions.

Appendix Table B.5: The Mediterranean Before and After the Conquests

	Dependent variable: Number of Coins			
	(1)	(2)	(3)	(4)
Crossing Mediterranean $\times$ After Conquests	-1.893*** (0.48)	-3.246*** (0.53)	-0.662 (0.63)	-1.736 (1.27)
Crossing Mediterranean $\times$ After Conquests $\times$ Islamic Coin		7.267*** (0.90)	4.789*** (0.95)	7.545*** (0.89)
Crossing Mediterranean $\times$ After Conquests $\times$ Roman Coin			-3.287*** (0.75)	-2.893*** (0.61)
Mint Cell $\times$ Empire FE	Yes	Yes	Yes	Yes
Mint Cell $\times$ Hoard Cell FE	Yes	Yes	Yes	Yes
After Conquests FE	Yes	Yes	Yes	
Mint Cell $\times$ After Conquests FE				Yes
Hoard Cell $\times$ After Conquests FE				Yes
Estimator	PPML	PPML	PPML	PPML
Observations	10480	10480	10480	6208

Standard errors in parentheses, clustered at the hoard  $\times$  era and mint  $\times$  era level.

+  $p < 0.10$ , \*  $p < 0.05$ , \*\*  $p < 0.01$

*Notes:* This table presents various specifications of equation (B.1). The dependent variable is the number of coins in a hoard cell from a mint cell  $\times$  dynasty  $\times$  era (where era is before vs after the conquests). The regression drops all mint  $\times$  dynasty combinations that have zero emitted coins. Hoard and mint cells are  $1^\circ \times 1^\circ$ . Flows before the conquests are those with mint date after 400 and  $tpq$  before 630; flows after the conquests are those with mint date after 713 and  $tpq$  before 900. Observation counts only include those that remain after dropping singletons and separated observations. “Crossing Mediterranean” is a dummy that is one if the geodesic line between hoard and mint cell intersects with the Mediterranean. “Islamic Coin” and “Roman Coin” are dummies equal to one if the coin is of Islamic issue (any dynasty) or Roman/Byzantine issue, respectively. “Empires” here are categorized as Sasanian, Roman-Byzantine, Franks, Islamic, Germanic Tribes, and Other Christian.

Appendix Table B.6: Estimation of the coin loss rate  $\lambda$

	Dependent variable: Log share of coins in bin $[k, k + n]$	
	(1)	(2)
$k/n$	-0.162*** (0.0100)	-0.356*** (0.031)
Bin size $n$	10	20
$R^2$	0.833	0.819
Observations	55	31

Standard errors in parentheses.

Appendix Table B.7: Tests of random sampling within region  $\times$  period

	N. coins	N. hoards	Test of equal distributions between hoards ( <i>p</i> -values)	
			Domestic vs foreign coins	Coin ages
			(Student's <i>t</i> )	(Kolmogorov-Smirnov)
al-Sham, Greater Syria (740-760)	13862	126	0.57	0.29
al-Andalus (380-400)	12364	89	1.00	0.65
Francia and Germania (880-900)	7725	25	0.53	0.85
Northern Italy (460-480)	1914	25	0.54	0.41
al-Sham, Greater Syria (680-700)	1625	15	0.61	0.33
Byzantine Heartlands (540-560)	833	109	0.59	0.54
Byzantine Heartlands (680-700)	565	22	0.35	0.60
Southern Italy (640-660)	107	14	0.52	0.13

*Notes:* We perform statistical tests for the region  $\times$  period containing the largest number of coins and hoards. For each region  $\times$  period, we randomly partition the sample in two sets of hoards, and aggregate all coins from those hoards within each set. We then run a test of equality between the two sets of the probability of a coin being domestic versus foreign (Student's *t* test) and of the distribution of coin ages (Kolmogorov-Smirnov test). We repeat this random partition in two sets of hoards 1,000 times, and report the average *p*-values of those tests. Note that all coins in Iberian hoards (al-Andalus) deposited in the ground in 380-400 are foreign (minted outside Iberia), so that the Student's *t* test is degenerate and the *p*-value equal to 1 by construction.

Appendix Table B.8: Test of random sampling between region  $\times$  period

A. Test of equal distributions of domestic vs foreign coins ( <i>p</i> -values for Student's t test)								
	al-Sham Greater Syria (740-760)	al-Andalus (380-400)	Francia and Germania (880-900)	Northern Italy (460-480)	al-Sham Greater Syria (680-700)	Byzantine Heartlands (540-560)	Byzantine Heartlands (680-700)	Southern Italy (640-660)
al-Sham, Greater Syria (740-760)	0.57	0.00	0.11	0.14	0.00	0.00	0.00	0.02
al-Andalus (380-400)		1.00	0.00	0.00	0.00	0.00	0.00	0.00
Francia and Germania (880-900)			0.53	0.85	0.00	0.00	0.00	0.00
Northern Italy (460-480)				0.54	0.00	0.00	0.00	0.00
al-Sham, Greater Syria (680-700)					0.61	0.00	0.00	0.94
Byzantine Heartlands (540-560)						0.59	0.56	0.00
Byzantine Heartlands (680-700)							0.35	0.00
Southern Italy (640-660)								0.52

B. Test of equal distributions of coin ages ( <i>p</i> -values for Kolmogorov-Smirnov test)								
	al-Sham Greater Syria (740-760)	al-Andalus (380-400)	Francia and Germania (880-900)	Northern Italy (460-480)	al-Sham Greater Syria (680-700)	Byzantine Heartlands (540-560)	Byzantine Heartlands (680-700)	Southern Italy (640-660)
al-Sham, Greater Syria (740-760)	0.29	0.00	0.00	0.00	0.00	0.00	0.00	0.08
al-Andalus (380-400)		0.65	0.00	0.00	0.00	0.00	0.00	0.00
Francia and Germania (880-900)			0.85	0.00	0.00	0.00	0.00	0.00
Northern Italy (460-480)				0.41	0.00	0.00	0.01	0.00
al-Sham, Greater Syria (680-700)					0.33	0.00	0.00	0.07
Byzantine Heartlands (540-560)						0.54	0.00	0.00
Byzantine Heartlands (680-700)							0.60	0.04
Southern Italy (640-660)								0.13

Notes: Off-diagonal elements—Panel A reports the *p*-value of a Student's t test of equality of the distribution of domestic versus foreign coins between two region  $\times$  period (row and column). Panel B reports the *p*-value of a Kolmogorov-Smirnov test of equality of the distribution of coin ages between two region  $\times$  period (row and column). Diagonal elements—same tests within each region  $\times$  period (randomly partitioned in two sets of hoards, 1,000 times, averaged), replicate the last two columns of table B.7.

Appendix Table B.9: Determinants of ancient trade costs: robustness

	Log Trade Costs			
	(1)	(2)	(3)	(4)
Log Travel Time	3.03 (0.02)	0.96 (0.03)	3.55 (0.03)	2.97 (0.02)
Political Border	0.49 (0.02)	3.4 (0.05)	2.37 (0.04)	1.28 (0.02)
Religious Border: East	1.97 (0.12)	0.0 (0.32)	0.15 (0.23)	0.88 (0.1)
Religious Border: West	4.59 (0.22)	4.05 (0.62)	5.2 (0.29)	7.71 (0.51)
Religious Border: Mediterranean	5.2 (0.18)	2.66 (0.19)	3.82 (0.21)	2.89 (0.1)
Time Interval	20 years	20 years	10 years	30 years
Coin Accounting	Number	Value	Number	Number
Sample	All	Gold/Silver	All	All
Observations	4,413	2,020	7,427	3,248

*Notes:* The table shows alternative specifications for the estimates of the trade cost parameters. Column 1 reproduces our baseline estimates, 20-year time intervals and the parameterization of trade costs in column 2 of table 3. Column 2 uses 20-year time intervals and weights coins by value (in equivalent grams of gold, assuming a constant exchange rate of 12g of silver for 1g of gold; and using gold and silver coins only). Columns 3 and 4 show variations of the baseline specification where time periods are aggregated to 10-year intervals (column 3) or 30-year time intervals (column 4), adjusting the coin loss rate to the period length (always 1.7% p.a.).

Appendix Table B.10: Military conflict and real consumption

	Dependent variable: Log Real Consumption $X_i/p_i$	
	(1)	(2)
(# Battles) $_{it}$	0.178 (0.14)	
(At least one battle) $_{it}$		0.833* (0.44)
20-year time period FE	Yes	Yes
Region FE	Yes	Yes
$R^2$	0.322	0.325
Observations	403	403

Standard errors in parentheses, clustered at the 20-year time interval level.

\*  $p < 0.10$ , \*\*  $p < 0.05$ , \*\*\*  $p < 0.01$

Appendix Table B.11: Plague events and real consumption

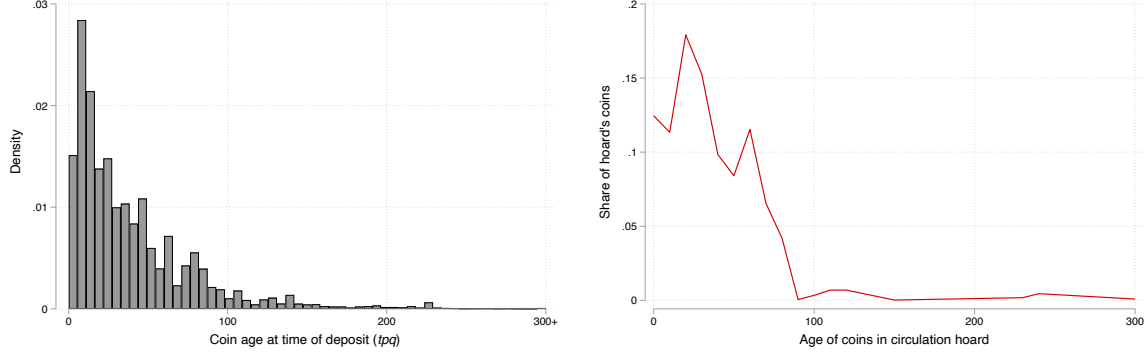
	Dep. var.: Log Real Consumption $X_n/p_n$			
	(1)	(2)	(3)	(4)
(# Plague years) $_{it}$	0.556*	0.0134		
	(0.31)	(0.24)		
(# Consecutive plague years) $_{it}$			0.554	0.433
			(0.90)	(0.61)
20-year time period FE	Yes	Yes	Yes	Yes
Region FE	Yes	Yes	Yes	Yes
Sample	Full	[540, 750)	Full	[540, 750)
$R^2$	0.324	0.703	0.319	0.704
Observations	403	143	403	143

Standard errors in parentheses.

\*  $p < 0.10$ , \*\*  $p < 0.05$ , \*\*\*  $p < 0.01$

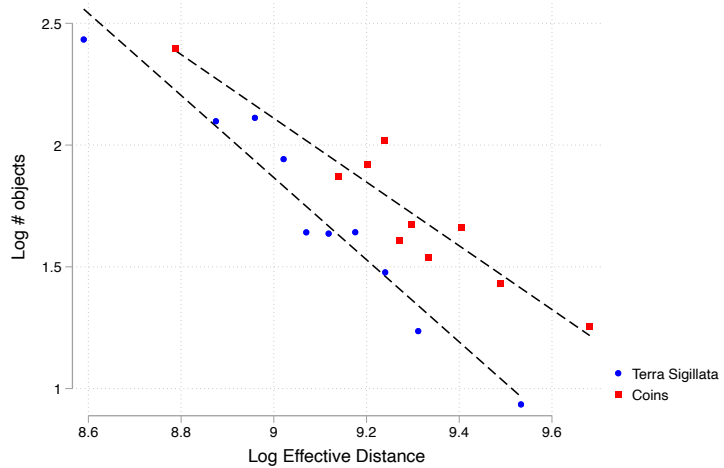
*Note:* The dependent variable is our estimate of  $\log X_n/p_n$ . The independent variables are the number of plague-years, and the number of consecutive plague-years in a 20-year time interval and region, from Stathakopoulos (2004). Columns (2) and (4) restrict the sample to the period [540, 750], which is the period from the onset of the Justinianic Plague to the end of period covered by Stathakopoulos (2004).

## Figures



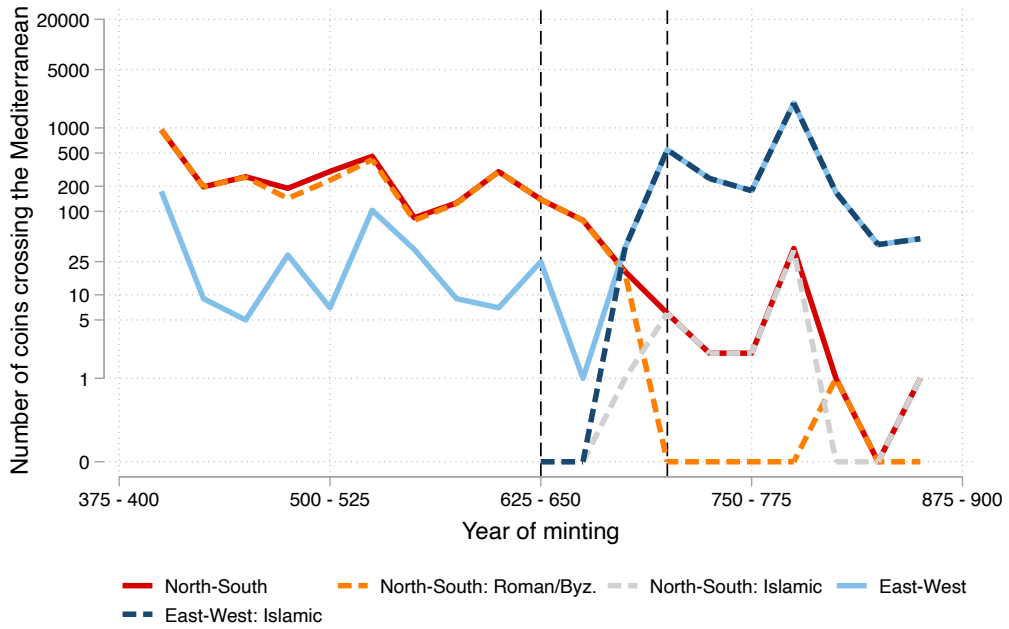
Appendix Figure B.1: Comparison with Circulation Hoards in [Banaji \(2016\)](#)

*Notes:* The left panel reproduces Figure 3b. The right panel shows the average share of coins in each 10-year age bin in the circulation hoards of [Banaji \(2016\)](#), Chapter 6, who reports the issuing emperors (but not mint dates) of the coins in these hoards. We draw mint dates uniformly from the ruling years of these emperors.



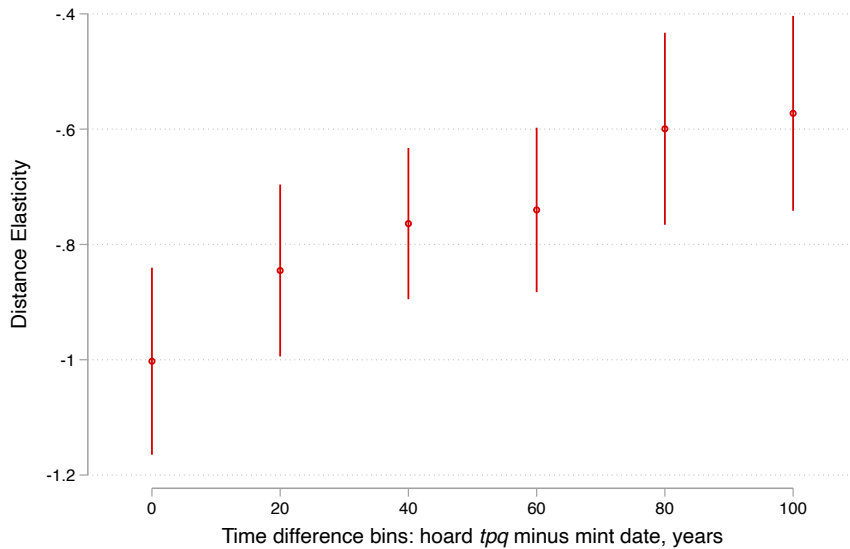
Appendix Figure B.2: Comparison with flows of West Roman Terra Sigillata ([Flückiger et al., 2022](#))

*Notes:* The figure shows a binscatter of the log number of objects flowing (either coins or number of Terra Sigillata) between two  $0.5 \times 0.5$  degree cells, against the log effective distance between cells. Both are de-meaned by origin and destination location. Cell definitions and effective distances are from [Flückiger et al. \(2022\)](#). The coin data is restricted to hoards with  $tpq$  up to 450 and that lie within the aforementioned cells.



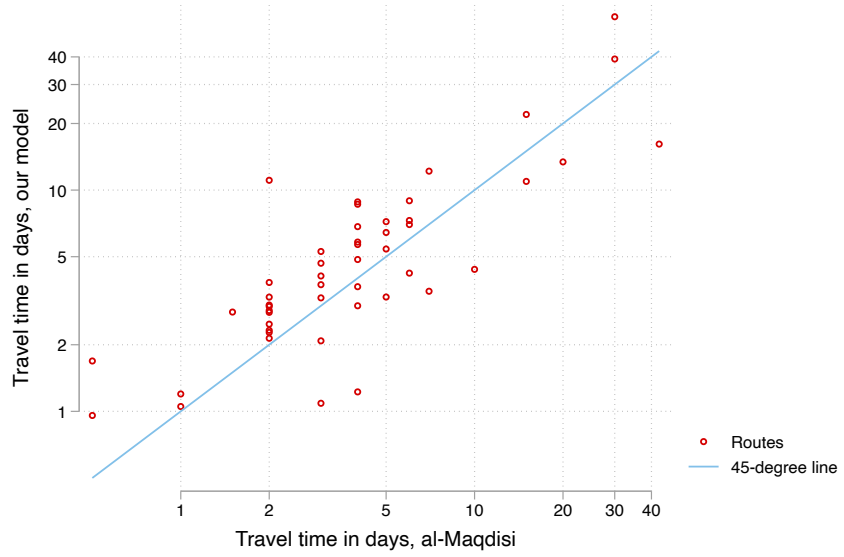
Appendix Figure B.3: Number of coins flowing across the Mediterranean

*Notes:* The figure shows the number of coins minted in the 25-year interval on the horizontal axis, that are minted on one side of the Mediterranean, and are found on the other. Flows include both directions. The north is defined to go from the Pyrenees to Byzantine Turkey, east from Byzantine Turkey to Egypt, south from Egypt to the Maghreb, and west from Maghreb to Aquitaine. Border regions are included in these definitions, so regions are partly overlapping.



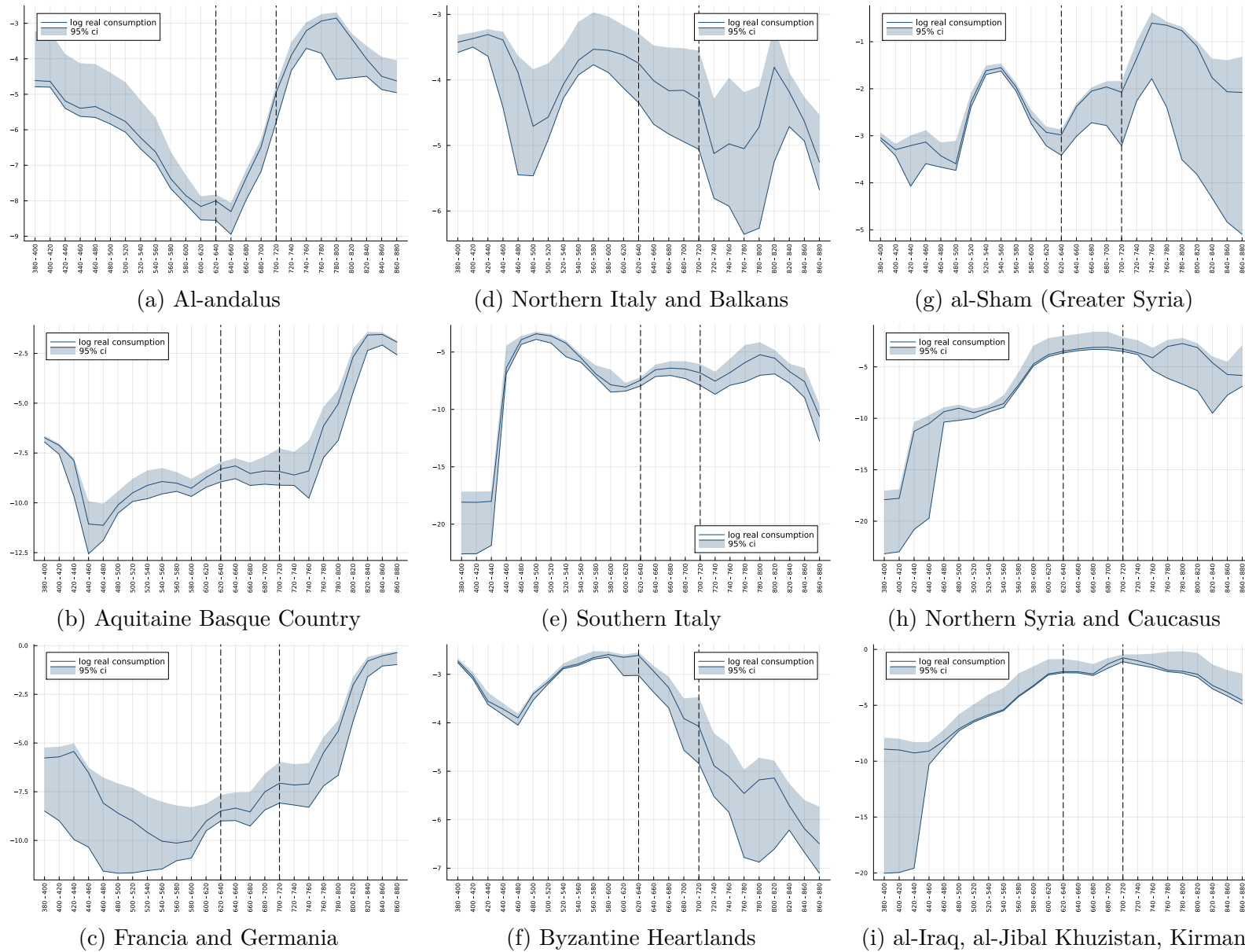
Appendix Figure B.4: The distance elasticity declines as coins age

*Notes:* The figure shows the distance elasticity estimates when estimating equation (B.2) using PPML.



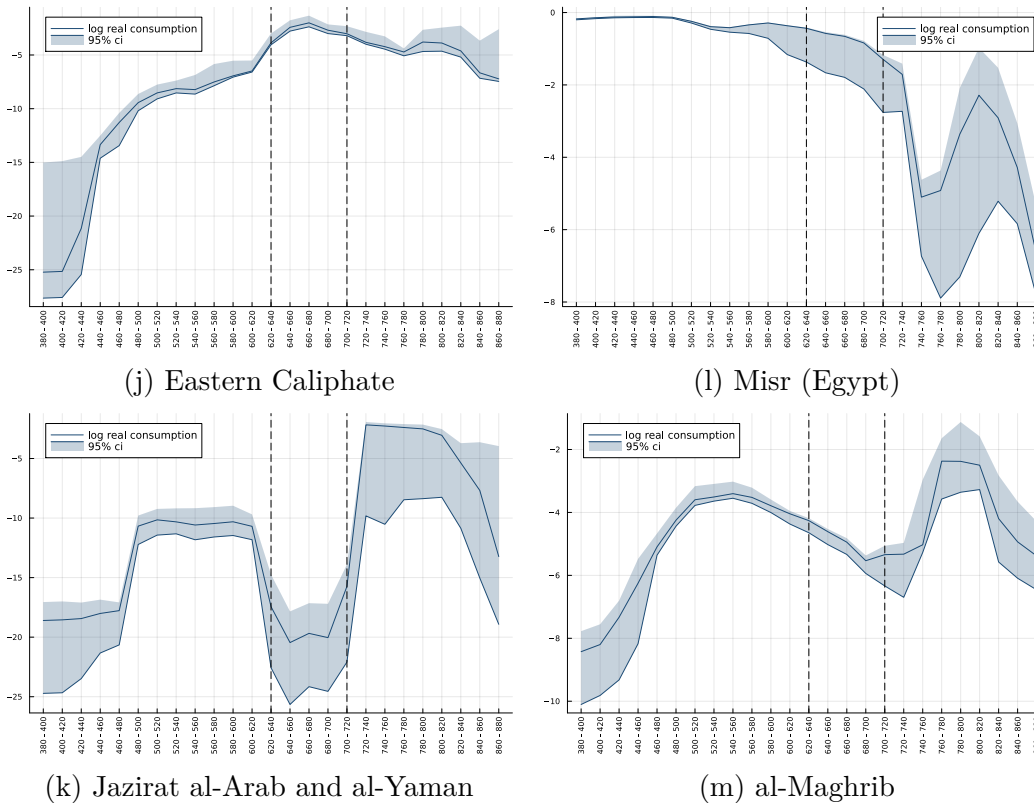
Appendix Figure B.5: Comparing travel times to Al-Muqaddasī (985)

*Notes:* Each dot refers to a city-to-city connection for which Al-Muqaddasī (985) lists the travel time in days. We exclude desert routes (where he reports travel times in nights or in watering stations, routes with cities cannot be found in al-Turayyā, as well as the route between Tahart and Fes, which he claims can be travelled in three days despite it being a distance of more than 600 kilometers (our model predicts 22 days)).



Appendix Figure B.6: Real consumption AD 380-880

*Notes:* The figures on this page and the next complement figure 10, showing for all 13 regions the time-series from AD 380 to AD 880 of (log) real consumption as a share of aggregate consumption. See section 4.1 for details on the computation of real consumption using estimates from the specification in column 2 of table 3. 95% confidence intervals (shaded areas) are computed from re-estimating our model on 100 bootstrapped samples from our coin hoard data.



Appendix Figure B.6: Real consumption AD 380-880 (continued)

## C Additional theoretical derivations

We propose a simple extension of our model with both monetized transactions and barter.

**Setup.** We assume that a fraction  $m_n[t]$  of transactions in region  $n$  and period  $t$  are monetized, and the remaining are barter: a fraction  $m_n[t]$  of wages and of consumption are paid in coins. The dynamic market clearing condition (7) becomes,

$$(m_i[t]w_i[t]L_i[t]) = \sum_n \pi_{ni}[t] \left( (1 - \lambda) (m_n[t-1]w_n[t-1]L_n[t-1]) + M_n[t] \right), \forall(i, t). \quad (\text{C.1})$$

The fraction of consumption ( $X_n[t]$ ) spent in coins is,

$$m_n[t]X_n[t] = (1 - \lambda) (m_n[t-1]w_n[t-1]L_n[t-1]) + M_n[t] \quad (\text{C.2})$$

The dynamic of coin stocks remains unchanged, as in (9).

Following the intuition from [Kiyotaki and Wright \(1989\)](#), we assume that monetization increases with real production. We approximate this relationship with an iso-elastic function,

$$m_n[t] = m(T_n^{1/\theta}[t]L_n[t]) = \min \left\{ \left( \frac{T_n^{1/\theta}[t]L_n[t]}{\overline{T}^{1/\theta}L} \right)^\mu, 1 \right\}. \quad (\text{C.3})$$

This parameterization captures several simple intuitions. First, there is a level of development  $\overline{T}^{1/\theta}L$  above which an economy becomes fully monetized. We assume that none of the regions in our sample period have reached this stage of full monetization. Second, as in [Kiyotaki and Wright \(1989\)](#), a larger economy is characterized by more transactions, such that the benefit from using money is larger because it allows for more indirect (non-barter) exchanges.

We further assume that the income elasticity of monetization is equal to the dispersion of productivity between sectors in our [Eaton and Kortum \(2002\)](#) model of trade,

$$\mu = \theta. \quad (\text{C.4})$$

This assumption captures in a reduced form the intuition in [Kiyotaki and Wright \(1989\)](#) that the degree of monetization depends on how beneficial the use of money is; with heterogeneous

productivity between sectors, the benefits from using money depend on comparative advantages which govern the gains from multilateral exchanges, and therefore the gains from using a universally accepted medium of exchange. In the [Eaton and Kortum \(2002\)](#) ricardian model of trade, the parameter governing the dispersion of productivity across sectors is  $\theta$ .

**Bringing the model to the data.** Because the dynamic of coin stocks remains unchanged compared to our baseline model (9), we follow the exact same maximum likelihood procedure as in section 3 to estimate the bilateral and seller terms,  $d_{ni}^{-\theta}[t]$  and  $\tilde{\beta}_i[t]$ , and minting,  $M_i[t]$ . As in our baseline, we directly recover trade shares,  $\pi_{ni}[t]$ , from those parameter estimates.

The post-estimation computation of real consumption is different. We start with the dynamic market clearing condition with endogenous monetization (C.1). Knowledge of trade shares and minting is enough to recover *monetized* nominal incomes,  $(m_n[t]w_n[t]L_n[t])$ . Note that the solution for *monetized* incomes is identical to the solution for incomes in our baseline, but their interpretation are different.

We then perform a simple manipulation of the expressions for monetized consumption (C.2) and for real consumption similar to the manipulation in (23),

$$\frac{X_n[t]}{p_n[t]} = \gamma^{-1} (\pi_{nn}[t])^{-1/\theta} (T_n^{1/\theta}[t]L_n[t]) \left( \frac{(1-\lambda)(m_n[t-1]w_n[t-1]L_n[t-1]) + M_n[t]}{(m_n[t]w_n[t]L_n[t])} \right). \quad (\text{C.5})$$

The first and last terms (openness and trade deficits) are directly computed from our solution for trade shares and monetized nominal incomes, and the trade elasticity  $\theta$ . We note that those first and last terms are numerically identical to the first and last terms in our baseline model (23), although their interpretation is different.

To compute  $T_n^{1/\theta}[t]L_n[t]$  from our empirical estimates, we manipulate the seller term in (11),

$$\begin{aligned}
\tilde{\beta}_n[t] &= (w_n[t]/T_n^{1/\theta}[t])^{-\theta} \\
\Rightarrow T_n^{1/\theta}[t]L_n[t] &= w_n[t]L_n[t] \left( \tilde{\beta}_n[t] \right)^{1/\theta} \\
&= (m_n[t])^{-1} (m_n[t]w_n[t]L_n[t]) \left( \tilde{\beta}_n[t] \right)^{1/\theta} \\
&= \left( \overline{T^{1/\theta} L} \right)^\theta (T_n^{1/\theta}[t]L_n[t])^{-\theta} (m_n[t]w_n[t]L_n[t]) \left( \tilde{\beta}_n[t] \right)^{1/\theta} \\
\Rightarrow T_n^{1/\theta}[t]L_n[t] &= \text{constant} \times (m_n[t]w_n[t]L_n[t])^{\frac{1}{1+\theta}} \left( \tilde{\beta}_n[t] \right)^{\frac{1}{\theta(1+\theta)}}. \tag{C.6}
\end{aligned}$$

We can directly compute this last remaining term, productive capacity, using our solution for monetized nominal incomes, our estimates for seller terms, and the trade elasticity  $\theta$ , up to a single (global) arbitrary multiplicative constant.

In practice this means that, compared to our baseline, we simply raise the productive capacity term labeled “ $T_n^{1/\theta}[t]L_n[t]$ ” in equation (23) to the power  $1/(1 + \theta)$  to account for endogenous monetization.

## References

- EATON, J. AND S. KORTUM (2002): “Technology, Geography, and Trade,” *Econometrica*, 70, 1741–1779.
- KIYOTAKI, N. AND R. WRIGHT (1989): “On Money as a Medium of Exchange,” *Journal of Political Economy*, 97, 927–954.

## D Coin hoard data (NOT FOR PUBLICATION)

Our numismatic data consists of two datasets: first, the set of hoards from the current release of the *Framing the Late Antique and Early Medieval Economy* project ([FLAME, 2023](#)). FLAME is a large collaborative effort of historians and numismatists that records data on coin hoards around the Mediterranean and Europe from between AD 325 and AD 725. We use the most recent release (January 2023) which has data on about 1.7m coins belonging to more than 9,000 hoards. Since the temporal and spatial focus of our study does not entirely overlap with that of FLAME, we complement their data by constructing a hand-coded dataset on hoards between AD 700 and AD 900, and hoards with a heavier emphasis on near eastern coins. We describe the hand-collected data and FLAME’s data in turn.

### D.1 Hand-collected data

We search the numismatic and archaeological literature for descriptions of coin hoards or coin finds with a *terminus post quem* (= date of the most recent content) of roughly between AD 700 and AD 950, that were discovered in Europe, North Africa, or the Middle East. For the sake of brevity we will refer to a single coin or a collection of coins that was found together in one place as a “hoard” (i.e. unless specifically mentioned, we do not distinguish between single finds, stray finds, mini-hoards, or full hoards). We exclude hoards that largely contain silver that was brought via the Viking route or that clearly have a Viking connection.<sup>4</sup> We likewise exclude records from excavations, unless they are described as a hoard or constitute a set of coins that were found together in the same location (e.g. in the same room of an excavated building).

An (at least approximate) findspot must be known for a hoard to be of use in our analysis. For each hoard we record the latitude and longitude of its findspot. When the findspot is known only with a low level of precision (e.g. at the country or region level) we code this in a separate dummy variable. Importantly, we do not record coins in museums or collections that have unknown findspots. While we digitize many descriptions of hoards that are incomplete, we omit hoards of which no information on the vast majority of coins has been published.

For each coin (or group of coins with identical properties) in a hoard we record, if documented

---

<sup>4</sup>Among the list from Appendix 3 of [McCormick \(2001\)](#), these are the hoards in Britain, Scandinavia, and Schleswig-Holstein (Germany). We also digitized the 10th century Máramaros county hoard ([Fomin and Kovács, 1987](#)), but drop it as its content (consisting of many imitations, as well as dirhams from the Samarkand and al-Shash mints) indicate that it was clearly brought in from the east.

by the authors of the hoard catalogue:

- The mint where the coin was minted, or believed to have been minted. When a coin is believed to have been an imitation, we note this separately.
- A time interval (consisting of a start year and end year) during which the coin was minted or is believed to have been minted. For some coins, such as most Islamic dirhams, this information is imprinted on the coin. For others, we code this as the shortest time interval during which the coin could have been minted, taking into account the denomination of the coin, the ruler under whose authority it has been issued, as well as his/her dynasty, and other information about coin types (e.g. pre/post-reform coinage). When the coin has been dated through the regnal year of the ruler or in the Islamic calendar, we convert this to Gregorian calendar years.

Beyond the attributes above, we record denomination, material, and issuing rulers and dynasties (mostly with dating of the coins in mind). This information, if known, is typically furnished by the authors of hoard catalogues in the numismatic literature. We do not distinguish between fragments and entire coins.

The geocodes of the hoards and mints are only approximate. We code Nomisma IDs for the mints based on the proximity of the place of minting, not based on the dynasty, e.g. “Siqilliyah” (Sicily) can be also used for non-Islamic issue.

### D.1.1 Hoards in the Near East and North Africa

Table D.3 shows the list of hand-coded hoards from the Near East and North Africa, along with references. These hoards consist mainly of Sasanian and/or Islamic coins, and sometimes Byzantine issue. We code approximate mint locations based on the proposals in the literature, typically giving preference to the suggestions of the authors of the original hoards.

A couple of notes on specific hoards:

- We digitize the Umm-Hajarah hoard based on the description by al 'Ush (1972a) but follow Noonan (1980) in treating the isolated Seljuk coin that Al-'Ush dates to 689-690 AH as not belonging to the hoard.

- We digitize Hoge (1997)'s description of a hoard from “North Africa (or Spain?)”, and assign Kairouan as approximate location (and note that the precise location of the hoard is immaterial to our exercise). We treat the Safavid dinar that is 650 years younger than the other coins (Hoge: “no doubt added to the other pieces ‘in trade?’”) as extraneous to the hoard.

### D.1.2 Islamic hoards in Spain and France

Tables D.4 and D.5 show the hand-digitized hoards from Islamic Spain (al-Andalus) and Islamic coin finds from southern France.

### D.1.3 Other Islamic and Byzantine hoards in Europe

We digitize the hoards, mini-hoards, and stray finds from McCormick (2001)'s survey of Arab and Byzantine coins in Europe (Appendix 3) between 668 and 900. We add those to our dataset, except when already covered in our other sources. We update hoard descriptions for which newer catalogues are available.<sup>5</sup> Finally, we exclude the contested Odoorn/Zuidbarge (1859–60) hoard, as the identity of it as a single hoard is not clear, some of the coins had been converted into jewellery, and the contents are not well described.<sup>6</sup>

### D.1.4 Byzantine hoards

The hoards reported in the corpora by Pennas (1991), Füeg (2007), and Nikolaou and Touratsoglou (2019) form the basis of our collection of Byzantine hoards (the corpus on earlier finds by Morrisson et al. (2006) is mostly already incorporated into FLAME). Information on particular regions come from Mirnik (1981) (Balkans), Arslan (2005) (Italy), Kovács (1989) (Hungary), and Wołoszyn (2009) (Central Europe). Hoard catalogues typically refer to collection catalogues (Sabatier, 1862, Wroth, 1908, Grierson, 1968, 1973) which we use to retrieve mint date intervals and likely mints.<sup>7</sup>

We exclude coin finds from running excavations, unless the coins were found as individual parcels in a specific location. Tables D.6 and D.7 show our hand-coded byzantine hoards.

---

<sup>5</sup>A35 (Steckborn): Ilisch (2005), A8 (Cagliari): Saccoccia (2005), who also mentions an Aghlabid semi-dirham of Muhammad I found in Crotone, Sicily. We update A28 (Porto Torres, Sardinia) based on the number and datings reported in Füeg (2007)'s corpus, likewise the dates from A34 (Reno River).

<sup>6</sup>See Coupland (2011a) for a discussion of these issues.

<sup>7</sup>For a large part of the time interval that is not covered by FLAME, Byzantine gold and silver coins are believed to have been exclusively issued at Constantinople (Grierson, 1968).

### D.1.5 Carolingian hoards

We follow Simon Coupland's *Checklist* (Coupland, 2011a, 2014, 2020) and digitize hoards and finds primarily based on the corpora presented by Völckers (1965), Duplessy (1985), and Haertle (1997), giving priority to more recent descriptions. Tables D.8 to D.12 show details. We follow the mint codings of Louis the Pious' *Christiana religio* coins given by Coupland (2011b). As mentioned above, we exclude the contested Odoorn/Zuidbarge hoard.

## D.2 FLAME

FLAME records their data in three different tables: coin finds, coin groups, and mints. In the coin find table each observation is a find that contains one or more coin groups; in the coin group table each observation is a set of coins with common recorded attributes (and linked to the coin find ID), including a mint and an interval for the year of minting. In the mint table each observation is a mint, and the mint name string allows these to be matched to coin groups. Mints and coin finds are geocoded.

The records in FLAME thus include a superset of the attributes in the hand-coded data above, except (i) the material of the coin, which we code based on the denomination; (ii) the weight and dimensions of the coins, which are sometimes (but not systematically) coded in the comments. We convert the FLAME data to the same structure as our handcoded data, including the following cleaning steps:

- A small number (6) of coin groups has a start year that's after the end year; we switch those around.
- FLAME contains start and end dates for the coin find itself. For a small number of coin groups the end date of the coin find falls in between the start and end dates of the coin group. This is often the case when very broad ranges have been given for the coin group, and so we truncate the coin group interval at the end date of the find.
- For Sasanian coins, we adhere to the mint codings in FLAME. A number of coins report the mint abbreviation but not the mint, we code and locate them analogously to how we coded them in the hand-coded coins (see below).

- A number of coin groups record a mint string that is not included in FLAME’s mint file. We code Nomisma ID’s for those mints, wherever possible.
- A large fraction of FLAME coins don’t have mints or dates: often large hoards are not recorded by coin (just the total number of coins). Out of 1.7m coins, about 340k have mint and dates.

## D.3 Locating mints

For FLAME data, we follow the attribution of mint locations done by the authors of the respective FLAME entries. For hand-collected data, we attempt to map the hand-coded mints to [Nomisma \(2023\)](#) IDs for the mints (`nmo:Mint`). Whenever a geocode for a mint is not available in Nomisma, or whenever the mint is not represented in Nomisma, we hand-code the geocodes. These geocodes should only be regarded as approximate and with a degree of precision required for our particular application in mind. Table D.1 shows the mints we add to Nomisma, along with our codings, and Table D.2 shows the codings for existing Nomisma mints without geocodes.

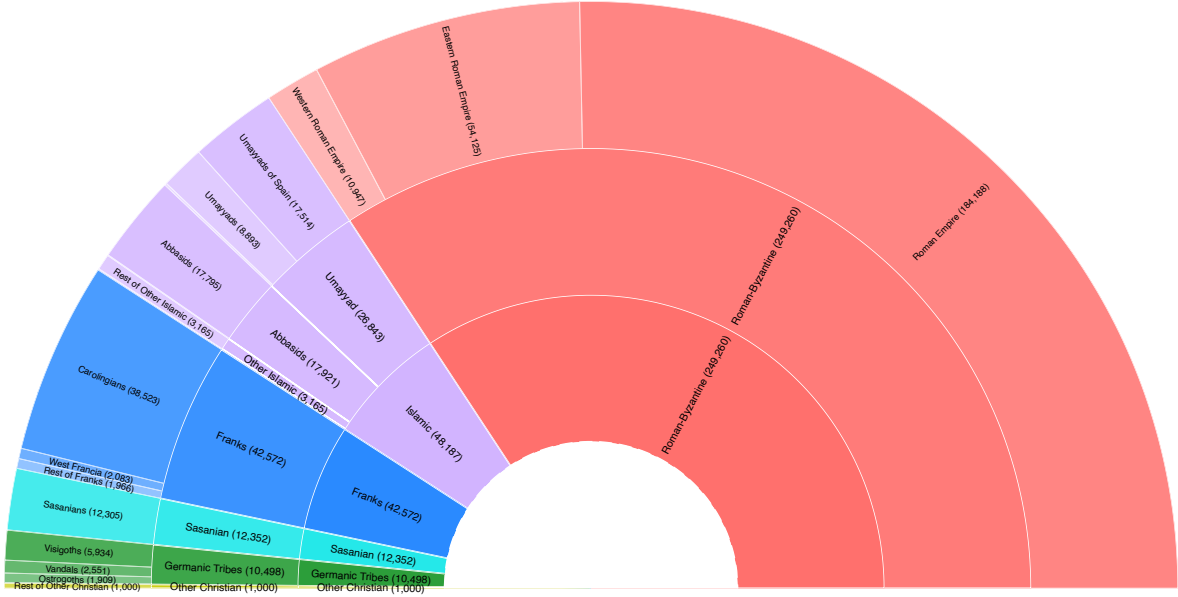
### D.3.1 Sasanian mints

The location of Sasanian mints and the identification of Sasanian mint signatures are contested. We generally follow the reading of the original hoard descriptions, except in situations where these are dated and the literature nowadays prefers different readings. Regarding the approximate location of the mints, we decided to code the approximate location for most signatures following the consensus in the literature; in some cases where the literature only agrees up to the region we chose Nomisma IDs from mints of that region. As with the other codings, the Nomisma IDs should only be seen as approximating the location of the mint, and do not carry any information on dating. Table D.14 summarizes our signature codings with their approximate mint locations.

## D.4 Political entities and the geography of hoards and mints

### D.4.1 Dynasties/Empires

We record dynasties/empires through the `dynastyname` field of FLAME data, and an equivalent field of the hand-coded data. We aggregate these to 10 more aggregate (“level 1”) dynasties/em-

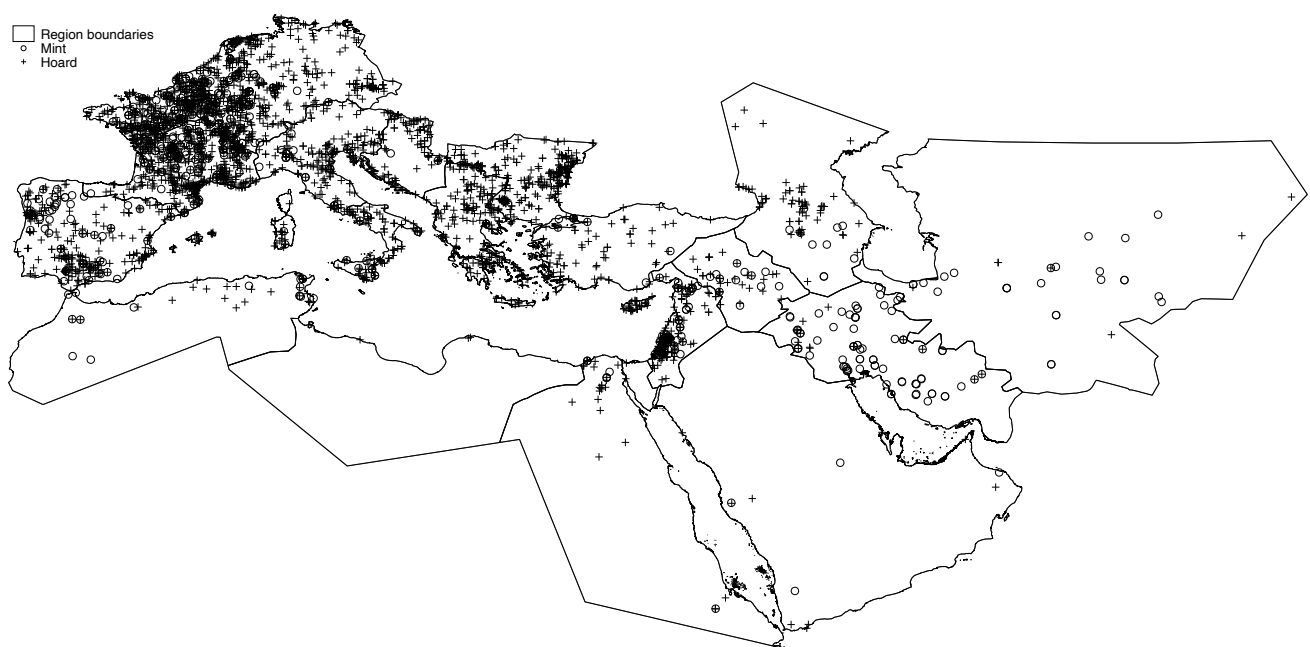


Appendix Figure D.1: Dynasties/Empires

pires, and seven most aggregate (“level 2”) dynasties/empires. Figure D.1 shows the breakdown of recorded dynasties in our final sample.

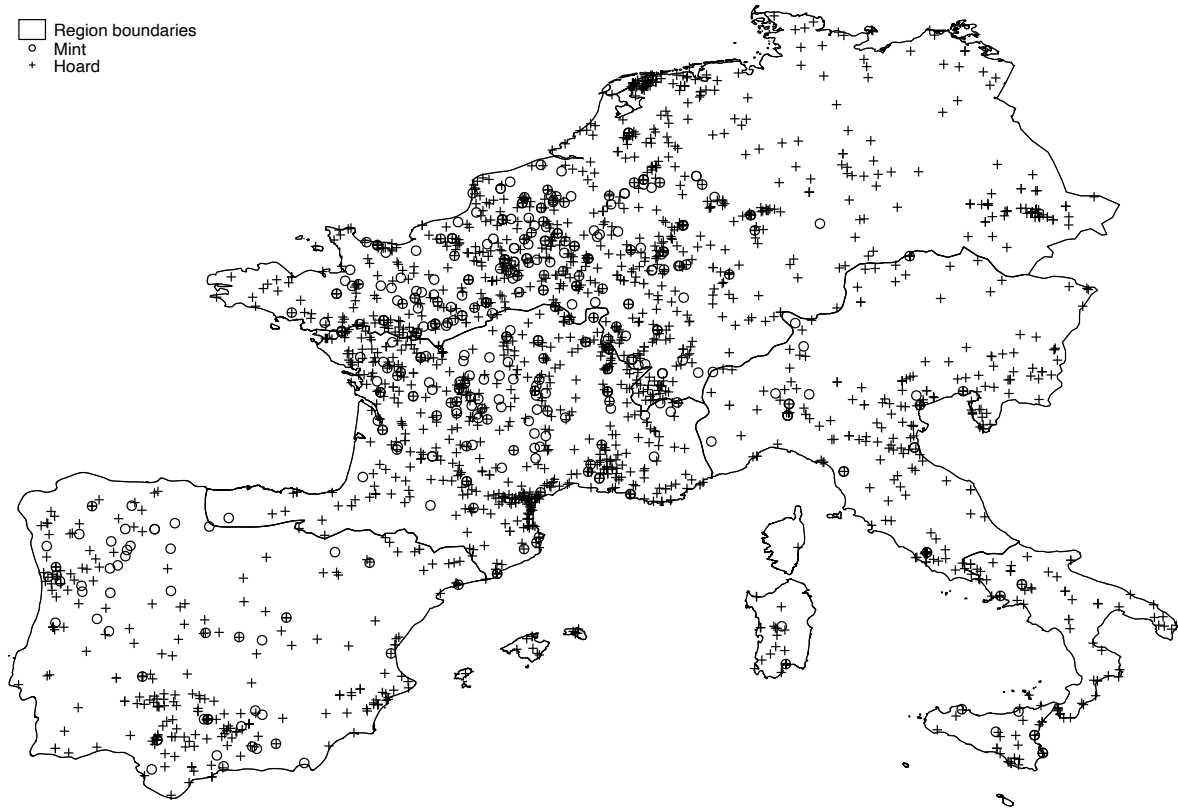
#### D.4.2 Location of hoards and mints

Figure D.2 show the location of mints and hoards of our final dataset. Only locations corresponding to coins that were minted after AD 400 are shown. Figure D.3 shows details for western Europe and the eastern Mediterranean.

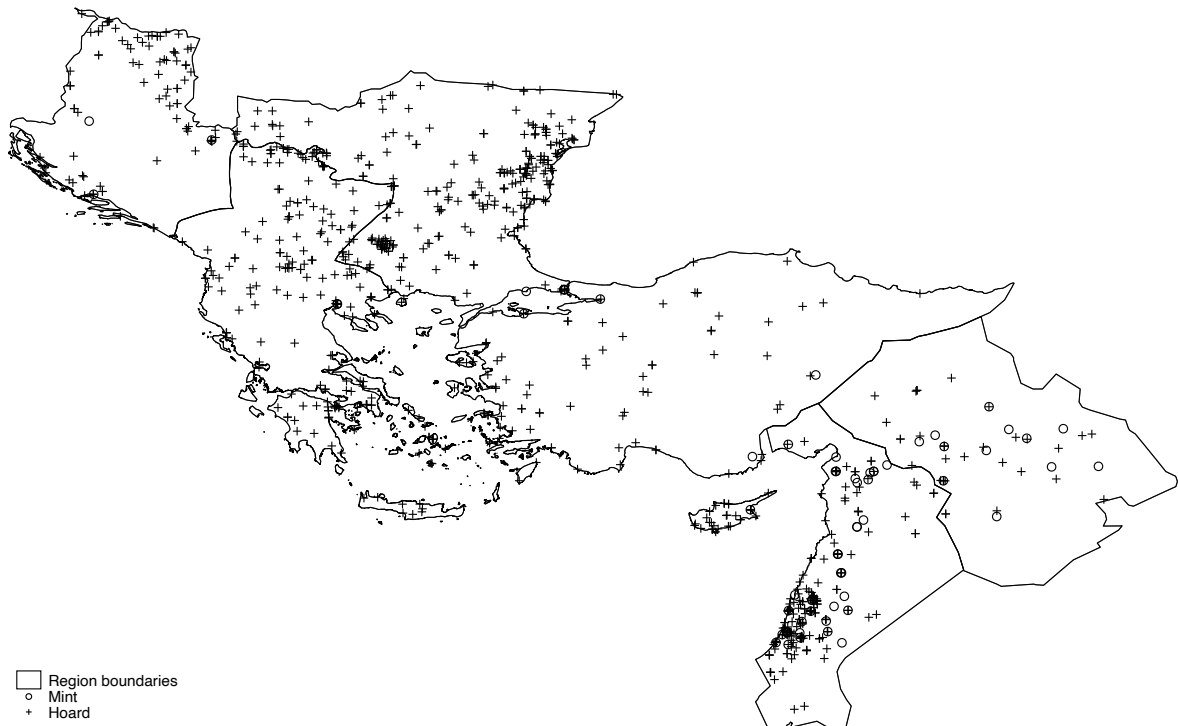


Appendix Figure D.2: Mints and Hoards

□ Region boundaries  
○ Mint  
+ Hoard



(a) Western Europe



(b) North-eastern Mediterranean

#### Appendix Figure D.3: Mints and Hoards: Details

Note: Maps show coins minted after AD 400

## D.5 Tables and references

Mint	id	Location	Latitude	Longitude	Notes
Abarqubadh	abarbqubadh		31.28027	47.49266	"This mint was in the district of Khusra-shadh Bahmân (the district of the Tigris) in Irâq, between Wâsit and al-Basra and near the border with Khuzistân." <a href="#">Lloyd (2023)</a>
Adurbadagan al Hashimiyyah	adurbadagan al-hashimiyyah	Ganzak Kufa	37.0123 32.05114	46.2019 44.44017	Sasanian mint (AT) Rare Abbasid mint during al-Mansur's reign, situated close to Kufah (138-146 AH).
al Rahba Arrajan	al-rahba arrajan	Mayadin	35.005 30.65388	40.4235 50.27472	A mint in Syria, on the Euphrates "[Bizamqubadh] was an alternative name for Arrajân in Fars, and also appears to have struck Arab-Sasanian issues." <a href="#">Lloyd (2023)</a>
Hulwan	hulwan		34.465	45.855	"This mint-name is that of a district (astân) in Irâq, which covered an area to the north-east of Baghdad. Le Strange notes that this district was also known as Shâd Firûz - presumably its former Sasanian name. The town of Hulwân itself evidently lay just over the border in Jibál province, although at this period it appears to have been included with 'Irâq for administrative purposes." <a href="#">Lloyd (2023)</a>
Madinat Elvira Mah al Basrah	madinat_elvira mah-al-basrah	Nihavand, Iran	37.23105 34.18879	-3.70848 48.37046	The archaeological site of Madinat Ilbira. "The term is the Arabic name for Nihavand." (British Museum x107840)
Mah al Kufah	mah-al-kufah	Dinawar, Iran	34.583333	47.43333	"Mah al-Kufah = Dinawar (sometimes incorrectly written Daynawar) in the middle ages was one of the most important towns in Djibal (Media); it is now in ruins. The exact location is 34 degrees 35 minutes Lat. N. and 47 degrees 26 minutes E. Long. (Greenwich)." <a href="#">Lockhart (2012)</a>
Masabadhan	masabadhan		33.52303	46.86539	A district with capital al-Sirawan; the location of al-Sirawan is from <a href="#">Cornu (1983)</a> 's atlas.
Maysan Panjshir Rev-Ardashir	maysan panjshir rev-ardashir	Naysan Panjshir Valley Bushehr	30.8093 35.254095 28.9119	47.5628 69.456014 50.8367	Sasanian mint Maysan (MY) Panjshir Valley, modern-day Afghanistan Sasanian mint (LYW/ LYWARTHST/KWN LY-W/GNC LYW); the location is from FLAME
Roda Sarakhs	roda sarakhs	Sarakhs, Iran	42.26478 36.5449	3.17887 61.1577	A carolingian mint in Rosas, Spain "A town in Khurâsân located roughly midway between Marw and Abrashahr. Sarakhs lay on the eastern bank of the Mashhad river, about forty or fifty miles north of its confluence with the Herât river." <a href="#">Lloyd (2023)</a>
Uman	oman	Oman	23.51234	58.27000	<a href="#">Lloyd (2023)</a> : "Modern Oman on the Persian Gulf."

Appendix Table D.1: Manual mint codings I: new mints

Nomisma ID	Nomisma Note	Latitude	Longitude	Note
al-Abbasiyah	"Earfly Abbasid site in North Africa"	35.62183407	10.18089991	According to <a href="#">Abdul Wahab (2012)</a> , three miles south-east of Kairouan.
al-Furat	"In the district of Shadh Bahman in Iraq, but its exact location unknown. Klat, 16."	30.53269083	47.87593421	Geocodes based on Fig. 11 in <a href="#">Morony (1982)</a> .
al-Madinat Mutawakkiliyah	al- "al-Madinat al-Mutawakkiliyah is just north of Sammara and was built by the Abbasids."	34.2621862	43.85500034	Close to Samarra, Iraq
al-Manadhir	"The name of two districts, with tehir chief-towns, named Greater Manadhir & Little Manadhir in Khuzistan, Iran"	31.97753445	48.69644554	<a href="#">Lloyd (2023)</a> : "Manâdhîr was a district within the province of Khuzistân, situated between the Dizfûl and Du-jayl rivers above their confluence north of Ahwâz. It was apparently divided into two parts named Greater and Little Manâdhîr, each containing a chief town with the same name."
al-Mubarakah basid)	(Ab- "Some place in North Africa"	36.30565739	10.13850323	Unknown location, coding it to modern-day Tunisia
al-Samiyah	"Al-Samiya was in the Shatt al-Arab area of lower Iraq."	30.6617666	47.78548511	Coding to Shatt al-Arab.
Bihqubadh af-Asfal	"Lower Bihqubach (sic) in Iraq on the Euphrates"	31.56718959	45.22725183	<a href="#">Lloyd (2023)</a> : "The three districts of Upper, Middle and Lower Bihqubâdh were located in 'Iraq to the west of the Euphrates. Bihqubâdh is taken from the Persian meaning "the good land of king Qubâdh. Al-Asfal means 'the lower,' and covered the land next to the Euphrates where it entered the Great Swamp." Coordinates based on Fig. 8 of <a href="#">Morony (1982)</a> .
Dastawa Ma'din Bajunays	"South of Qazvin" "Province north of Lake Van"	35.75554989 40.223509	50.08839336 43.8355181	Location very approximate in western Armenia.
Mani	Klat is uncertain of its location although the prefix Mah occurs in older names for Dinavar & Nihavand. Quarter of Jibal. Klat"	34.38582341	47.97904114	<a href="#">Lloyd (2023)</a> puts it either at Mah al Basrah (Nihavand) or Mah al Kufa (Dinavar). Our chosen geocode is halfway between the two.
Nahr Tira	"Exact location on the river or canal of the same name in Khuzistan not know. Klat, p.. 18"	30.8755	49.7131	From FLAME.
Qumis	"A small province which stretches along the foot of the Great Alburz chain of mouintains. Klat, p. 17."	35.96088616	54.03571139	Wikipedia "Qumis (region)"
Surraq	"Surraq or DAWRAQ (or Dawraq al-Fors), name of a district (k̄'ra; Moqaddasf', pp. 406-07), also known as Sorraq, and of a town that was sometimes its chef-lieu in medieval Islamic times."	30.65094882	48.67463446	Coding to Shadegan, Iran.
Tabaristan	"Tabaristan, also known as Tapuria, was the name of the former historic region in the southern coasts of Caspian Sea roughly in the location of the northern and southern slopes of Elburz range in Iran."	36.5656	53.0588	From FLAME
Tudghah	"Unknown location in Morroco"	31.523	-5.5313	<a href="#">al 'Ush (1982)</a> identifies it with "Todr'a", and cites <a href="#">Renou (1846)</a> (incorrectly as authored by "Lavoix") saying that it was located fourty kilometers west of Sijilmasa, at a river of the same name. That would place it close to Tinghir, Morocco.

Appendix Table D.2: Manual mint codings II: geocoding existing Nomisma mints

Hoard Name	Date	# Coins described	Reference	Location	Latitude	Longitude
Abu Saida	ca. 721	15	Royal Numismatic Society (1975)	Qaryat Abū Ṣaydā as Ṣaghīrah, Iraq	33.924	44.761
Afaq	773-932	1674	Gachet (1993)	Afak, Iraq	32.064	45.247
Afghanistan	86-112 AH	131	Album (1971)	Afghanistan	33.000	66.000
Agrigento	699-828	370	Lagumina (1904)	Agrigento, Italy	37.311	13.577
Al Raqa	698-750	1187	Sears (2000)	Ar Raqqah, Syria	35.953	39.008
Al Wajh		35	Hakiem (1977)	Al Wajh, Saudi Arabia	26.246	36.452
Al-Khobar	tpq 784/85	42	Noonan (1980)	Khobar, Saudi Arabia	26.279	50.208
Amman	AH 79-125	12	Kirkbride (1951)	Amman, Jordan	31.955	35.945
Āmūdā I	tpq 874	646	Ilisch (1990)	‘Āmūdā, Syria	37.104	40.930
Āmūdā II	779-941	643	Ilisch (1990)	‘Āmūdā, Syria	37.104	40.930
Awarta (Nablus I )	602-685	29	Dajani (1951)	‘Awartā, Palestine	32.161	35.284
Bab Tuma	tpq 748	854	Gyselen and Kalus (1983)	Damascus, Syria	33.510	36.291
Babylone, Egypt	157 AH - 241 AH	114	Jungfleisch (1949)	Cairo, Egypt	30.063	31.250
Buseyra	769-943	3108	Al Chomari (2020)	Al Buṣayrah, Syria	35.156	40.427
Capernaum		288	Wilson (1989)	Kfar Nahum, Israel	32.881	35.575
Damascus	548-736	3815	al 'Ush (1972b)	Damascus, Syria	33.510	36.291
Damascus	679-721	546	al 'Ush (1954-1955)	Damascus, Syria	33.510	36.291
Denizbaji	tpq 811	2496	Artuk (1966)	Denizbaci, Turkey	37.139	38.390
Diyarbakir	802-902	224	Ilisch (1979)	Diyarbakır, Turkey	37.914	40.217
En Nebk	tpq 747	102	Royal Numismatic Society (1977)	An Nabk, Syria	34.024	36.728
Gazira	3rd to 9th century	2820	Gyselen and Nègre (1982)	Al Jazīrah, Iraq	36.000	42.000
Godhlaniya		127	American Numismatic Society (2023)	Syrian Arab Republic, Syria	35.000	38.000
Hamah	tpq 950	214	Ilisch (1990)	Hamāh, Syria	35.132	36.758
Huszt		368	Fomin and Kovács (1987)	Khust, Ukraine	48.172	23.298
Iran 1970	tpq 820	668	Noonan (1980)	Islamic Republic of Iran, Iran	32.000	53.000
Isfahan	777-936	582	Lowick (1975)	Isfahan, Iran	32.652	51.675
Jarash		36	Treadwell and Rogan (1994)	Jarash, Jordan	32.281	35.899
Jazira (Illisch)	tpq 886	48	Ilisch (1990)	Al Jazīrah, Iraq	36.000	42.000
Kerman	about 632-651	43	Heidemann et al. (2014)	Kerman, Iran	30.283	57.079
Khdir Elias	tpq 1014	2865	Al-Naqshbandi (1954)	Republic of Iraq, Iraq	33.000	44.000
Khorasan	705-774	196	Hebert (1966)	Mashhad, Iran	36.298	59.606
Khirbat al-Minya	716-734	2	Schneider (1952)	Horbat Minnim, Israel	32.865	35.536
Kufah	tpq 808/09	178	Noonan (1980)	Kufa, Iraq	32.051	44.440
Marv	tpq 815	855	Khodzhanizayev and Treadwell (1998)	Mary, Turkmenistan	37.594	61.830
Near Fez		36	Royal Numismatic Society (1978)	Fès, Morocco	34.033	-5.000
Nippur (Bates)	704-794	76	Bates (1978)	Atṭālā Nafar, Iraq	32.136	45.221
Nippur (Sears)	597-743	97	Sears (1994)	Atṭālā Nafar, Iraq	32.136	45.221
North Africa (Spain?)	tpq 860	87	Hoge (1997)	Kairouan, Tunisia	35.678	10.096
Orif, Nablus	691-742	19	Ma'ayeh (1962)	Urif, Palestine, West Bank	32.159	35.224
Ouenza	789-798	12	Troussel (1942)	Ouenza, Algeria	35.953	8.129
Qamishliyyah	tpq 816	1519	Gyselen and Kalus (1983)	Al Qāmishlī, Syria	37.052	41.231
Ra's al-Khaimah	921-975	43	Lowick and Nisbet (1968)	Ras Al Khaimah City, UAE	25.790	55.943
Sinaw	589-841	948	Lowick (1983)	Sināw, Oman	22.501	58.030
Tabaristan	about 718-760	810	Malek (1996)	Mazandaran Province, Iran	36.250	52.333
Tiflis	ca. 280-330 AH	112	Bartolomei (1857)	Tbilisi, Georgia	41.694	44.834
Umm Hajarah	tpq 808/09	408	al 'Ush (1972a)	Umm Hajarah, Syria	36.195	41.074
Utaifyah	154-193 AH	294	al Bakri (1973)	Baghdad, Iraq	33.341	44.401
Volubilis	tpq 125 AH (742)	232	Eustache (1956)	Oualili, Morocco	34.073	-5.555
Yarubiyah	tpq 815/816	1415	American Numismatic Society (2023)	Al Ya'rubiyyah, Syria	36.811	42.062
Zahu/Zakho	tpq 808-9	3306	Al-Naqshbandi (1949, 1950, 1951, 1952)	Zaxo, Iraq	37.149	42.686

Appendix Table D.3: Near East and North Africa Hoards

Hoard name	Date	# Coins described	Reference	Location	Latitude	Longitude
Alcaudete	698-734	14	Cano Ávila (1989)	Alcaudete	N 37° 35' 27"	W 4° 4' 56"
Algeciras	710-727	29	Canto García and Martín Escudero (2009)	Algeciras	N 36° 7' 59"	W 5° 27' 1"
Alhama	770-876	459	Codera y Zaidín (1892)	Alhama	N 37° 0' 24"	W 3° 59' 22"
Arrabal Occidental	929-1021	373	Canto García et al. (2020a)	Cordoba	N 37° 53' 29"	W 4° 46' 21"
Azanuy	699-733	6	Codera y Zaidín (1913)	Azanuy	N 41° 59' 10"	E 0° 18' 58"
Badajoz	927-1011	99	Prieto (1934)	Badajoz	N 38° 52' 40"	W 6° 58' 14"
Baena	699-754	160	Martín Escudero (2001)	Baena	N 37° 39' 22"	W 4° 20' 4"
Barrio de los Olivos Borrachos	941-1004	165	Marcos Pous and Vicent Zaragoza (1992)	Cordoba	N 37° 53' 29"	W 4° 46' 21"
Benferri	941-958	12	Doménech Belda (1997)	Benferri	N 38° 8' 28"	W 0° 57' 43"
Bormujos	929-965	11	Cano Ávila (2016)	Bormujos	N 37° 21' 41.9"	W 6° 06' 38.1"
Calle San Jose	936-950	16	Doménech Belda (1997)	Xàtiva	N 38° 59' 25"	W 0° 31' 6"
Calle San Pedro	967-1031	19	Canto García and Jabłońska (2019)	Murcia	N 37° 59' 13"	W 1° 7' 48"
Calle Santa Julia	929-1012	263	Segovia Sopo (2014)	Mérida	N 38° 54' 58"	W 6° 20' 37"
Campo de la Verdad	775-912	176	Martín and Martín (2006)	Cordoba	N 37° 53' 29"	W 4° 46' 21"
Carmona	698-753	146	Canto García and Escudero (2012)	Carmona	N 37° 28' 17"	W 5° 38' 46"
Castillejos de Quintana	933-1010	39	Cravioto (2016)	Castillejos de Quintana	N 36° 46' 58.7"	W 4° 41' 30.9"
Castro Marim	788-885	53	Rodrigues Marinho (1995)	Castro-Marim	N 37° 13' 14"	W 7° 26' 36"
Cerro da Villa	831-900	239	Heidemann et al. (2018)	Cerro da Villa	N 37° 4' 48"	W 8° 7' 13"
Crevillent	770-1269	34	Doménech Belda and Treliš (1990)	Crevillent	N 38° 14' 59"	W 0° 48' 35"
Cihuela	912-1016	296	Navascués y de Palacios (1961a)	Cihuela	N 41° 24' 26"	W 1° 59' 59"
Consuegra	835-1010	173	Martín Escudero (2011)	Consuegra	N 39° 27' 44"	W 3° 36' 28"
Cordoba I	817-1010	25	Navascués y de Palacios (1961b)	Cordoba	N 37° 53' 29"	W 4° 46' 21"
Cordoba II	933-953	328	Navascués y de Palacios (1958)	Cordoba	N 37° 53' 29"	W 4° 46' 21"
Cordoba III	933-1021	379	Navascués y de Palacios (1958)	Cordoba	N 37° 53' 29"	W 4° 46' 21"
Cordoba IV	708-796	119	Canto García (1988)	Cordoba	N 37° 53' 29"	W 4° 46' 21"
Cova del Randerro	768-835	54	Doménech Belda (1997)	Pedreguer	N 38° 47' 35"	E 0° 2' 2"
Cuba	932-1010	9	Martín Escudero (2011)	Cuba	N 38° 10' 24"	W 7° 53' 46"
Domingo Perez	767-865	367	Martín and Martín (2002)	Domingo Pérez	N 37° 29' 45"	W 3° 30' 33"
Elche	841-1173	316	Doménech Belda (1992)	Elche	N 38° 15' 43"	W 0° 42' 3"
Electromecanicas I	941-1005	169	Marcos Pous and Vicent Zaragoza (1992)	Cordoba	N 37° 53' 29"	W 4° 46' 21"
Electromecanicas II	928-1016	102	Marcos Pous and Vicent Zaragoza (1992)	Cordoba	N 37° 53' 29"	W 4° 46' 21"
El Pedroso	928-1021	144	Cano Ávila and Martín Gómez (2006)	Hacienda Montegil, El Pedroso	N 37° 43' 51.9"	W 5° 51' 39.8"
El Pedroso III	832-1021	144	Cano Ávila and Gómez (2008)	El Pedroso	N 37° 51' 0"	W 5° 46' 0"
El Rebollar	810-818	5	Salido Domínguez et al. (2020)	Boalo	N 40° 42' 57"	W 3° 54' 59"
Finca la Marquesa	941-1036	246	Doménech Belda (1997)	Montilla	N 37° 36' 07.2"	W 4° 37' 11.7"
Fontanar	941-977	764	Canto García and Martín Escudero (2007)	Cordoba	N 37° 53' 29"	W 4° 46' 21"
Fuente de Cantos	837-883	15	Segovia Sopo (2006)	Fuente de Cantos	N 38° 15' 0"	W 6° 18' 0"
Hospital Militar	970-1032	23	Martín Escudero (2003)	Zaragoza	N 41° 39' 21"	W 0° 52' 38"
Huesca	710-756	100	Martín Escudero (2012)	Huesca region	N 37° 39' 56.1"	W 4° 23' 41.6"
Izcar	778-886	50	Ariza Armada (1988)	Cortijo de Izcar	N 37° 15' 27"	W 4° 18' 30"
Iznajar	768-912	1047	Canto García and Marsal Moyano (1988)	Iznajar	N 37° 15' 27"	W 4° 18' 30"
Jaen	711-713	4	González García and Martínez Chico (2017)	Jaen region	N 37° 15' 27"	W 4° 18' 30"
Jerez de los Caballeros	770-782	277	Canto García (2019)	Jerez de los Caballeros	N 38° 19' 14"	W 6° 46' 21"
La Almagra	820-822	7	Museo Arqueológico de Murcia (2014)	La Almagra	N 38° 2' 15"	W 1° 25' 57"
La Fuensanta	770-812	18	Cravioto and Ayala (1995)	Cerro la Fuensanta	36° 55' 13.7"N	4° 23' 23.7"W
Lantejuela	773-887	175	Ruiz Asencio (1967)	La Lantejuela	N 37° 19' 17.5"	W 5° 13' 27.6"
La Rinconada	770-912	315	Cano Ávila and Martín Gómez (2005)	La Rinconada	N 37° 29' 10"	W 5° 58' 51"
Las Torres	757-976	18	Martínez Enamorado (2004)	Gavilanes	N 40° 15' 44"	W 4° 51' 30"
L'Elca	933-950	31	Doménech Belda (1997)	Oliva	N 38° 55' 10"	W 0° 7' 9"
Lleida	770-1463	40	Soler Balaguer (1993)	Lleida	N 41° 37' 7"	E 0° 34' 29"
Lora del Rio	941-1021	165	Pellicer i Bru (1985)	Lora del Rio	N 37° 39' 32"	W 5° 31' 39"
Los Villares	942-1028	112	Valle (1987)	Caudete de las Fuentes	N 39° 33' 34"	W 1° 16' 42"

Appendix Table D.4: Hoards in al-Andalus, Part I

Hoard name	Date	# Coins described	Reference	Location	Latitude	Longitude
Madinat Iyyuh	711-856	20	Doménech Belda and Gutiérrez Lloret (2006)	El Tolmo de Minateda	N 38° 28' 34"	W 1° 36' 20"
Marroquies Altos	933-1010	270	Asencio (1962)	Jaen	N 37° 46' 9"	W 3° 47' 25"
Marroquies Bajos	941-1015	201	Canto García et al. (1997)	Jaen	N 37° 46' 9"	W 3° 47' 25"
Martos	817-875	24	Canto García (1993)	Cortijo del Mimbre	N 37° 38' 26.0"	W 3° 57' 04.9"
Merida	726-901	60	Rodríguez Palomo and Martín Escudero (2022)	Merida	N 38° 54' 58"	W 6° 20' 37"
Mertola	932-1036	81	Poiares (2000)	Mertola	N 37° 38' 34"	W 7° 39' 40"
Mijas Costa	932-976	533	Ayala Ruiz and Gozalbes Cravioto (1996)	La Cala de Mijas	N 36° 33' 56"	W 4° 40' 11"
Montellano	949-1010	23	Cano Ávila (2014)	Montellano	N 37° 00' 06.1"	W 5° 33' 02.1"
Moraleja	767-854	16	Álvarez (1993)	Moraleja	N 40° 0' 58"	W 6° 41' 51"
Moreria	857-1015	134	Palma García and Segovia Sopo (2007)	Merida	N 38° 54' 58"	W 6° 20' 37"
Niebla	805-884	36	Cano Ávila and Martín Gomez (2011)	Sierra de Alcantara	N 37° 28' 33.8"	W 6° 38' 36.2"
Osuna	954-1022	3	Alfaro Asins (1992)	Osuna	N 37° 14' 15"	W 5° 6' 11"
Parque Cruz conde	852-1021	3341	Canto García et al. (2020b)	Cordoba	N 37° 53' 29"	W 4° 46' 21"
Partida de Atzbares	941-970	26	Doménech Belda (1997)	Atzavares Baix (Elche)	N 38° 15' 43"	W 0° 42' 3"
Pascul de Gayangos	778-1204	159	Marinho (1993)	Algarve		
Pinos Puente	770-816	169	Martín Escudero (2011)	Pinos Puente	N 37° 15' 3"	W 3° 44' 58"
Pozoblanco	948-976	15	Marcos Pous and Vicent Zaragoza (1992)	Pozoblanco	N 38° 22' 44"	W 4° 50' 53"
Priego de Cordoba	770-856	54	Ávila and Pareja (1999)	Priego de Cordoba	N 37° 26' 17"	W 4° 11' 42"
Puebla de Cazalla	770-892	911	Ibrahim and Canto García (1991)	La Puebla de Cazalla	N 37° 13' 17"	W 5° 18' 41"
Puente de Miluze	934-1057	164	Canto García (2001)	Pamplona	N 42° 49' 0"	W 1° 38' 35"
Recopolis	772-785	9	Priego and Enciso (2016)	Recopolis	N 40° 19' 15.1"	W 2° 53' 37.7"
Sagrada Familia	945-1012	316	Marcos Pous and Vicent Zaragoza (1992)	Cordoba	N 37° 53' 29"	W 4° 46' 21"
San Andres de Ordoiz	782-908	167	Uranga (1950)	Estella-Lizarra	N 42° 40' 19"	W 2° 01' 56"
Saqunda	707-930	467	Martín Escudero et al. (2023)	Cordoba	N 37° 53' 29"	W 4° 46' 21"
Sevilla	711-1011	497	Saenz-Diéz (1993)	Sevilla	N 37° 22' 58"	W 5° 58' 23"
Sierra Cazorla	928-1021	237	Pellicer i Bru (1982)	Sierra Cazorla	N 37° 54' 45"	W 2° 58' 34"
Silves	770-875	79	Miles (1960)	Silves	N 37° 11' 21"	W 8° 26' 17"
Sinarcas	942-1037	57	Arroyo Ilera (1989)	Sinarcas	N 39° 44' 0"	W 1° 14' 0"
Solar del Museo Arqueologico	953-1007	16	Marcos Pous and Vicent Zaragoza (1992)	Cordoba	N 37° 53' 29"	W 4° 46' 21"
South France	692-886	204	Parvére (2014, 2019)	South France		
Spain single finds (felus)	699-901	57	Martín Escudero (2012)	Spain		
Tarancon	929-1014	451	Canto García (2014)	Tarancon	N 40° 0' 30"	W 3° 0' 26"
Teatro romano	805-819	25	Segovia Sopo and Jiménez (2011)	Merida	N 38° 54' 58"	W 6° 20' 37"
Tignar	864-913	35	Motos Guirao and Díaz García (1985)	Albolote	N 37° 13' 51"	W 3° 39' 18"
Tijan	976-1021	377	Fontenla Ballesta (1998)	Sierra de Cabrera	N 37° 06' 30.3"	W 1° 55' 49.2"
Trujillo	711-1014	384	Navascués y de Palacios (1957)	Trujillo	N 39° 27' 28"	W 5° 52' 55"
Valencia de Ventoso	933-1006	7	Grañeda Miñón (2021)	Valencia del Ventoso	N 38° 16' 0"	W 6° 28' 0"
Valeria	936-1009	250	Puertas (1982)	Valeria	N 39° 47' 0"	W 2° 9' 0"
Valle de Guadajoz	931-1013	204	Ortega et al. (2006)	Fuentidueña (Baena)	N 37° 43' 42.1"	W 4° 16' 54.3"
Vega Baja	-200-1500	184	Priego (2020)	Toledo	N 39° 51' 29"	W 4° 1' 21"
Vera	941-1024	370	Doménech Belda (1997)	Vera	N 37° 14' 36"	W 1° 51' 32"
Villaviciosa	705-817	1361	Peña Martín and Vega Martín (2007)	Villaviciosa de Cordoba	N 38° 5' 0"	W 5° 1' 0"
Yecla	705-726	5	Codera y Zaidín (1913)	Yecla	N 38° 39' 18"	W 1° 7' 46"
Zafra	789-892	43	Canto García (2019)	Zafra	N 38° 25' 31"	W 6° 25' 2"
Zamora	943-999	10	Cerrato and Esquivel (2019)	Zamora	N 41° 30' 22"	W 5° 44' 40"

Appendix Table D.5: Hoards in al-Andalus, Part II

Hoard Name	Country	Reference	Latitude	Longitude
Ankara 1960?	Turkey	Pennas (1991) 122	39.9388	32.8594
Argos 1983	Greece	Pennas (1991) 8	37.6353	22.7277
Ayies Paraskies/Crete 1962	Greece	Pennas (1991) 59 / Füeg (2007)	35.209	25.2041
Bajagic	Croatia	Mirnik (1981)	43.7581	16.6657
Balchik Stray Find I	Bulgaria	Curta (2005)	43.4119	28.1628
Berezeni	Romania	Oberländer-Târnoveanu (2001) p.67	46.378	28.1523
Bratimir	Bulgaria	Pennas (1991) 90	43.8682	26.7044
But	Italy	Arslan (2005) 2280	46.4768	13.0246
Byala 1954	Bulgaria	Pennas (1991) 73	42.8739	27.8886
Calarasi 1947	Romania	Pennas (1991) 111, Dimian (1957)	44.2029	27.3115
Camarina	Italy	Arslan (2005) 6170	36.8279	14.5241
Camarina ed. 18	Italy	Arslan (2005) 6185	36.8279	14.5241
Camarina ed. 1a	Italy	Arslan (2005) 6181	36.8279	14.5241
Camarina ed. 6	Italy	Arslan (2005) 6182	36.8279	14.5241
Capo Schiso 1950	Italy	Arslan (2005) 6910	37.8244	15.2684
Chryse/Edhessa 1935	Greece	Pennas (1991) 50 / Füeg (2007)	40.81	22.0446
Cleja	Romania	Pennas (1991) 113, Dimian (1957)	46.4019	26.9427
Constanta Stray I	Romania	Dimian (1957)	44.1777	28.6442
Constanta Stray II	Romania	Dimian (1957)	44.1777	28.6442
Corinth 15 May 1934 (South Basilica)	Greece	Pennas (1991) 3	37.9373	22.932
Corinth 1934	Greece	Pennas (1991) 7	37.9373	22.932
Corinth 1965 (Roman Bath)	Greece	Pennas (1991) 1	37.9373	22.932
Corinth 1965 (Roman Bath)	Greece	Pennas (1991) 4 (BCH 90, 1966, 751, 754)	37.9373	22.932
Corinth (St John's monastery)	Greece	Pennas (1991) 9	37.9373	22.932
Didyma (single find)	Turkey	Baldus (2006)	37.3731	27.2639
Drobeta - Turnu Severin	Romania	Oberländer-Târnoveanu (2001) p.68	44.6425	22.6587
Drobeta 1928	Romania	Oberländer-Târnoveanu (2001) p.67	44.6425	22.6587
Dubravice	Croatia	Mirnik (1981)	43.8506	15.9398
Dubrovnik 1982	Croatia	Mosser (1935) p.71 ("Ragusa"), Mirnik (1981) 359	42.6489	18.094
Elazig	Turkey	Füeg (2007)	38.6747	39.2229
Elbistan	Turkey	Füeg (2007)	38.2016	37.1924
Eskisehir	Turkey	Füeg (2007)	39.7743	30.5138
Gabrica	Bulgaria	Sophoulis (2011)	43.5082	26.9736
Govora	Romania	Oberländer-Târnoveanu (2001) p.68	45.0681	24.2302
Hadrianoupolis Acropolis Kimistene	Turkey	Lafli et al. (2016)	40.9231	32.4867
Hadrianoupolis Basilica A	Turkey	Lafli et al. (2016)	40.9231	32.4867
Hadrianoupolis Bath A	Turkey	Lafli et al. (2016)	40.9231	32.4867
Hadrianoupolis Bath B	Turkey	Lafli et al. (2016)	40.9231	32.4867
Hadrianoupolis Building 4	Turkey	Lafli et al. (2016)	40.9231	32.4867
Hadrianoupolis Domus	Turkey	Lafli et al. (2016)	40.9231	32.4867
Hagios Nikolaos, Hydra (Greece)	Greece	Pennas (1996), p. 270	37.3011	23.3967
Iatrus 1962	Bulgaria	Pennas (1991) 77	43.6262	25.587
Iatrus 1975	Bulgaria	Pennas (1991) 75	43.6262	25.587
Ipsala	Turkey	Füeg (2007)	40.9201	26.3828
Istria Stray Finds 869-877	Croatia	Miškć (2002)	45.1439	13.8259
Kavaklı	Turkey	Ünal (2018)	37.755	28.305
Kenchreai 1963	Greece	Pennas (1991) 2	37.8833	22.9873
Kozojedy, Bohemia	Czechia	Profantova (2009)	50.2548	13.8153
Kyme near Aliaga	Croatia	Carroccio, cited by Morrisson (2017)	38.7592	26.9367
Kyulevcha Grave	Bulgaria	Curta (2005)	43.2559	27.111
Lagbe	Turkey	Füeg (2007), Newell (1945)	36.8276	30.4112
Libice, Bohemia	Czechia	Profantova (2009)	50.1285	15.1815
Liopesi (around 1946)	Greece	Pennas (1991) 35 / Vryonis (1971)	37.9545	23.8521
Ljubimets	Bulgaria	Dimian (1957), Sophoulis (2011)	41.8466	26.0781
Luka Krnicka	Croatia	Miškć (2002)	44.9723	14.0171
Macvanska Mitrovica	Serbia	Pennas (1991) 72	44.9655	19.5975
Malthi (Dorion)	Greece	Pennas (1991) 6	37.267	21.8824
Maluk Povorets 1934	Romania	Pennas (1991) 74	43.7133	26.7652
Matera Piazza S. Francesco	Italy	Arslan (2005) 4140	40.6654	16.6087
Medias	Romania	Oberländer-Târnoveanu (2001) p.68, Dimian (1957)	46.1621	24.3567
Melito Porto Salvo	Italy	Arslan (2005) 0450	37.9197	15.7857
Mikulcice	Czechia	Profantova (2009)	48.8167	17.0516
Monemvasia Stray Find	Greece	Pennas (1996), p. 270	36.6876	23.0559
Naxos	Greece	Füeg (2007)	37.0567	25.4638
Nea Syllata/Chalkidiki 1977	Greece	Pennas (1991) 52	40.3275	23.136
Nin	Croatia	Mirnik (1981)	44.2392	15.1791
Odartsı	Bulgaria	Sophoulis (2011)	43.44	27.9616
Osava near Ram	Serbia	Füeg (2007)	44.8006	21.3433
Osvetimany	Czechia	Profantova (2009)	49.0562	17.2496

Appendix Table D.6: Hoards with Byzantine coins, Part I

Hoard Name	Country	Reference	Latitude	Longitude
Oszony, Komarom	Hungary	Oberländer-Târnoveanu (2001) p.68	47.7295	18.1751
Piran	Italy	Arslan (2005) 2808	45.5279	13.5694
Pliska	Bulgaria	Füeg (2007)	43.362	27.1228
Prague, Tynsky dur	Czechia	Profantova (2009)	50.073	14.4286
Rakvice (Breclav)	Czechia	Profantova (2009)	48.8559	16.813
Rasova 1934	Romania	Pennas (1991) 112, Dimian (1957)	44.2403	27.9414
Reggio Calabria	Italy	Arslan (2005) 0670	38.0947	15.6455
Rhodos Stray Find 859	Greece	Kasdagli (2018)	36.436	28.2221
Rhodos V.12 (Kattavia)	Greece	Kasdagli (2018)	35.9534	27.7683
Rome / Tiber	Italy	Morrisson and Barrandon (1988)	41.8882	12.4768
Salamis (South of Amphitheatre, 1964-1974)	Turkey	Füeg (2007)	35.1914	33.8979
Santorini (Thira) 1895-1902	Greece	Pennas (1991) 57	36.4058	25.4588
Sicily (Fagerlie)	Italy	Fagerlie (1974)	37.5732	14.2114
Songurlu / Mosser	Turkey	Füeg (2007) / Mosser (1935)	40.1627	34.3767
Stare Mesto	Czechia	Profantova (2009)	49.0727	17.4463
Stimanga 1955	Greece	Pennas (1991) 5 (BCH 80, 1956, 256)	37.909	22.6989
Streda nad Bodrogom	Slovakia	Profantova (2009)	48.3785	21.758
Syracuse Via G. Di Natale	Italy	Arslan (2005) 7335	37.0724	15.2845
Tegani/Samos 1914	Greece	Pennas (1991) 58	37.6904	26.9417
Telerig Stray Miliaresion	Bulgaria	Curta (2005)	43.8457	27.671
Thessaloniki	Greece	Füeg (2007)	40.652	22.9304
Thessaloniki 1891	Greece	Pennas (1991) 51	40.652	22.9304
Tichilesti	Romania	Dimian (1957)	45.1291	27.9045
Tralleis/Aydin	Turkey	Ünal (2015)	37.8591	27.8335
Trilj	Croatia	Mirnik (1981)	43.6187	16.7241
Unknown Provenance (Turkey) 1987	Turkey	Pennas (1991) 123	39.2963	32.9327
Urluia 1936	Romania	Dimian (1957), Sopoulis (2011)	44.1016	27.9132
Velul lui Trajan	Romania	Pennas (1991) 105	44.1647	28.4621
Velul lui Trajan 1999/2000	Romania	Măncu-Adameșteanu (2016)	44.1647	28.4621
Voila, Romania	Romania	Dimian (1957)	45.818	24.8405
Vukovar - Ljeva Bara	Croatia	Mirnik (1981)	45.3382	19.0079
Yakimovo (Progorelets) 1960	Bulgaria	Pennas (1991) 91	43.6337	23.3621
Yunak	Bulgaria	Pennas (1991) 76	43.0763	27.6109

Appendix Table D.7: Hoards with Byzantine coins, Part II

Hoard Name	Date	Reference	Location	Latitude	Longitude
Aalst	840-855	Bijsterveld et al. (2000)	Aalst	51.39611	5.477
Aalsum	814-855	Morrison and Grunthal (1967)	Aalsum	53.3403	6.00538
Achlum	768-840	Morrison and Grunthal (1967)	Achlum	53.14779	5.48239
Alfocea	943-977	Parvéria (2018)	Alfocea	41.724097	-0.953131
Amerongen	768-877	Coupland (2014)	Amerongen	52.0025	5.46024
Ampurias	768-814	Doménech-Belda et al. (2013)	Ampurias	42.134477	3.111418
Andalusia	814-848	Parvéria (2018)	Andalusia		
Angeac-Champagne	840-877	Duplessy (1985)	Angeac-Champagne	45.60769	-0.29771
Angers I	814-840	Morrison and Grunthal (1967)	Angers	47.4707	-0.55324
Angers II (Saint-Julien)	819-877	Haertle (1997)	Angers	47.4707	-0.55324
Anglure	864-887	Morrison and Grunthal (1967)	Anglure	48.58345	3.81356
ANS find	768-922	Morrison and Grunthal (1967)	France		
Anse I	818-823	Guillemain (1993)	Anse	45.937639	4.717512
Anserall	768-815	Doménech-Belda et al. (2013)	Anserall	42.37829	1.456511
Apremont	793-822	Morrison and Grunthal (1967)	Apremont-sur-Allier	46.906	3.048
Aquitaine	814-887	Coupland (1991)	Aquitaine		
Ardres	888-923	Haertle (1997)	Ardres	50.856432	1.978355
Arras	843-922	Morrison and Grunthal (1967)	Arras	50.29039	2.778414
Ashdon	843-898	Blackburn (1989)	Ashdon	52.05544	0.31373
Aspres-lès-Corps	901-924	Schulze (1984)	Aspres-lès-Corps	44.80162	5.98217
Assebroek	843-877	Morrison and Grunthal (1967)	Assebroek	51.18793	3.27363
Assen	800-911	Morrison and Grunthal (1967)	Assen	52.99421	6.55957
Auxerre	813-877	Haertle (1997)	Auxerre	47.796587	3.570535
Auzeville	814-848	Sarah et al. (2016)	Auzeville	43.5257	1.49342
Avallon	843-877	Coupland (2020)	Avallon	47.488712	3.907758
Avignon	843-887	Morrison and Grunthal (1967)	Avignon	43.95344	4.80601
Bakonyszombathely	898-973	Morrison and Grunthal (1967)	Bakonyszombathely	47.47208	17.96018
Balloo	843-855	Haertle (1997)	Balloo	54.472363	-5.69076
Barbentane	814-840	Morrison and Grunthal (1967)	Barbentane	43.89948	4.74635
Barcelona	814-840	Doménech-Belda et al. (2013)	Barcelona	41.395937	2.174552
Bassenheim	814-876	Coupland (2019)	bassenheim	50.359028	7.462443
Bátorove Kosihy	888-950	Kovács (1989)	Bátorove Kosihy	47.83083	18.41083
Beaumont	843-877	Morrison and Grunthal (1967)	Beaumont (Chalo	48.409016	2.042742
Saint Mars)					
Bel-Air	768-814	Morrison and Grunthal (1967)	Lausanne	46.57957	6.605807
Bellpuig	887-928	Doménech-Belda et al. (2013)	Bellpuig	41.626531	1.011607
Belvédet	768-840	Morrison and Grunthal (1967)	Belvédet	44.08433	4.36426
Bikbergen	814-855	Cruijssen and der Veen (2015)	Bikbergen	52.287933	5.196186
Bjerndrup	817-924	Coupland (2020)	Bjerndrup	54.93391	9.32867
Blendecques	814-840	Coupland (2020)	Blendecques	50.716982	2.282169
Bligny	814-887	Morrison and Grunthal (1967)	Bligny	48.1725	4.6172
Blois	898-940	Moesgaard (1997)	Blois	47.58696	1.33139
Bondeno	768-814	Morrison and Grunthal (1967)	Bondeno	44.89098	11.41096
Bonnevaux	800-887	Morrison and Grunthal (1967)	Bonnevaux	44.367837	4.030289
Borne	794-813	Coupland (2011a)	Borne	52.30137	6.75779
Bourges	840-877	Morrison and Grunthal (1967)	Bourges	47.08585	2.39293
Bourges	800-887	Coupland (2020)	Bourges	47.08585	2.39293
Bourgneuf	814-888	Morrison and Grunthal (1967)	Bourgneuf	46.167624	-1.022216
Bourgneuf-en-Retz	843-877	Coupland (2010)	Bourgneuf-en-Retz	47.04229	-1.9543
Bray-sur-Seine	840-877	Vandenbossche and Coupland (2012)	Bray-sur-Seine	48.41451	3.24057
Bressuire	814-840	Coupland (1995)	Bressuire	46.84008	-0.49253
Breuvery-sur-Coole	768-813	Dhémin (1989)	Breuvery-sur-Coole	48.86311	4.31164
Brion	814-840	Denais (1908)	Brion	47.4425	-0.1553
Brioux-sur-Boutonne	814-840	Morrison and Grunthal (1967)	Brioux-sur-Boutonne	46.14349	-0.21823
Bruère-Allichamps	814-954	Morrison and Grunthal (1967)	Bruère-Allichamps	46.7695	2.4325
Burgum	843-877	Haertle (1997)	Burgum	53.19527	5.98694
Caden	843-877	Coupland (2020)	Caden	47.630822	-2.287131
Caen	936-954	Coupland (2020)	Caen	49.183512	-0.363489
Calatrava la vieja		Parvéria (2018)	Calatrava la Vieja	39.074099	-3.833274
Campeaux	813-877	Haertle (1997)	Campeaux	48.952844	-0.93197
Carcassonne	768-814	Coupland (2014)	Carcassonne	43.206463	2.363268
Castelsarasin	888-898	Morrison and Grunthal (1967) and Lafaurie (1965)	Castelsarasin	44.039071	1.106969
Catalonia	768-905	Balaguer (1999) and Doménech-Belda et al. (2013)	Calalonia		
Cauroir	843-882	Coupland (2011a)	Cauroir	50.17283	3.30174
Cerdanyola	814-840	Doménech-Belda et al. (2013)	Cerdanyola	41.49201	2.137338
Cerveník	826-950		Cerveník	48.45	17.75

Appendix Table D.8: Carolingian Hoards, Part I

Hoard Name	Date	Reference	Location	Latitude	Longitude
Chaley	936-954	Morrison and Grunthal (1967)	Chaley	45.9552	5.53122
Chalo-Saint-Mars	840-877	Morrison and Grunthal (1967)	Chalo-Saint-Mars	48.4267	2.067
Chalon-sur-Saône I	800-887	Morrison and Grunthal (1967)	Chalon-sur-Saône	46.782132	4.858459
Chalon-sur-Saône II	800-887	Haertle (1997)	Chalon-sur-Saône	46.782132	4.858459
Charente-Maritime	888-898	Coupland (2011a)	Charente-Maritime		
Chartes	923-977	Duplessy (1985)	Chartres	48.446659	1.488596
Chartres II	751-768	Morrison and Grunthal (1967)	Chartres	48.446659	1.488596
Château Roussillon	793-877	Haertle (1997)	Château Roussillon	42.710278	2.946667
Chateauneuf sur Cher	843-954	Morrison and Grunthal (1967)	Chateauneuf sur Cher	46.857333	2.320522
Chaumoux-Marcilly	814-877	Morrison and Grunthal (1967)	Chaumoux-Marcilly	47.12628	2.77884
Chauvigny	843-877	Société des antiquaires de l'Ouest (1982)	Chauvigny	46.56974	0.64345
Chef-Boutonne	800-922	Haertle (1997) and Rondier (1869)	Chef-Boutonne	46.10934	-0.06806
Chester	888-924	Webster et al. (1953)	Chester	53.1903	-2.89437
Chézy-sur-Marne	768-814	Duplessy (1985)	Chézy-sur-Marne	48.989611	3.366294
Choisy-au-Bac	888-898	Haertle (1997)	Choisy-au-Bac	49.44777	2.88097
Ciney Dinant	898-922	Coupland (2020)	Ciney	50.286773	5.098966
Clermont Ferrand	843-918	Coupland (2020)	Clermont-Ferrand	45.778063	3.083696
Compiègne I	877-882		Compiègne	49.41762	2.82513
Compiègne II	843-882	Morrison and Grunthal (1967)	Compiègne	49.41762	2.82513
Corrèze	843-877	Coupland (2014)	Corrèze		
Cosne d'Allier	814-840	Coupland (2014)	Cosne d'Allier	46.474799	2.830127
Cosne-Cours-sur-Loire II	814-877	Morrison and Grunthal (1967)	Cosne-Cours-sur-Loire	47.40983	2.92425
Cosne-Cours-sur-Loire III	877-840	Haertle (1997)	Cosne-Cours-sur-Loire	47.40983	2.92425
Croydon	814-877	Morrison and Grunthal (1967)	Croydon	51.379287	-0.09975
Csorna	888-947	Kovács (1989)	Csorna	47.6167	17.25
Cuerdale	843-922	Morrison and Grunthal (1967)	Cuerdale	53.7553	-2.638
Dalen	843-976	Morrison and Grunthal (1967)	Dalen	52.69847	6.75641
Dauphiné	814-848	Coupland (2014)	Dauphiné		
Deux-Sèvres	814-877	Société de statistique, sciences, lettres et arts du département des Deux-Sèvres (1882)	Deux-Sèvres		
Dijon	770-780	Bompaire and Depierre (1989)	Dijon	47.3268	5.04619
Dommartin-Lettrée	923-936	Duplessy (1985)	Dommartin-Lettrée	48.7669	4.29933
Dordives	750-950	Coupland (2014)	Dordives	48.144081	2.766333
Dorestad	768-877	Morrison and Grunthal (1967)	Dorestadt	51.97212	5.344769
Drantum	814-840	Haertle (1997)	Drantum	52.81942	8.19537
Eichstetten	911-922	Morrison and Grunthal (1967)	Eichstetten	48.094296	7.745429
Ejstrup	814-840	Coupland (2020)	Ejstrup	55.503525	9.377413
Ekeren	819-877	Haertle (1997)	Ekeren	51.276405	4.417467
Ellikon an der Thur	887-915	Zäch (2001)	Ellikon an der Thur	47.56253	8.82386
Emmen	814-877	Morrison and Grunthal (1967)	Emmen	52.49784	6.23039
Entrammes	814-877	Coupland (2014)	Entrammes	47.999133	-0.716154
Espana 1-4	800-1009	Parvérie (2018)	Calatayud	41.352868	-1.641101
Etampes	843-882	Morrison and Grunthal (1967)	Etampes	48.434768	2.162027
Etréchy	832-877	Morrison and Grunthal (1967)	Etréchy	48.88411	3.94374
Evreux	840-954	Duplessy (1985) and Moesgaard (2003)	Evreux	49.02754	1.15028
Extremadura		Parvérie (2018)	Extremadura		
Eyguières	814-840	Coupland (2020)	Eyguières	43.696133	5.030134
Fécamp	900-999	Duplessy (1985)	Fécamp	49.75765	0.37632
Flacey	814-840	Coupland (2020)	Flacey	48.147247	1.349598
Flanders	814-877	Coupland (2020)	Flanders		
Florange		Duplessy (1985) and Simmer (2000)	Florange	49.32743	6.12273
Foissy-lès-Vézelay	864-877	Duplessy (1985)	Foissy-lès-Vézelay	47.43637	3.76447
Fontaines	814-877	Duplessy (1985)	Fontaines	46.85083	4.773055
Frankfurt	814-840	Morrison and Grunthal (1967)	Frankfurt am Main	50.11208	8.68341
Freiburg im Breisgau	898-922	Morrison and Grunthal (1967)	Freiburg im Breisgau	47.99853	7.84965
Fresnes		Duplessy (1985)	Fresnes	48.75043	2.322063
Fridolfing	768-814	Coupland (2020)	Fridolfing	47.998573	12.826917
Frisia	814-855	Morrison and Grunthal (1967)	Grou	53.11035	5.848604
Gannat	800-887	Morrison and Grunthal (1967)	Gelderland	46.10192	3.19692
Gelderland	768-814	Morrison and Grunthal (1967)	Giekau	54.31793	10.50529
Giekau	814-911	Wiechmann (2004)	Glisy	49.8756	2.39788
Glisy	800-922	Morrison and Grunthal (1967)	Gnadendorf	48.61549	16.39885
Gnadendorf	898-905	Daim and Lauermann (2006)	Goutum	53.178037	5.806018
Goutum	814-877	Coupland (2020)	Slagelse	55.3028	11.2647
Grisebjerggård	898-922		Groningen	53.25713	6.93525
Groningen	814-877	Morrison and Grunthal (1967)	Guardamiglio	45.11055	9.68215
Guardamiglio	843-884	Coupland (2011a)			

Appendix Table D.9: Carolingian Hoards, Part II

Hoard Name	Date	Reference	Location	Latitude	Longitude
Györ I	888-950	Kovács (1989)	Györ	47.69739	17.6527
Györ II	888-951	Kovács (1989)	Györ	47.69739	17.6527
Halimba	902-947	Kovács (1989)	Halimba	47.03345	17.53546
Häljarp	814-840	Morrison and Grunthal (1967)		55.85578	12.910919
Harkirke	843-905	Morrison and Grunthal (1967)	Crosby	53.48919	-3.048081
Harlingen	840-855	Haertle (1997)	Harlingen	53.1735	5.4246
Haute Isle	814-922	Morrison and Grunthal (1967)	Haute Isle	49.083426	1.65697
Haza de Carmen	888-954	Coupland (2020)	Cordoba	37.881495	-4.776125
Hermenches	822-840	Morrison and Grunthal (1967)	Hermenches	46.640456	6.757567
Hoen	814-855	Morrison and Grunthal (1967)	Hoen	60.2204	10.25852
Hole	796-840	Coupland (2020)	Hole	58.897156	6.018229
Holy Family	800-887	Parvéria (2018) and Morrison and Grunthal (1967)	Cordoba	37.888028	-4.7734
Hradec Hilfort	768-814	Coupland (2020)	Hradec-Kralove	50.209703	15.832231
Huriel	800-887	Morrison and Grunthal (1967)	Le Moulin-Gargot (Huriel)	46.37468	2.47842
Ibaneta	800-888	Doménech-Belda et al. (2013)	Puerto d'Ibaneta	43.020083	-1.324207
Ibersheim	768-814	Morrison and Grunthal (1967)	Ibersheim	49.72085	8.40065
Ilanz I	843-905	Morrison and Grunthal (1967)	Ilanz	46.77451	9.20463
Ilanz II	664-814	Bernareggi (1977, 1983), Völckers (1965), McCormick (2001)	Ilanz	46.77451	9.20463
Île Agois	864-877	Johnston (1986)	Île Agois	49.24935	-2.18641
Île-de-France	888-936	Dhémin (2006)	Ile de France		
Imbleville	864-877	Haertle (1997)	Imbleville	49.71539	0.95198
Imphy	751-814	Morrison and Grunthal (1967)	Imphy	46.934537	3.259903
Indre	814-865	Morrison and Grunthal (1967)	Indre		
Indre II	814-848	Coupland (2014)	Indre		
Indre-et-Loire	814-877	Coupland (2011a)	Indre-et-Loire		
Indre-et-Loire II	888-910	Coupland (2011a)	Indre-et-Loire		
Indre-et-Loire III	888-898	Coupland (2020)	Indre-et-Loire		
Isle-Aumont I	814-840	Haertle (1997)	Isle-Aumont	48.21131	4.12459
Isle-Aumont II	864-898	Haertle (1997)	Isle-Aumont	48.21131	4.12459
Issy l'Evêque	843-922	Morrison and Grunthal (1967)	Issy l'Evêque	46.70818	3.9734
Jedomelice	814-840	Coupland (2020)	Jedomelice	50.23411	13.971234
Jelsum	768-814	Morrison and Grunthal (1967)	Jelsum	53.23455	5.783862
Juaye-Mondaye	800-922	Morrison and Grunthal (1967)	Juaye-Mondaye	49.20803	-0.68508
Jura	768-814	Morrison and Grunthal (1967)	Jura		
Karden	814-822	Morrison and Grunthal (1967)	Karden	50.179051	7.299583
Karos-Eperjesszög I	888-915	Révész (1996)	Karos	48.32959	21.73712
Karos-Eperjesszög II	900-911	Gedai (1993)	Karos	48.32959	21.73712
Kättilstorp	814-877	Morrison and Grunthal (1967)	Kättilstorp	58.041694	13.711198
Katwijk I	800-922	Kluge (1993)	Katwijk	52.195273	4.421091
Katwijk II	794-800	Van der Velde (2008)	Katwijk	52.195273	4.421091
Kecel	888-924	Huszár (1955)	Kecel	46.52644	19.24647
Kenézlő	826-950	Huszár (1955)	Kenézlő	48.2	21.53333
Kimsword-Pingjum I	814-877	Morrison and Grunthal (1967)	Kimsword	53.1289	5.4387
Kimsword-Pingjum II	814-878	Morrison and Grunthal (1967)	Kimsword	53.1289	5.4387
Kiskundorozsma-Hosszúhát	826-950	Múzeum Móra Ferenc (2002)	Szeged	46.275	20.06278
Kiskunfélegyháza	881-918	Kovács (1989)	Kiskunfélegyháza	46.71246	19.85279
Koblenz	823-830	Reinhold Fischer Auktionshaus (2010)	Koblenz	50.359618	7.59383
Krinkberg	768-814	Morrison and Grunthal (1967)	Pöschendorf	54.03055	9.472156
La Cornouaille	814-877	Coupland (2020)	La Cornouaille	47.578279	-0.797543
La Couvertoirade	881-898	Coupland (2011a)	La Couvertoirade	43.91127	3.31355
La Roche en Ardenne	750-950	Coupland (2014)	La-Roche-en-Ardenne	50.183528	5.575243
La Tessoualle	814-877	Haertle (1997)	La Tessoualle	47.00535	-0.8494
La Tour-de-Peilz	755-768	Geiser (1990)	La-Tour-de-Peilz	46.45302	6.85686
Ladánybene	888-922	Huszár (1955)	Ladánybene	47.03333	19.45
Lamairé	843-877	Baigl et al. (1995)	Lamairé	46.75707	-0.1263
Lamotte Beuvron	814-877	Coupland (2020)	Lamotte-Beuvron	47.602363	2.025245
Langon	814-877	Morrison and Grunthal (1967)	Langon	44.55389	-0.24833
Langres I	843-922	Morrison and Grunthal (1967)	Langres	47.85816	5.33113
Langres II	864-884	Coupland (2011a)	Langres	47.85816	5.33113
Larino	768-840	De Benedittis and Lafaurie (1998)	Larino	41.7968	14.9128
Lauterach	840-924	Zách and Tabernero (2002)	Lauterach	47.4745	9.730031
Lauzès	814-877	Morrison and Grunthal (1967)	Lauzès	47.4707	-0.55324
Lavelanet	888-898	Coupland (2020)	Lavelanet	42.932652	1.848583
Laxfield	843-877	Morrison and Grunthal (1967)	Laxfield	52.30114	1.36237
Leiderdorp	768-840	Coupland (2020)	Leiderdorp	52.151653	4.529015

Appendix Table D.10: Carolingian Hoards, Part III

Hoard Name	Date	Reference	Location	Latitude	Longitude
Lésigny-sur-Creuse	814-898	Jeanne-Rose (1996)	Lésigny-sur-Creuse	46.84996	0.76421
Levice-Géna	926-950	Minarovicova (2007)	Levice-Géna	48.21639	18.60806
Lillebonne	814-877	Coupland and Moesgaard (2012)	Lillebonne	49.51802	0.53681
Limoux	849-877	Haertle (1997)	Limoux	43.053658	2.217421
Lisówek	848-922	Morrison and Grunthal (1967)	Lisówek	51.9	20.9333
Llanbedrgoch	814-878	Coupland (2020)	Llanbedrgoch	53.300117	-4.236622
Llerida	887-928	Doménech-Belda et al. (2013)	Lleida	41.61879	0.621737
Loire River Bank	814-840	Coupland (2014)	Loire River		
Loiret	843-1027	Duplessy (1985)	Loiret		
Lokeren	843-864	Haertle (1997)	Lokeren	51.10473	3.9865
Longjumeau	843-884	Moesgaard (2010)	Longjumeau	48.69173	2.29005
Loppersum	814-877	Morrison and Grunthal (1967)	Loppersum	53.33276	6.74398
Lucca	947-961	Saccoccia et al. (2004)	Lucca	43.84201	10.51534
Lussac-les-Châteaux	845-848	Haertle (1997)	Lussac-les-Châteaux	46.403093	0.723563
Lutkesaaxum	843-864	Haertle (1997)	Lutkesaaxum	53.364638	6.489072
Luzancy	814-877	Sombart (2008)	Luzancy	48.97205	3.1865
Lyon	751-771	Coupland (2020)	Lyon	45.758973	4.830895
Maine et Loire	751-878	Coupland (2014)	Maine-et-Loire		
Marçay	840-898	Morrison and Grunthal (1967)	Marçay	47.10002	0.21706
Marssum	814-855	Coupland (2011a)	Marssum	53.21056	5.73008
Marsum	814-887	Morrison and Grunthal (1967)	Marsum	53.339476	5.73008
Matha	778-877	Coupland (2014)	Matha	45.867625	-0.321187
Melle I	875-877	Haertle (1997)	Melle	46.221471	-0.147358
Melle II	843-877	Haertle (1997)	Melle	46.221471	-0.147358
Melle IV	823-825	Coupland (2018)	Melle	46.221471	-0.147358
Mercurey	822-877	Duplessy (1985) and Haertle (1997)	Mercurey	46.833364	4.722119
Méréville	814-877	Morrison and Grunthal (1967)	Méréville-Saint-Pierre	48.59069	6.15058
Metz	843-877	Morrison and Grunthal (1967)	Metz	49.11566	6.1732
Meurthe et Moselle	898-922	Coupland (2014)	Meurthe-et-Moselle		
Midlaren	814-877	Morrison and Grunthal (1967), Haertle (1997)	Midlaren	53.1111	6.67616
Midlum	900-961	Morrison and Grunthal (1967)	Midlum	53.18204	5.44716
Mikulčice	887-900	Slovenská akadémia vied. Archeologický ústav (1979)	Mikulčice	48.81667	17.05
Molliens-Vidame	817-877	Haertle (1997)	Molliens-Dreuil	49.8839	2.02
Monchy-au-Bois	840-922	Morrison and Grunthal (1967)	Monchy-au-Bois	50.17999505	2.656698281
Montmain	768-814	Coupland (2020)	Montmain	49.410716	1.252625
Montreux-en-Sologne II	800-922	Morrison and Grunthal (1967)	Montreux-en-Sologne	47.55408	1.72638
Montreux-en-Sologne III	864-898	Morrison and Grunthal (1967)	Montreux-en-Sologne	47.55408	1.72638
Moreria		Parvéria (2018)	Moreria	38.916776	-6.349645
Mourlieu	900-925	Caron (1882)	Mourlieu	46.564931	0.512703
Muizen	822-877	Morrison and Grunthal (1967)	Muizen	51.01056	4.514722
Mullaghboden	814-877	Morrison and Grunthal (1967)	Mullaghboy	54.83536	-5.72671
Muret	814-840	Coupland (2020)	Muret	43.460924	1.327252
Nagyszokoly	926-947	Kovács (1989)	Nagyszokoly	46.72132	18.21182
Nagyvázsony	902-947	Kovács (1989)	Nagyvázsony	46.9835	17.69408
Neufchateau I	800-922	Coupland (2014)	Neufchateau	48.356071	5.692627
Neufchateau II	814-848	Coupland (2014)	Neufchateau	48.356071	5.692627
Neuvy-au-Houlme	814-877	Morrison and Grunthal (1967), Duplessy (1985)	Neuvy-au-Houlme	48.8181	-0.19966
Niederlahnstein	855-869	Coupland (2020)	Niederlahnstein	50.315193	7.598382
Nourray	843-877	Morrison and Grunthal (1967)	Nourray	47.71903	1.06023
Nr.Trier	768-855	Coupland (2014) and Morrison and Grunthal (1967)	Trier	49.755513	6.640075
Odoorn	843-961	Morrison and Grunthal (1967)	Odoorn	52.85033	6.847823
Orléans	814-864	Haertle (1997)	Orléans	47.90143	1.90496
Oudwoude	814-877	Morrison and Grunthal (1967)	Oudwoude	53.27968	6.11413
Palma de Majorque	800-888	Doménech-Belda et al. (2013)	Palma de Majorque	39.570589	2.648991
Paule	843-877	Coupland (2014)	Paule	48.235953	-3.4444348
Pilligerheck	814-877	Petry and Wittenbrink (2021), Coupland (2011b)	Muenstermaifeld	50.20461	7.31152
Pingjum	900-911	Morrison and Grunthal (1967)	Pingjum	53.11519	5.44004
Place Unknown	954-986	Morrison and Grunthal (1967)			
Plessé	875-877	Haertle (1997)	Plessé	47.54109	-1.88812
Poitou Charentes	814-877	Coupland (2020)	Poitou-Charente		
Pommern	887-924	Coupland (2020)	Pommern	50.169368	7.269726
Pont Saint-Pierre	864-877	Coupland (2011a)	Pont-Saint-Pierre	49.33388	1.2745
Postsaal	814-1024	Coupland (2020)	Bavière		
Pouzauges	875-898	Haertle (1997)	Pouzauges	46.7822	-0.8361

Appendix Table D.11: Carolingian Hoards, Part IV

Hoard Name	Date	Reference	Location	Latitude	Longitude
Questembert	814-877	Haertle (1997)	Questembert	47.66097	-2.4521
Raalte	814-877	Coupland (2011a)	Raalte	52.38724	6.27462
Regensburg	843-877	Haertle (1997)	Regensburg	49.016213	12.097468
Rennes	843-922	Morrison and Grunthal (1967)	Rennes	48.10761	-1.68448
Rijs	814-877	Morrison and Grunthal (1967)	Rijs	52.86298	5.49838
Rijswijk	814-840	Coupland (2020)	Rijswijk	52.039942	4.325633
Rochefort	900-911	Coupland (2020)	Rochefort	45.935077	-0.962458
Roches l'Evêque	814-922	Morrison and Grunthal (1967)	Roches l'Evêque	47.7772	0.8922
Roermond	222-877	Haertle (1997), Coupland (2011b), Zuyderwyk and Besteman (2010)	Roermond	51.193179	5.98624
Rome I (Forum)	887-950	Metcalf (1992)	Rome	41.90509	12.46194
Rome II (Vatican)	898-922	Morrison and Grunthal (1967)	Rome	41.90509	12.46194
Rosas	814-840	Doménech-Belda et al. (2013)	Rosas	42.265002	3.178593
Roswinkel	768-882	Morrison and Grunthal (1967)	Roswinkel	52.83787	7.03843
Rotterdam	814-840	Coupland (2020)	Rotterdam	51.919909	4.47544
Saint Bris le Vineux	814-877	Coupland (2020)	Saint-Bris-le-Vineux	47.74291	3.651349
Saint Ponc	884-887	Doménech-Belda et al. (2013)	Saint-Ponç	41.963245	1.603627
Saint Yrieix la Perche	888-898	Coupland (2020)	Saint-Yrieix-la-Perche	45.51359	1.203618
Saint-Brieuc	864-875	Haertle (1997)	Saint-Brieuc	48.5136	-2.7653
Saint-Calais	768-877	Paty (1848)	Saint-Calais	47.9211	0.7439
Saint-Cyr-en-Talmondais	814-877	Morrison and Grunthal (1967)	Saint-Cyr-en-Talmondais	46.4614	-1.3356
Saint-Denis	793-875	Haertle (1997)	Saint-Denis	48.9364	2.3547
Saint-Martin-sur-le-Pré		Coupland (2014)	Saint-Martin-sur-le-Pré	48.9778	4.3394
Saint-Même-le-Tenu	814-877	Coupland (2014)	Saint-Même-le-Tenu	47.020808	-1.794104
Saint-Michel-de-Chavaignes		Haertle (1997)	Saint-Michel-de-Chavaignes	48.018584	0.570918
Saint-Pierre-de-Maillé	814-840	Benoit and Braunstein (1983)	Saint-Pierre-de-Maillé	46.6797	0.8444
Saint-Pierre-des-Fleurs I	823-877	Coupland and Moesgaard (2012)	Saint-Pierre-des-Fleurs	49.2514	0.9667
Saint-Pierre-des-Fleurs II	888-898	Cardon et al. (2008)	Saint-Pierre-des-Fleurs	49.2514	0.9667
Saint-Seine-l'Abbaye		Coupland (2014)	Saint-Seine-l'Abbaye	47.440003	4.788637
Santa Elena	961-966	Doménech-Belda et al. (2013)	Irun	43.337137	-1.786251
Santiago de Compostela	800-888	Doménech-Belda et al. (2013)	Santiago de Compostela	42.880265	-8.543118
Sarlat	814-877	Coupland (2020)	Sarlat-la-Canéda	44.889865	1.216381
Sarzana	768-814	Morrison and Grunthal (1967)	Sarzana	44.11186	9.95886
Saumeray	843-877	Morrison and Grunthal (1967)	Saumeray	48.25027	1.32157
Saumur-Thouars	843-898	Morrison and Grunthal (1967)	Saumur	47.1218	-0.1704
Saverne		Duplessy (1985)	Saverne	48.73947	7.36602
Savigné-sous-le-Lude	843-898	Morrison and Grunthal (1967)	Savigné-sous-le-Lude	47.61845	0.05801
Savigny en Véron	814-877	Coupland (2020)	Savigny-en-Véron	47.205554	0.147106
Seiches sur le Loir	751-814	Coupland (2014)	Seiches-sur-le-Loir	47.578315	0.362977
Séranon	814-840	Coupland (2020)	Séranon	43.772823	6.704362
Sevilla region	888-898	Parvérie (2018)	Sevilla	37.393305	-5.993535
's-Hertogenbosch	814-840	Coupland (2014)	's-Hertogenbosch	51.698578	5.303773
Sigean	768-814	Coupland (2020)	Sigean	43.0287	2.978539
Silverdale	800-898	Coupland (2014)	Silverdale	54.167322	-2.82505
Minor Finds	751-1027	Morrison and Grunthal (1967)			
Søndre Bø	814-883	Morrison and Grunthal (1967)	Søndre Bø	58.11019	6.88224
Strasbourg-Basel	843-954	Morrison and Grunthal (1967)	Strasbourg/Basel	48.171	7.6473
Szabadbattyán	826-950	Huszár (1955)	Szabadbattyán	47.11798	18.3629
Szabadegyháza	888-924	Kovács (1989)	Szabadegyháza	47.07845	18.69228
Szedeg-othalom	902-924	Coupland (2014)	Szeged	46.265179	20.140614
Szekszárd	902-947	Huszár (1955)	Szekszárd	46.34779	18.70626
Tarrega	887-928	Doménech-Belda et al. (2013)	Tarrega	41.648564	1.140707
Taizy	864-877	Coupland (2020)	Taizy	49.51967	4.25832
Teloché	864-877	Hucher (1845)	Teloché	47.88987	0.26731
Ter Apel	900-911	Morrison and Grunthal (1967)	Ter Apel	52.878359	7.063981
Ter Heijde	814-840	Coupland (2020)	Ter Heijde	52.02903	4.164265
Terslev	814-966	Morrison and Grunthal (1967)	Terslev	55.37476	11.9693
Thoiry	875-894	Haertle (1997)	Thoiry	48.86519	1.79463
Thouars	822-855	Morrison and Grunthal (1967)	Thouars	46.977604	-0.21579
Tiel	898-922	Coupland (2011a)	Tiel	51.88809	5.43069
Tiszaeszlár I	814-950	Kovács (1989)	Tiszaeszlár	48.05	21.46667
Tiszaeszlár II	926-950	Kovács (1989)	Tiszaeszlár	48.05	21.46667
Tiszanána	888-946	Kovács (1989)	Tiszanána	47.56111	20.52382

Appendix Table D.12: Carolingian Hoards, Part V

Hoard Name	Date	Reference	Location	Latitude	Longitude
Troyes	814-840	Coupland (2014)	Troyes	48.299055	4.077872
Troyes II	843-877	Coupland (2020)	Troyes	48.58345	3.81356
Tuscany	888-973	Ciampoltrini et al. (2001)	Tuscany		
Tytsjerksteradiel	814-855	Coupland (2020)	Burgum	53.195748	5.987155
Tzummarum I	819-855	Haertle (1997)	Tzummarum	53.238297	5.549116
Tzummarum II	855-865	Coupland (2020)	Tzummarum	53.238297	5.549116
Unknown	954-986	Morrison and Grunthal (1967)	France		
Vale of York	898-922	Williams and Ager (2010)	Vale of York	54.20361	-1.36398
Valence	819-840	Haertle (1997)	Valence	44.93347	4.890808
Vallée de la Risle	814-877	Coupland and Moesgaard (2012)	Vale of Risle	49.424	0.725
Vercelli	768-814	Morrison and Grunthal (1967)	Vercelli	45.32255	8.41844
Verdun I	875-877	Haertle (1997)	Verdun	49.15952	5.382316
Verdun II	881-887	Morrison and Grunthal (1967)	Verdun	49.15952	5.382316
Vereb	858-024	Morrison and Grunthal (1967)	Vereb	47.31867	18.61802
Vernon	814-877	Coupland (2020)	Vernon	49.091052	1.483426
Vicq sur Gartempe	814-877	Coupland (2020)	Vicq sur Gartempe	46.721302	0.862012
Vire	843-877	Morrison and Grunthal (1967)	Vire-Normandie	48.83919	-0.89
Vrigny	843-877	Haertle (1997)	Vrigny	48.08167	2.243889
Wagenborgen	814-877	Haertle (1997)	Wagenborgen	53.25713	6.93525
Westerkief I	814-877	Sarfati et al. (1999)	Westerkief	52.89494	4.93322
Westerkief II	814-877	Besteman (2006)	Westerkief	52.89494	4.93322
Wiesbaden-Biebrich	717-814	Morrison and Grunthal (1967)	Wiesbaden-Biebrich	50.050115	8.237668
Wijk bij Duurstede I	793-822	Morrison and Grunthal (1967)	Wijk-Bij-Duurstede	51.971869	5.344562
Wijk bij Duurstede II	752-768	Van Es and Verwers (1980)	Wijk-Bij-Duurstede	51.971869	5.344562
Wijk bij Duurstede III	768-820	Van Es and Verwers (1980)	Wijk-Bij-Duurstede	51.971869	5.344562
Wijk bij Duurstede IV	823-840	Dijkstra (2005)	Wijk-Bij-Duurstede	51.971869	5.344562
Wijk bij Duurstede V	751-768	Coupland (2020)	Wijk-Bij-Duurstede	51.971869	5.344562
Wirdum	814-877	Coupland (2020)	Wirdum	53.149585	5.803308
Worms	814-840	Coupland (2020)	Worms	49.632241	8.36221
Yde	814-877	Morrison and Grunthal (1967)	Yde	53.11143	6.58365
Yonne	814-840	Coupland (2014)	Yonne	47.89753	3.588695
York	751-887	Dolley (1965)	York	53.95333	-1.08342
Yronde	843-877	Morrison and Grunthal (1967)	Yronde	45.6133	3.25481
Zelzate	814-877	Morrison and Grunthal (1967)	Zelzate	51.19753	3.81463
Zetel	768-793	Völckers (1965)	Zetel	53.4146	7.9699
Zillis	888-949	Zäch (2001)	Zillis	46.6355	9.44514
Zuidlaren	875-894	Haertle (1997)	Zuidlaren	53.09231	6.679414

Appendix Table D.13: Carolingian Hoards, Part VI

Signatures	Approx. Nomisma ID	Location	Notes
AHM	hamadhan		
AIRAN, AYLAN	hulwan	Eran-asankar-Kavad	
AM	amol	Amol, Khorasan	
APL, APR	nishapur		
ART, TART	ardashir_khurrah	TART: Tawwaj as dependency of Ardashir Khurra	
AT	adurbadagan		
AU, AW	suq_al-ahwaz	AU is used by Al-Ush, we interpret it as "AW", Hormizd-Ardashir	
AY, AYL	al-sus	Eran-khvarrah-Shapur. AYL: British Museum says "possibly referring to Susa."	
AS	ctesiphon	Following the coding in FLAME.	
BBA	ctesiphon	Court mint, probably at Ctesiphon (Gyselen)	
BCLA, BJRA, DS, DST	al-basrah	Mallon-McCorgray interprets BCLA as al-Basra. Accoring to <a href="#">Schindel (2005)</a> BJRA is al-Basra.	
BISH, BYS, BYSH	bishapur		
BN, BRMKRMAN, DL, DR, GLM,	kirman	Multiple mints that are in Kirman province.	
KL, KLMAN, KLMANLCN, KR,			
KRAMAN H P, KRMAN, KRMAN			
W ST, KRMAN-GY, KRMAN-NAR,			
KRMAN-NAW, NAL, NAR			
D', DA, DAP	darabjird		
DAP	fasa		
GD	jayy		
GU, GW	gorgan	We follow <a href="#">Schindel (2005)</a> in attributing GW to Gorgan (after Yazdegerd I). <a href="#">Gyselen (1977)</a> attributes GU to Gorgan.	
HL	harat		
HWC	jundi_sabur		
LAM, RAM	ramhurmuz		
LD, RD	rayy		
LYW, RIU	rev-ardashir	<a href="#">Bivar (1970)</a> associates RIU with LYW, and confirms Nö's interpretation as Rev-Ardashir	
MA	masabadhan		
MB, MY, PL	maysan		
ML, MR	marw		
NH, NIHJ, NYHC, WH, WYHC	ctesiphon*	NH, WH: Veh-Ardashir. On WYHC, <a href="#">Album (2011)</a> : "A mint in northern Iraq, ostensibly the treasury mint near Ktesiphon prior to the AH50s, and thereafter, for a series dated AH67-73, Arrajan". We follow <a href="#">Album (2011)</a> , <a href="#">Schindel (2005)</a> , and others in attributing it to Ctesiphon before AH50, then Arrajan.	
NHR	nahr_tira		
NIH, WYH	bihqubadh_af-asfal		
NIHJ	arrajan	Almost certainly the same as WYHC.	
NY, NYH	antiocheia_persis	NY: Nihawand. For NYH, <a href="#">Schindel (2005)</a> suggests Nihawand.	
SHI	shiraz		
SK	zaranj, sijistan		
ST	istakhr		
SY	fars_shiraz	Unlocated mint, probably in Fars province (or Kirman, as has sometimes been suggested).	
TPWRSTAN	tabaristan		
YZ, ZR, GZ	yazd		

Appendix Table D.14: Sasanian mint codings

## References

- ABDUL WAHAB, H. (2012): “al-Abbāsiyya,” in *Encyclopaedia of Islam*, ed. by P. Bearman, T. Bianquis, C. Bosworth, E. van Donzel, and W. Heinrichs, Brill.
- AL BAKRI, M. D. (1973): “Kanz al-’Utayfiyah al-fiddi,” *al-Maskukat*, 4.
- AL CHOMARI, A. A. (2020): *Le commerce régional et international au Xe siècle en Syrie: D’après le trésor monétaire de Buseyra et d’autres trésors de l’époque*, Archaeopress.
- AL-NAQSHBANDI, N. (1949): “Rare Islamic coins in the Iraq Museum,” *Sumer*, 5, 199–202.
- (1950): “The Zakho Treasure,” *Sumer*, 6, 177–188.
- (1951): “The Zakho Treasure,” *Sumer*, 7, 165–172.
- (1952): “The Zakho Treasure,” *Sumer*, 8, 220–227.
- (1954): “Khidr Elias Treasure,” *Sumer*, 10, 180–196.
- AL ’USH, A.-F. (1954-1955): “Al-Kanz al-dhahabī al-umawī,” *Annales Archeologiques de Syrie*, IV-V, 21–28.
- (1972a): *Kunz umm hajarah al-fiddi (Trésor de monnaies d’argent trouvé à Umm Hajarah)*, Damascus.
- (1972b): *The silver hoard of Damascus: Sasanian, Arab-Sasanian, Khuwarizmian, and Umayyad kept in the National Museum of Damascus*, Damascus: Direction General of Antiquities and Museums.
- (1982): *Monnaies Aghlabides, étudiées en relation avec l’histoire des Aghlabides*, Institut Français de Damas.
- ALBUM, S. (1971): “An Umayyad hoard from Afghanistan,” *Museum Notes (American Numismatic Society)*, 17, 241–246.
- (2011): “Checklist of Islamic Coins, 3rd Edition,” .

ALFARO ASINS, C. (1992): “La colección de moneda hispano-árabe del Museo Arqueológico Nacional de Madrid,” *III Jarique de Numismática hispano-árabe. Actas (Museo Arqueológico Nacional. Madrid, 13-16 diciembre 1990)*, 39–75.

ÁLVAREZ, M. D. L. Á. P. (1993): “Tesorillo de monedas árabes de Moraleja (Cáceres),” *Alcántara: revista del Seminario de Estudios Cacereños*, 37–44.

AMERICAN NUMISMATIC SOCIETY (2023): “MANTIS Database,” <https://numismatics.org/collection>, accessed: 2023-07-01.

ARIZA ARMADA, A. (1988): “Un tesorillo de dirhames de Baena (Cordoba),” *Arqueología Medieval*, 2, 137–140.

ARROYO ILERA, R. (1989): “Descripción y análisis de las monedas árabes de Sinarcas (Valencia),” in *Actas del VII Congreso Nacional de Numismática, Madrid, Museo Casa de la Moneda*, 467–479.

ARSLAN, E. A. (2005): “Il Repertorio dei ritrovamenti di moneta altomedievale (489-1002),” .

ARTUK, I. (1966): *Denizbaci definesi*, Ankara: Türk Tarih Kurumu.

ASENCIO, J. M. R. (1962): “Tesoro de dirhemes califales hallado en Jaén,” *Boletín del Instituto de Estudios Giennenses*, 109.

ÁVILA, R. C. AND A. R. H. PAREJA (1999): “Un conjunto monetario andalusí de plata emiral procedente de la Junta de los Ríos (Priego de Córdoba),” *Antiquitas*, 125–136.

AYALA RUIZ, J. A. AND C. GOZALBES CRAVIOTO (1996): “Un tesorillo califal aparecido en la Cala de Mijas-Costa (Málaga),” *Gaceta Numismática*, 121, 61–76.

BAIGL, J.-P., A. CLAIRAND, AND O. JEANNE-ROSE (1995): “Troupailles récentes de monnaies carolingiennes dans les Deux-Sèvres: petits trésors et monnaies isolées,” *Bulletin de la Société française de numismatique*, 50, 1152–1154.

BALAGUER, A. M. (1999): *Història de la moneda dels comtats catalans*, vol. 2, Institut d’Estudis Catalans.

BALDUS (2006): *Didyma. III. Ergebnisse der Ausgrabungen und Untersuchungen seit dem Jahre 1962. 3. Fundmünzen aus den Jahren 1962-1998*, Deutsches Archäologisches Institut.

BARTOLOMEI, I. A. (1857): “Description d’une trouvaille de 200 dirhems koufiques, faite aux environs de Tiflis, en 1857,” *Bulletin de l’Académie impériale des sciences de St. Petersburg*, 3.

BATES, M. L. (1978): “A hoard of dirhams found at Nippur,” *Excavations at Nippur, twelfth season*, 126–138.

BENOIT, P. AND P. BRAUNSTEIN (1983): *Mines, carrières et métallurgie dans la France médiévale*, Paris: Edition du CNRS.

BERNAREGGI, E. (1977): “I tremissi longobardi e carolingi del ripostiglio di Ilanz nei Grigioni,” *Quaderni ticinesi di numismatica*, VI.

——— (1983): “Carolingian gold coins from the Ilanz hoard,” in *Studies Philip Grierson*, 127–135.

BESTEMAN, J. (2006): “Westerklief II, a second Viking silver hoard from the former island of Wieringen; with a contribution by Gert Rispling and Simon Coupland,” *Jaarboek voor Munt-en Penningkunde*, 93, 5–80.

BIJSTERVELD, A., N. NEUFEGLISE, AND B. VAN DER VEEN (2000): “Een heilige plaats onder de grond. Aalst en zijn middeleeuwse kerk,” *Brabants Heem*, 52, 81–92.

BIVAR, A. D. H. (1970): “Appendix: The Sasanian Coin from Qūmis,” *Journal of the Royal Asiatic Society of Great Britain and Ireland*, 156–158.

BLACKBURN, M. A. (1989): “The Ashdon (Essex) hoard and the currency of the Southern Danelaw in the late ninth century,” *British Numismatic Journal*, 59, 13–38.

BOMPAIRE AND DEPIERRE (1989): “le trésor carolingien de dijon, rue du chapeau rouge,” Tech. rep., bulletin de la société française de numismatique.

CANO ÁVILA, P. (1989): “Algunos dirhemes hallados cerca de Alcaudete (Jaén),” in *VII Congreso Nacional de Numismática: Memoria*, 489–503.

——— (2014): “Hallazgo de dírhemes del califato Omeya de Al-andalus en Montellano (Sevilla),” *Revista Numismática OMNI*, 149–164.

- (2016): “Hallazgo de dírhems del Califato omeya de al-Andalus en Bormujos (Sevilla),” in *Patrimonio numismático y museos: actas XV Congreso Nacional de Numismática. Madrid, 28-30 de octubre de 2014*, Museo Casa de la Moneda, 1133–1148.
- CANO ÁVILA, P. AND C. M. GÓMEZ (2008): “Hallazgo de un tesorillo de dírhemes del imamato fatimí y del califato omeya de al-Andalus en El Pedroso (Sevilla). El Pedroso III,” in *Moneda y arqueología: actas XIII Congreso Nacional de Numismática*, Universidad de Cádiz, 799–824.
- CANO ÁVILA, P. AND C. MARTÍN GÓMEZ (2006): “Hallazgo de un tesorillo de dírhemes del califato omeya de al-Andalus en El Pedroso (Sevilla),” in *Actas XII Congreso Nacional de Numismática: Madrid. 25-27 de octubre de 2004*, Real Casa de la Moneda, Fábrica Nacional de Moneda y Timbre, 443–464.
- CANO ÁVILA, P. AND C. I. MARTÍN GÓMEZ (2005): “Tesoro de dirhemes emirales hallado en La Rinconada (Sevilla),” in *XIII Congreso Internacional de Numismática, Madrid, 2003: actas-proceedings-actes*, Ministerio de Cultura, 1553–1566.
- CANO ÁVILA, P. AND C. I. MARTÍN GOMEZ (2011): “Hallazgo de dírhemes del emirato omeya de al-Ándalus en Niebla (Huelva),” in *Ars metallica. Monedas y medallas: Nules-Valencia, 25-27 de octubre de 2010*, Museo Casa de la Moneda, 817–834.
- CANTO GARCÍA, A. (1988): “Tesoro de moneda emiral del siglo II de la Hégira, conservado en el MAn [Museo Arqueológico nacional],” *Actas I Jarique de Estudios Numismáticos Hispano-Árabes, Zaragoza, Institución Fernando el Católico*, 147–162.
- (1993): “Sobre un pequeño hallazgo de moneda emiral en Martos (Jaén),” *Antiquitas*, 63–66.
- (2001): “La moneda hispanoárabe y su circulación por Navarra,” in *La moneda en Navarra: Museo de Navarra, Pamplona: exposición 31 de mayo a 25 de noviembre de 2001*, Fundación Caja Navarra, 73–82.
- (2014): “El tesoro de Tarancón (Cuenca, 1893): nuevos datos e imágenes sobre el mismo,” *Revista Numismática OMNI*, 21–64.
- (2019): “Hallazgos de Moneda Andalusi y Documentacion,” Tech. rep., Universidad Autónoma de Madrid.

CANTO GARCÍA, A., R. CLAPÉS, AND W. JABLÓNSKA (2020a): “Un hallazgo de monedas califales en el arrabal occidental de Córdoba,” .

CANTO GARCÍA, A. AND F. M. ESCUDERO (2012): “El tesoro de monedas árabes de Carmona y una rectificación de A. Vives Escudero,” *Cuadernos de Prehistoria y Arqueología de la Universidad Autónoma de Madrid*, 38.

CANTO GARCÍA, A., G. GARCÍA RUIZ, AND L. RUIZ QUINTANAR (1997): “Hallazgo de monedas califales de Marroquíes Bajos (Jaén),” *Arqueología y territorio medieval*, 4, 81–101.

CANTO GARCÍA, A. AND W. JABLÓNSKA (2019): “Algunas precisiones sobre el hallazgo de dinares califales de la calle San Pedro (Murcia),” *Tudmir: Revista del Museo Santa Clara, Murcia*, 5–13.

CANTO GARCÍA, A. AND E. MARSAL MOYANO (1988): “Hallazgo de moneda emiral de Iznájar (Granada),” *Al-Qantara*, 9, 427.

CANTO GARCÍA, A. AND F. MARTÍN ESCUDERO (2007): “El hallazgo de moneda califal de Fontanar (Córdoba),” *Documenta & Instrumenta*, 129–156.

——— (2009): “Hallazgos monetarios islámicos en Algeciras,” *Caetaria: revista bianual de Arqueología*, 125–130.

CANTO GARCÍA, A., F. MARTÍN ESCUDERO, AND W. JABLONSKA (2020b): *El hallazgo de monedas califales del Parque Cruz Conde (Córdoba)*, Museo Casa de la Moneda.

CARDON, T., J. C. MOESGAARD, R. PROT, AND P. SCHIESSER (2008): “Le premier trésor monétaire de type viking en France. Denier inédit d’Eudes pour Beauvais,” *Revue numismatique*, 6, 21–40.

CARON, E. (1882): *Monnaies féodales françaises*, vol. 1, Rollin et Feuardent.

CERRATO, C. B. AND A. M. ESQUIVEL (2019): “Conjunto de dírhams califales hallado en Zamora: estudio e interpretación,” *Archivo español de arqueología*, 92, 287–306.

CIAMPOLTRINI, G., E. ABELA, AND S. BIANCHINI (2001): “Lucca: un contesto con monete del X secolo dell’area dell’ex ospedale Galli Tassi,” *Bollettino di Numismatica*, 153–166.

- CODERA Y ZAIDÍN, F. (1892): “Tesoro de monedas árabes, descubierto en Alhama de Granada,” *Boletín de la Real Academia de la Historia*, XX, 442–449.
- (1913): “Monedas árabes orientales encontradas en Aragón,” *Boletín de la Real Academia de la Historia*, LXIII, 552–556.
- CORNU, G. (1983): *Atlas du monde Arabo-Islamique à l'époque classique: IX.-X. siècles*, Brill.
- COUPLAND, S. (1991): “The early coinage of Charles the Bald, 840-864,” *The Numismatic Chronicle (1966-)*, 121–158.
- (1995): “Bilan Société Française de Numismatique,” Tech. rep., Société Française de Numismatique.
- (2010): “Le trésor de Bourgneuf-en-Retz et les monnaies de Melle au monogramme d'un roi Charles’,” *Bulletin de la Société française de numismatique*, 65, 190–3.
- (2011a): “A checklist of Carolingian coin hoards 751-987,” *The Numismatic Chronicle*, 171, 203–256.
- (2011b): “The Roermond coins reconsidered,” *Medieval and Modern Matters*, 2, 25–50.
- (2014): “A supplement to the checklist of Carolingian coin hoards, 751-987,” *The Numismatic Chronicle (1966-)*, 174, 213–222.
- (2018): “Les monnaies de Melle sous Louis le Pieux’,” *Mine, métal, monnaie, Melle. Les voies de la quantification de l'histoire monétaire du haut Moyen Âge*, 259–278.
- (2019): “Der Karolingschatz von Bassenheim,” Tech. rep., Münzfunde aus Rheinland-Pfalz 36.
- (2020): “A Second Supplement to the Checklist of Carolingian coin hoards, 751-987,” *The Numismatic Chronicle*, 180, 259–289.
- COUPLAND, S. AND J. C. MOESGAARD (2012): “Trésors monétaires peut-être enfouis lors des premiers raids vikings dans la vallée de la Seine’,” *Bulletin de la Société française de numismatique*, 67, 222–229.

CRAVIOTO, C. G. (2016): “Tesorillo de monedas andalusíes de Castillejos de Quintana (Pizarra, Málaga),” in *Patrimonio numismático y museos: actas XV Congreso Nacional de Numismática. Madrid, 28-30 de octubre de 2014*, Museo Casa de la Moneda, 1353–1360.

CRAVIOTO, C. G. AND J. A. AYALA (1995): “Un tesorillo de monedas del emirato independiente hallado en el Cerro de la Fuensanta (Antequera-Casabermeja-Colmenar. Málaga),” *Mainake*, 235–242.

CRUYSHEER, A. AND B. J. V. DER VEEN (2015): “De Karolingische schatvondst Bikbergen 1992,” Tech. rep., De Beeldenaar.

CURTA, F. (2005): “Byzantium in Dark-Age Greece (the numismatic evidence in its Balkan context),” *Byzantine and Modern Greek Studies*, 29, 113–146.

DAIM, F. AND E. LAUERMANN (2006): *Das frühungarische Reitergrab von Gnadendorf (Niederösterreich)*, Verlag des Römisch-Germanischen Zentralmuseums.

DAJANI, A. (1951): “A hoard of Byzantine gold coins from Awarta, Nablus,” *Annual of the Department of Antiquities, Jordan*, 1, 41–43.

DE BENEDITTIS, G. AND J. LAFaurie (1998): “Trésor de monnaies carolingiennes du VIIIe siècle trouvé à Larino (Italie, Molise),” *Revue Numismatique*, 6, 217–243.

DENAIS, J. (1908): “Catalogue illustré du musée de Beaufort-en-Vallée,” Tech. rep.

DHÉNIN, M. (1989): “Le trésor monétaire de Breuvery-sur-Coole (Marne),” *Comptes rendus des séances de l'Académie des Inscriptions et Belles-Lettres*, 133, 811–823.

DHÉNIN, M. (2006): “Les monnaies carolingiennes d’Arpajon (anciennement Chartres), Essonne,” *Bulletin de la Société Française de Numismatique*, 61, 226–230.

DIJKSTRA, M. F. P. (2005): “Middeleeuwse gulle gaven, greppels en waterputten. De opgraving Wijk bij Duurstede-David van Bourgondieweg.,” 26.

DIMIAN, I. (1957): “Cîteva descoperiri monetare bizantine pe teritoriul RPR,” *Studii si cercetari de numismatica*, 1, 189–216.

DOLLEY, M. (1965): “New Light on the Pre-1760 Coney Street (York) Find of Coins of the Duurstede Mint.”, ” *Jaarboek Voor Munt-en Penningkunde*, 52, 1966.

DOMÉNECH BELDA, C. (1992): “Revisión de un hallazgo de monedas árabes de Elche (Alicante),”

——— (1997): “Circulación monetaria durante el período islámico en el País Valenciano,” .

DOMÉNECH BELDA, C. AND S. GUTIÉRREZ LLORET (2006): “Viejas y nuevas monedas en la ciudad emiral de Madīnat Iyyuh (El Tolmo de Minateda, Hellín, Albacete),” *Al-Qantara*, 27, 337–374.

DOMÉNECH BELDA, C. AND J. TRELIS (1990): “Hallazgos numismáticos de época islámica en Crevillente (Alicante),” *III Jarique de Numismática Hispano-árabe*.

DOMÉNECH-BELDA, C. ET AL. (2013): “La circulation de monnaie carolingienne dans la péninsule ibérique. À propos d'un denier de l'atelier de Roda,” *Revue Numismatique*, 6, 383–410.

DUPLESSY, J. (1985): “Les trésors monétaires médiévaux et modernes découverts en France, vol. 1, 751-1223,” .

EUSTACHE, D. (1956): “Monnaies musulmanes trouvées à Volubilis,” *Hespéris: Archives berbères et bulletin de l'institut des hautes études-marocaines*, XLIII.

FAGERLIE, J. M. (1974): “A Byzantine “Sicilian” Hoard,” in *Studies George C. Miles*, 175–183.

FLAME (2023): “Framing the Late Antique and early Medieval Economy,” <https://coinage.princeton.edu/>, accessed: 2023-07-01.

FOMIN, A. V. AND L. KOVÁCS (1987): *The tenth century Máramaros County (“Huszt”” dirham hoard*, Magyar Numizmatikai Társulat.

FONTENLA BALLESTA, S. (1998): “Un tesorillo de plata medieval del Tijan (Turre, Almeria),” Tech. rep., Axarquia 3.

FÜEG, F. (2007): *Corpus of the Nomismata from Anastasius II to John I in Constantinople, 713-976*, Classical Numismatic Group.

GACHET, A. (1993): *Présentation d'un trésor monétaire des premiers temps de l'Islam : le trésor d'Afak.*

GEDAI, I. (1993): “The denars of Luis the Child in a grave find in Hungary,” *Numismatica e antichità classica*, 273–278.

GEISER, A. (1990): *Un trésor de monnaies de Pépin le Bref trouvé à La Tour-de-Peilz (VD), nécropole du Clos d'Aubonne*, Gazette numismatique suisse.

GONZÁLEZ GARCÍA, A. AND D. MARTÍNEZ CHICO (2017): “Cuatro hallazgos aislados de dinares epigráficos latinos hispano-musulmanes en Jaén,” .

GRAÑEDA MIÑÓN, P. (2021): “Reexcavando en el Museo Arqueológico Nacional: los tesoros de Valencia del Ventoso (Badajoz) y Osuna (Sevilla),” Tech. rep., XVI Congreso Nacional de Numismática: Tesoros y hallazgos monetarios: protección, estudio y musealización (Barcelona, 28-30 de noviembre de 2018).

GRIERSON, P. (1968): *Catalogue of the Byzantine Coins in the Dumbarton Oaks Collection and in the Whittemore Collection, 2: Phocas to Theodosius III, 602-717*, Dumbarton Oaks.

——— (1973): *Catalogue of the Byzantine Coins in the Dumbarton Oaks Collection and in the Whittemore Collection, 3: Leo III to Nicephorus III, 717-1081*, Dumbarton Oaks.

GUILLEMAIN, J. (1993): “Deux trouvailles de monnaies médiévales au nord de Lyon,” *Bulletin de la Société Française de Numismatique*.

GYSELEN, R. (1977): “Trésor de monnaies sasanides trouvé à Suse. I. Inventaire,” *Cahiers de la Délégation archéologique française en Iran*, 7, 61–74.

GYSELEN, R. AND L. KALUS (1983): *Deux trésors monétaires des premiers temps de l'Islam*, Bibliothèque Nationale de France, Paris.

GYSELEN, R. AND A. NÈGRE (1982): “Un trésor de Gazīra (Haute-Mésopotamie): monnaies d'argent sasanides et islamiques enfouies au début du IIIe siècle de l'Hégire/IXe siècle de notre ère,” *Revue Numismatique*, 6, 170–205.

HAERTLE, C. M. (1997): *Karolingische Münzfunde aus dem 9. Jahrhundert*, Böhlau.

- HAKIEM, A. A.-A. D. (1977): “A critical and comparative study of early Arabian coins on the basis of Arabic textual evidence and actual finds,” Ph.D. thesis, University of Leeds.
- HEBERT, R. J. (1966): “Notes on an Umayyad hoard from Khurāsān,” *Museum Notes (American Numismatic Society)*, 12, 157–163.
- HEIDEMANN, S., J. RIEDERER, AND D. WEBER (2014): “A Hoard from the Time of Yazdgard III in Kirmān,” *Iran*, 52, 79–124.
- HEIDEMANN, S., T. SCHIERL, AND F. TEICHNER (2018): “Coins from the seaside. An Emiral silver coin hoard from a harbour settlement on the Cerro de Vila (Vilamoura, Algarve, Portugal),” *Al-Qantara*, 39, 169–224.
- HOGE, R. (1997): “A Parcel of Mainly’Abbāsid Gold Coins,” *The Numismatic Chronicle*, 157, 239–247.
- HUCHER, E. F. F. (1845): *Essai sur les monnaies frappées dans le Maine*, de Gallienne.
- HUSZÁR, L. (1955): *Das Münzmaterial in den Funden der Völkerwanderungszeit im mittleren Donaubecken*, Akadémiai Kiadó.
- IBRAHIM, T. B. H. AND A. CANTO GARCÍA (1991): “Hallazgo emiral en Puebla de Cazalla (Sevilla),” *Numisma: revista de Estudios Numismáticos*, 69–86.
- ILISCH, L. (1979): “Ein Dirhamfund des frühen 10. Jahrhunderts aus der Gegend von Diyarbakir,” *Münstersche Numismatische Zeitung*.
- (1990): “Whole and fragmented Dirhams in near eastern hoards,” in *Sigtuna papers: proceedings of the Sigtuna symposium on Viking-age coinage, 1-4 june 1989*, ed. by K. Jonsson and B. Malmer, Kungl. Vitterhets Historie och Antikvitets Akademien.
- (2005): “Der Steckborner Schatzfund von 1830 und andere Funde nordafrikanischer Dirhams im Bereich des Karlsreiches,” in *Simposio Simone Assemani sulla monetazione islamica*, ed. by G. Gorini, Esedra.
- JEANNE-ROSE, O. (1996): “Trovailles isolées de monnaies carolingiennes en Poitou: inventaire provisoire,” *Revue numismatique*, 6, 241–283.

- JOHNSTON, P. (1986): *The archaeology of the Channel Islands*, Phillimore.
- JUNGFLEISCH, M. (1949): “La trouvaille du cimetière de Sainte-Barbe à Babylone d’Egypte,” *Revue Numismatique*, 11, 165–169.
- KASDAGLI, A.-M. (2018): *Coins in Rhodes: From the monetary reform of Anastasius I until the Ottoman conquest (498 - 1522)*, Archaeopress.
- KHODZHANIYAZOV, T. AND L. TREADWELL (1998): “The Marv hoard of early Islamic dirhams,” *Iran*, 36, 85–94.
- KIRKBRIDE, A. (1951): “Recent Finds of Arabic Coins,” *Annual of the Department of Antiquities, Jordan*, 1, 17–19.
- KLUGE, B. (1993): “Fernhandel und Geldwirtschaft: Beiträge zum deutschen Münzwesen in sächsischer und salischer Zeit,” .
- KOVÁCS, L. (1989): *Münzen aus der ungarischen Landnahmezeit: archäologische Untersuchung der arabischen, byzantinischen, westeuropäischen und römischen Münzen aus dem Karpatenbecken des 10. Jahrhunderts*, Akadémiai kiadó.
- LAFAURIE, J. (1965): “Deux trésors monétaires carolingiens: Saumeray (Eure-et-Loir), Rennes (Ille-et-Vilaine),” *Revue Numismatique*, 6, 262–305.
- LAFLI, E., C. LIGHTFOOT, AND M. RITTER (2016): “Byzantine coins from Hadrianopolis in Paphlagonia,” *Byzantine and Modern Greek Studies*, 40, 187–206.
- LAGUMINA, B. (1904): “Ripostiglio di monete arabe rinvenuto in Girgenti,” *Archivio storico siciliano*, 29.
- LLOYD, S. (2023): “Post-Reform Umayyad Dirhams and their Mint Towns,” <https://www.angelfire.com/ny3/vaguebrit/>, accessed: 2023-07-01.
- LOCKHART, L. (2012): “Dīnawar,” in *Encyclopaedia of Islam*, ed. by P. Bearman, T. Bianquis, C. Bosworth, E. van Donzel, and W. Heinrichs, Brill.
- LOWICK, N. (1975): “An early tenth century hoard from Isfahan,” *The Numismatic Chronicle*, 110–154.

- (1983): “The Sinaw Hoard of Early Islamic Coins,” *The journal of Oman studies*, 6, 199–230.
- LOWICK, N. AND J. NISBET (1968): “A hoard of dirhems from Ra’s al-Khaimah,” *The Numismatic Chronicle*, 231–240.
- MA’AYEH, F. S. (1962): “A Hoard of Omayyad Dinars from Orif,” *Annual of the Department of Antiquities, Jordan*, 6/7, 76–97.
- MALEK, H. M. (1996): “A Hoard Group Of Drachms of the Dābūyid Ispahbads and Early’Abbāsid Governors of Ṭabaristān,” *The Numismatic Chronicle*, 156, 175–191.
- MĂNUCU-ADAMEȘTEANU, G. (2016): *Monede bizantine descoperite în Dobrogea: monede bizantine descoperite în mediul rural din nordul Dobrogei, Secolele VII-XV*, Muzeul Municipiului București.
- MARCOS POUS, A. AND A. M. VICENT ZARAGOZA (1992): “Los tesorillos de moneda hispano-árabe del Museo Arqueológico de Córdoba,” *III Jarique de Numismática Hispano-Árabe*, 192–215.
- MARINHO, J. R. (1993): “As moedas hispano-muçulmanas da coleção Justino Cumano numa carta de Pascual de Gayangos,” Tech. rep., III Jarique de numismática hispano-arabe.
- MARTÍN, M. V. AND S. P. MARTÍN (2002): “Del hallazgo de dirhames emirales en Domingo Pérez (Iznalloz, Granada),” *Al-Qantara*, 23, 155–192.
- (2006): “Sobre el hallazgo emiral del Campo de la Verdad (Córdoba),” in *Actas XII Congreso Nacional de Numismática: Madrid. 25-27 de octubre de 2004*, Real Casa de la Moneda, Fábrica Nacional de Moneda y Timbre, 403–416.
- MARTÍN ESCUDERO, F. (2001): “El hallazgo omeya de Baena: un tesoro olvidado,” in *IV Jarique de numismática andalusí*, Universidad de Jaén, 81–94.
- (2003): “Sobre el hallazgo de dinares del Hospital Militar de Zaragoza (1858),” in *XI Congreso Nacional de Numismática: actas, Zaragoza, 2002*, Real Casa de la Moneda, Fábrica Nacional de Moneda y Timbre, 257–268.

- (2011): “Las monedas de Al-Andalus: de actividad ilustrada a disciplina científica,” *Las monedas de Al-Andalus*, 1–394.
- (2012): “Monedas que van, monedas que vienen... circulación monetaria en época de cambios,” *De Mahoma a Carlomagno. Los primeros tiempos (siglos vii–ix). XXXIX Semana de Estudios Medievales de Estella*, 311–350.
- MARTÍN ESCUDERO, F., M. T. CASAL GARCÍA, AND A. CANTO GARCÍA (2023): “Feluses, dírhams y monedas en el arrabal de Šaqunda (Córdoba): análisis y clasificación tipológica,” .
- MARTÍNEZ ENAMORADO, V. (2004): “Frontera de al-Andalus. El Valle del Tiétar en el contexto de la Tagr al-Awsat,” .
- MCCORMICK, M. (2001): *Origins of the European economy: communications and commerce AD 300-900*, Cambridge University Press.
- METCALF, D. M. (1992): „The Rome (forum) hoard of 1883 ,” *British Numismatic Journal*, 62, 63–96.
- MILES, G. C. (1960): “A Hoard of Arab Dirhems from Algarve, Portugal,” *Museum Notes (American Numismatic Society)*, 9, 219–230.
- MINAROVICOVA, E. (2007): “Novoobjavený rímsky denár z hromadného nálezu rímskych mincí z Vyškovieč nad Iplom, okr. Levice,” Tech. rep., Slovenska Numizmatika.
- MIRNIK, I. A. (1981): *Coin hoards in Yugoslavia*, BAR Publishing.
- MIŠKEC, A. (2002): *Die Fundmünzen der römischen Zeit in Kroatien. Abt. 18. Istrien*, von Zabern.
- MOESGAARD, J. C. (1997): “A hoard from the Blois region and the proto-feudal coinage of Blois, c. 920/40,” *The Numismatic Chronicle (1966-)*, 157, 196–205.
- (2003): “Le trésor de Saint-Taurin à Evreux (Xe siècle),” *Cahiers Numismatique*, 158, 23–40.
- (2010): “Le “maillon manquant” entre Quentovic et Rouen?” *Bulletin de la Société française de numismatique*, 65, 57–61.

- MORONY, M. G. (1982): “Continuity and Change in the Administrative Geography of Late Sasanian and Early Islamic al-’Irāq,” *Iran*, 20, 1–49.
- MORRISON, K. F. AND H. GRUNTHAL (1967): *Carolingian Coinage*, New York: American Numismatic Society.
- MORRISSON, C. (2017): “Coinage in Byzantine Anatolia,” in *The Archaeology of Byzantine Anatolia. From the End of Late Antiquity to the Coming of the Turks*, ed. by P. Niewöhner, Oxford University Press.
- MORRISSON, C. AND J.-N. BARRANDON (1988): “La trouvaille de monnaies d’argent byzantines de Rome (VIIe-VIIIe s.): Analyses et chronologie,” *Revue numismatique*, 6, 149–165.
- MORRISSON, C., V. POPOVIĆ, AND V. IVANIŠEVIĆ (2006): *Les Trésor monétaires byzantins des Balkans et d’Asie Mineure (491-713)*, Lethielleux.
- MOSSER, S. M. (1935): *A bibliography of Byzantine coin hoards*, New York: American Numismatic Society.
- MOTOS GUIRAO, E. AND A. DÍAZ GARCÍA (1985): “Tesorillo árabe de Tígnar,” *Miscelánea de estudios árabes y hebraicos. Sección Árabe-Islam. Vol. 34 (1985)*.
- MUSEO ARQUEOLÓGICO DE MURCIA (2014): “Tesoros. Materia ley y forma. Catalogue of the exhibition December 2014 to April 2015,” Tech. rep., Museo Arqueológico de Murcia.
- MÚZEUM MÓRA FERENC (2002): *Studia archaeologica VIII*, Szeged: Múzeum Móra Ferenc.
- NAVASCUÉS Y DE PALACIOS, J. (1957): “Tesoro hispano-árabe encontrado en Trujillo (Cáceres),” *Numario Hispánico*, 6, 5–28.
- (1958): “Tesorillo de monedas de plata del califato cordobés y fatimíes,” *Numario Hispánico*, 7, 207–210.
- (1961a): “Tesoro de Cihuela (Soria),” *Numario Hispánico*, X, 173–175.
- (1961b): “Tesoro de moneda califal,” *Numario Hispánico*, X, 169–173.

NIKOLAOU, Y. AND I. TOURATSOGLOU (2019): *The Circulation of Byzantine Coinage in Mainland Greece and the Balkans. The Hoard Evidence: 5th - 15th centuries*, Athens: Friends of the Numismatic Museum.

NOMISMA (2023): “The Nomisma.org project,” <https://nomisma.org/>, accessed: 2023-07-01.

NOONAN, T. S. (1980): “When and how dirhams first reached Russia: a numismatic critique of the Pirenne theory,” *Cahiers du monde russe et soviétique*, 401–469.

OBERLÄNDER-TÂRNOVEANU, E. (2001): “From the Late Antiquity to the Early Middle Ages—the Byzantine Coins in the territories of the Iron Gates of the Danube from the second half of the 6th Century to the first half of the 8th Century,” *Etudes byzantines et post-byzantines*, 4, 29–69.

ORTEGA, M. R. R., J. B. ESTELLA, R. G. TORRES, AND M. M. M. MARQUÉS (2006): “Estudio de un conjunto monetario de época califal procedente del Valle del Guadajoz (Córdoba),” in *Actas XII Congreso Nacional de Numismática: Madrid. 25-27 de octubre de 2004*, Real Casa de la Moneda, Fábrica Nacional de Moneda y Timbre, 417–441.

PALMA GARCÍA, F. AND R. SEGOVIA SOPO (2007): “Un tesorillo de moneda islámica aparecido en Morería (Mérida),” Tech. rep., Biblioteca Virtual Miguel de Cervantes.

PARVÉRIE, M. (2014): “Corpus des monnaies arabo-musulmanes des VIII et IX siècles découvertes dans le Sud de la France,” *Revista Numismática OMNI*, 79–100.

——— (2018): “La circulation des deniers de l’Aquitaine carolingienne en Al-Andalus; un réexamen des trésors ‘Espanya-1, 2 et 3’,” *Bulletin de la Société numismatique de Limousin*, 25, 4–16.

——— (2019): “Supplément au corpus des monnaies arabomusulmanes découvertes en France,” *Revista Numismática OMNI*, 283–294.

PATY, E. (1848): “Étude archéologique sur Saint Calais et son canton,” Tech. rep., Bulletin de la Société royale d’agriculture, science et arts de la Sarthe.

PELLICER I BRU, J. (1982): “Un tresor de dirhems àrabs a SC.-J.” *Acta numismàtica*, 139–166.

——— (1985): “El tresoret de moneda àrab LR-P dels anys 331-418 AH,” *Acta numismàtica*, 157–182.

PEÑA MARTÍN, S. AND M. VEGA MARTÍN (2007): “La amonedación canónica del emirato omeya andalusí antes de Abd-al-Rahman II, según el hallazgo de dirhams de Villiciosa (Córdoba),” .

PENNAS, V. (1991): “Byzantine Monetary Affairs during the 8th, 9th, 10th and 11th Centuries,” D.phil thesis, University of Oxford.

——— (1996): “Life in Byzantine Cities of Peloponnesos: The Numismatic Evidence (8th-12th Century),” in *Mneme Martin Jessop Price*, Hellenic Numismatic Society.

PETRY, K. AND S. WITTENBRINK (2021): *Der karolingische Münzschatzfund von Pilligerheck (Landkreis Mayen-Koblenz), vergraben nach 855*, Verein der Münzfreunde für Westfalen und Nachbargebiete.

POIARES, A. (2000): “Diremes califais encontrados ao norte de Mértola,” *Arqueólogo Português*, 201–268.

PRIEGO, M. C. (2020): “Estratos, vellones,” feluses” y tremises: Estratigrafía y numismática en el yacimiento de la Vega Baja de Toledo (ss. VII-XV dC),” in *El sitio de las cosas: la Alta Edad Media en contexto*, Servicio de Publicaciones, 123–160.

PRIEGO, M. C. AND L. O. ENCISO (2016): “Dírhams, feluses y contextualización arqueológica en el centro de la Península: nuevos hallazgos de época emiral (s. VIII-IX dC) en Recópolis,” in *Patrimonio numismático y museos: actas XV Congreso Nacional de Numismática. Madrid, 28-30 de octubre de 2014*, Museo Casa de la Moneda, 1097–1114.

PRIETO, A. (1934): “Tesoro de monedas musulmanas encontrado en Badajoz,” *Al-Andalus*, 2, 299.

PROFANTOVA, N. (2009): “Byzantine Coins from the 9th-10th century from the Czech Republic,” in *Byzantine Coins in Central Europe between the 5th and 10th century*, ed. by M. Wołoszyn, Polish Academy of Arts and Sciences, Institute of Archaeology.

PUERTAS, A. F. (1982): “Catálogo de los fondos numismáticos hispanomusulmanes del Museo de Cuenca,” *Cuadernos de la Alhambra*, 115–142.

REINHOLD FISCHER AUKTIONSHAUS (2010): “Auction 114,” Tech. rep.

RENOU, E. J. (1846): *Description géographique de l'empire de Maroc*, vol. 8, Imprimerie Royale.

RODRIGUES MARINHO, J. (1995): “Um Achado de Dirhames do Emirado Ândalus em Castro Marim,” *O Arqueólogo Português IV*, 13–15.

RODRÍGUEZ PALOMO, D. AND F. MARTÍN ESCUDERO (2022): “Moneda en contexto arqueológico en Márida (siglos VIII-IX). Estudio e interpretación,” *Arqueología y territorio medieval*, 29.

RONDIER, R. F. (1869): “Trovailles de monnaies près de Chef-Boutonne,” *Revue de l'Aunis, de la Saintonge et du Poitou*.

ROYAL NUMISMATIC SOCIETY (1975): *Coin Hoards, Volume 1*, London.

——— (1977): *Coin Hoards, Volume 3*, London.

——— (1978): *Coin Hoards, Volume 4*, London.

RUIZ ASENSIO, J. M. (1967): “Tesorillo de dirhemes del Emirato hallado en la Lantejuela,” Tech. rep., nvmisma.

RÉVÉSZ, L. (1996): “A karosi honfoglalás kori temetők : régészeti adatok a Felső-Tisza-vidék X. századi történetéhez,” Tech. rep.

SABATIER, J. (1862): *Description générale des monnaies byzantines frappées sous les empereurs d'Orient depuis Arcadius jusqu'à la prise de Constantinople par Mahomet II*, Rollin et Feuardent.

SACCOCCI, A. (2005): “Ritrovamenti di monete islamiche in Italia continentale e in Sardegna (secc. VII-XVI),” in *Simone Assemani Symposium sulla monetazione islamica. Simone Symposium on Islamic Coinage*, 137–149.

SACCOCCI, A. ET AL. (2004): “Il ripostiglio dall'area “Galli Tassi” di Lucca e la cronologia delle emissioni pavesi e lucchesi di X secolo,” *Bollettino di Numismatica*, 36, 165–203.

SAENZ-DIÉZ, J. I. (1993): “Museo municipal de Sevillla : fondos islamicos de la colección Gago,” Tech. rep., III Jarique de numismática hispano-arabe.

SALIDO DOMÍNGUEZ, J., R.-L. GARCÍA LERGA, R. GÓMEZ OSUNA, E. GARCÍA ARAGÓN, M. BLANCO DOMÍNGUEZ, AND J. BARRIO MARTÍN (2020): “Un nuevo conjunto de monedas emirales del centro peninsular: los dírhams del yacimiento arqueológico de El Rebollar (El Boalo, Madrid),” .

SARAH, G., V. GENEVIÈVE, AND C. GUERROT (2016): “Le trésor carolingien découvert à Auzeville (Haute-Garonne) en 1878. Étude des monnayages toulousains de Charles le Chauve et de Pépin II d’Aquitaine,” *Revue numismatique*, 6, 417–498.

SARFATIJ, H., W. J. H. VERWERS, AND P. WOLTERING (1999): *In discussion with the past: Archaeological studies presented to WA van Es*, Foundation for Promoting Archaeology (Stichting Promotie Archeologie).

SCHINDEL, N. (2005): “Sasanian coinage,” *Encyclopædia Iranica*.

SCHNEIDER, A. M. (1952): “Hirbet el-Minje am See Genesareth,” *Annales Archéologiques Syriennes*, 2, 23–45.

SCHULZE, M. (1984): “Das ungarische Kriegergrab von Apres-Lès-Corps. Untersuchungen zu den Ungarneinfällen nach Mittel-, West- und Südeuropa (899–955 n. Chr.) mit einem Exkurs zur Münzchronologie altungarischer Gräber,” *Jahrbuch des Römisch-Germanischen Zentralmuseums Mainz*, 31, 473–514.

SEARS, S. D. (1994): “A late Umayyad hoard from Nippur,” *The Numismatic Chronicle*, 133–146.

——— (2000): “An Abbasid Revolution Hoard from the Western Jazira (al-Raqqa?),” *American Journal of Numismatics*, 12, 171–193.

SEGOVIA SOPO, R. (2006): “Tesorillo de moneda del Emirato Independiente hallado en Fuente de Cantos y su contextualización en las Guerras de Ibn Marwan contra la corte cordobesa,” in *VI Jornada de Historia de Fuente Cantos: Actas*, Asociación Cultural Lucerna, 145–178.

——— (2014): “El tesorillo numismático andalusí de la C/Santa Julia de Mérida (Badajoz): circulación y ocultación monetaria durante la ‘Fitna’ del Califato de Córdoba,” *Cuadernos emeritenses*, 1–396.

SEGOVIA SOPO, R. AND A. V. JIMÉNEZ (2011): “Un inédito tesorillo de moneda emiral independiente hallado en el Teatro Romano de Mérida,” in *Ars metallica. Monedas y medallas: Nules-Valencia, 25-27 de octubre de 2010*, Museo Casa de la Moneda, 795–816.

SIMMER, A. (2000): “Le trésor carolingien d’Ebange-Florange,” *Les cahiers lorrains*, 3–18.

SLOVENSKÁ AKADÉMIA VIED. ARCHEOLOGICKÝ ÚSTAV (1979): *Rapports du IIIe Congrès international d'archéologie slave: Bratislava, 7-14 septembre 1975*, vol. 1, Veda.

SOCIÉTÉ DE STATISTIQUE, SCIENCES, LETTRES ET ARTS DU DÉPARTEMENT DES DEUX-SÈVRES (1882): “Sur un trésor carlovingien provenant de Brioux,” *Bulletins de la Société de statistique du département des Deux-Sèvres*, V.

SOCIÉTÉ DES ANTIQUAIRES DE L’OUEST (1982): “Communications,” *Bulletins de la Société des antiquaires de l’Ouest*, 6.

SOLER BALAGUERO, M. (1993): “Las monedas árabes del gabinete numismático del IEI,” in *III Jarique de numasmitica hispano-arabe*.

SOMBART, S. (2008): “Le trésor carolingien de Luzancy (77138), enfoui ou perdu vers 865-870,” *Bulletin de la Société française de numismatique*, 63, 128–9.

SOPHOULIS, P. (2011): “Byzantine coin-circulation in early medieval Bulgaria (mid 8th - early 9th c.),” .

TREADWELL, L. AND E. ROGAN (1994): “An Ottoman report of an Umayyad coin hoard: Jarash, 1898,” *Yarmouk Numismatics*, 6, 20–29.

TROUSSEL, M. (1942): “Monnaies d’argent (dirhams) idrissites et abbassides trouvées à Ouenza,” *Recueil des notices et mémoires de la Société archéologique de Constantine*, 65, 105–123.

ÜNAL, C. (2015): “The Tralleis Hoard and the Reflection of the Iconoclastic Idea in Byzantine Coin Iconography,” *American Journal of Numismatics*, 27, 199–205.

——— (2018): “Kavaklı Definesi: II. Constans Dönemine Ait Altın Sikkeler,” *Cedrus*, 6, 465–483.

URANGA, J. E. (1950): “El hallazgo de” dírhemes” del Emirato en San Andrés de Ordoiz (Estella, Navarra),” *Príncipe de Viana*, 11, 85–101.

VALLE, A. M. (1987): “El tesoro califal de “Los Villares” (Caudete, Valencia),” *Acta numismática*, 177–196.

VAN DER VELDE, H. (2008): “Cananefaten en Friezen aan de monding van de Rijn,” *ADC Monografie*, 5, 536.

VAN ES, W. A. AND W. J. H. VERWERS (1980): *Excavations at Dorestad. 1: The Harbour, Hoogstraat*, Amersfoort: Rijksdienst voor het oudheidkundig bodemonderzoek.

VANDENBOSSCHE, É. AND S. COUPLAND (2012): “Une trouvaille de deniers carolingiens dans la région de Bray-sur-Seine,” *The Numismatic Chronicle*, 172, 307–321.

VÖLCKERS, H. H. (1965): *Karolingische Münzfunde der Frühzeit, 751-800: Pippin, Karlmann, Karl der Große, I. und II. Münzperiode*.

VRYONIS, S. J. (1971): “An Attic Hoard of Byzantine Gold Coins (668-741) from the Thomas Whittemore Collection and the Numismatic Evidence for the Urban History of Byzantium (1963),” in *Byzantium: its internal history and relations*.

WEBSTER, G., R. DOLLEY, AND G. DUNNING (1953): “A Saxon treasure hoard found at Chester, 1950,” *The Antiquaries Journal*, 33, 22–32.

WIECHMANN, R. (2004): “Karolingische Denare aus Bardowick–Münzumlauf an der nördlichen Peripherie des Frankenreichs,” in *Delectat et docet. Festschrift zum 100jährigen Bestehen des Vereins der Münzenfreunde in Hamburg*, Hamburg, 13–44.

WILLIAMS AND AGER (2010): “The Vale of York Hoard,” Tech. rep., British Museum Objects in Focus.

WILSON, J. (1989): “The gold hoard,” in *Excavations at Capernaum I (1978-1982)*, ed. by V. Tzaferis, Eisenbrauns.

WOŁOSZYN, M. (2009): *Byzantine Coins in Central Europe between the 5th and 10th century*, Polish Academy of Arts and Sciences, Institute of Archaeology.

WROTH, W. (1908): *Catalogue of the Imperial Byzantine Coins in the British Museum*, Order of the Trustees, British Museum.

ZÄCH, B. (2001): *Kanton St. Gallen I: Mittelalterliche und neuzeitliche Münzfunde*, Schweizerische Akademie der Geistes-und Sozialwissenschaften.

ZÄCH, B. AND J. D. TABERNERO (2002): “Zwei Münzfunde des 9. und 10. Jahrhunderts aus dem Alpenrheintal: Lauterach (1868) und Chur (1997),” *Schweizerische numismatische randschau=Revue suisse de numismatique*, 93–128.

ZUYDERWYK, J. AND J. BESTEMAN (2010): “The Roermond hoard: a Carolingian mixed silver hoard from the ninth century,” *Medieval and Modern Matters*, 1, 73–154.

# E Identification (NOT FOR PUBLICATION)

## E.1 Asymptotic identification proof

Our identification proof proceeds in three steps.

First (section E.1.1), we show that under our random sampling assumption (18) for the data generating process (see appendix tables B.7 and B.8 for empirical evidence in support of this assumption), our maximum likelihood estimator exactly recovers the true shares of coins within the coin stock of a single region  $\times$  period from data on a single hoard for that region  $\times$  period. Second (section E.1.2), we extend this result to all hoards and show that arbitrarily normalizing the total hoard sizes has no impact on the estimation of true shares of coins within hoards. Third (section E.1.3), we show constructively how to uniquely recover all parameters of the true model (up to the normalizations defined in section 3) from knowledge of shares of coins within hoards.

### E.1.1 Asymptotic recovery of coin shares by maximum likelihood, single hoard

Under our data generating process assumption in equation (18), i.e. hoards in our dataset are random samples from the coins in circulation, sample shares (within a single hoard) are asymptotically equal to model predicted shares. Let define  $\mathcal{N}$ , the number of coins found in a given  $(h, T)$  hoard buried in region  $h$  at time  $T$  ( $tpq$ ). From the law of large numbers,

$$\lim_{\mathcal{N} \rightarrow +\infty} \frac{H_{m,h}[t, T]}{H_h[T]} = \mathbb{E} \left[ \frac{H_{m,h}[t, T]}{H_h[T]} \right] = \frac{S_{m,h}[t, T] (\Theta^{true})}{\sum_{m', t' \leq T} S_{m', h}[t', T] (\Theta^{true})} \equiv (H(t, T))_{m,h}^{true}.$$

Observed coin shares within hoards ( $H_{m,h}[t, T]/H_h[T]$ ) are asymptotically equal to model-predicted true shares within coin stocks ( $S_{m,h}[t, T] (\Theta^{true})/\sum_{m', t' \leq T} S_{m', h}[t', T] (\Theta^{true})$ ), which we label  $(H(t, T))_{m,h}^{true}$ .

The next step is to prove, for a single hoard  $(h, T)$ , that the likelihood of observing coin shares is (asymptotically) maximized when predicted shares,  $(H(t, T))_{m,h}^{pred}$  are equal to realized shares  $(H(t, T))_{m,h}^{true}$ . Section E.1.2 trivially extends this result for multiple hoards.

Arbitrarily choosing one reference region  $\times$  period  $(m_0, t_0)$  as shares add up to one,

$$\begin{aligned} \arg \max_{\left(\cdots, (H(t, T))_{m,h}^{pred}, \cdots\right)_{(m,t) \neq (m_0, t_0)}} & \\ \left\{ \mathcal{L} = \left( \sum_{m,t} (H(t, T))_{m,h}^{true} \ln (H(t, T))_{m,h}^{pred} \right) + \left( 1 - \sum_{m',t'} (H(t', T))_{m',h}^{true} \right) \ln \left( 1 - \sum_{m'',t''} (H(t'', T))_{m'',h}^{pred} \right) \right\} \\ &= \left( \cdots, (H(t, T))_{m,h}^{true}, \cdots \right)_{(m,t) \neq (m_0, t_0)} \end{aligned}$$

**Proof.** From the FOC's wrt each share  $(H(t, T))_{m,h}^{pred}$ :

$$\frac{(H(t, T))_{m,h}^{true}}{(H(t, T))_{m,h}^{pred}} - \frac{\left( 1 - \sum_{m',t'} (H(t', T))_{m',h}^{true} \right)}{\left( 1 - \sum_{m',t'} (H(t', T))_{m',h}^{pred} \right)} = 0, \forall m, t \Rightarrow (H(t, T))_{m,h}^{pred} = (H(t, T))_{m,h}^{true}, \forall m, t$$

■

### E.1.2 Irrelevance of coin hoard sizes for maximum likelihood, multiple hoards

From section E.1.1, any strictly monotonically increasing transformation (e.g. logged and multiplied by a positive constant  $\alpha(h, T) > 0$ ) of the likelihood of observing a distribution of coin types within a single hoard is maximized for predicted shares equal to true shares,

$$\begin{aligned} \arg \max_{\left(\cdots, (H(t, T))_{m,h}^{pred}, \cdots\right)_{(m,t) \neq (m_0, t_0)}} & \\ \alpha(h, T) \sum_{m,t \leq T} (H(t, T))_{m,h}^{true} \ln (H(t, T))_{m,h}^{pred} \\ &= \left( \cdots, (H(t, T))_{m,h}^{true}, \cdots \right)_{(m,t)}, \forall (h, T), \forall \alpha(h, T) > 0, \end{aligned}$$

because the scalar  $\alpha(h, T) > 0$  cancels out from the FOC's in E.1.1.

Adding up the log-likelihood for multiple hoards, we get,

$$\begin{aligned} \arg \max_{\left(\cdots, (H(t, T))_{m,h}^{pred}, \cdots\right)_{(m,t) \neq (m_0, t_0)}} & \\ \sum_{h,T} \alpha(h, T) \sum_{m,t \leq T} (H(t, T))_{m,h}^{true} \ln (H(t, T))_{m,h}^{pred} \\ &= \left( \cdots, (H(t, T))_{m,h}^{true}, \cdots \right)_{(m,h,t,T)}, \forall \alpha(h, T) > 0. \end{aligned}$$

The FOC's wrt coin shares for one hoard is independent from the FOC's for other hoards, so the system of FOC's for each  $(h, T)$  hoard implies  $(H(t, T))_{m,h}^{pred.} = (H(t, T))_{m,h}^{true}, \forall m, t, \forall \alpha(h, T) > 0$ .

In other words, any selection bias that increases the likelihood of hoards being buried/discov-  
ered/documentated does not affect our estimates.

### E.1.3 Unique recovery of parameters from coin shares within hoards

We now proceed to the proof that knowledge of the (asymptotic) shares of coins within hoards is sufficient to uniquely recover the true structural parameters governing the flow of coins.<sup>8</sup> This proof considers a simplified setting with a single determinant of bilateral trade flows (travel times) and zero saving. Extending the proof to include political and religious borders is straightforward. Extending the proof to include positive saving is also straightforward but extremely tedious.

#### Problem Formulation

**Latent Coin Dynamics.** We define a dynamic system evolving over discrete periods  $t = 1, \dots, T$ . For any periods  $t < s$ , the coin stock matrix  $S(t, s) \in \mathbb{R}_{++}^{N \times N}$  is defined as in (10):

$$S(t, s) = (1 - \lambda)^{s-t} M(t) \Pi(t+1) \dots \Pi(s) \quad (\text{E.1})$$

where:

- $\lambda \in (0, 1)$  is a known coin loss rate.
- $M(t)$  is an unknown  $N \times N$  invertible diagonal matrix of minting in period  $t$ .
- $\Pi(s)$  is an unknown  $N \times N$  row-stochastic trade share matrix in period  $s$ .

**Parametric Structure.** The trade matrices  $\Pi(s)$  follow a gravity structure governed by an iso-elastic function of travel times as in (11) and (15):

$$\Pi(s) = A(s) \Delta B(s) \quad (\text{E.2})$$

- $\Delta$  is the matrix of bilateral trade terms with entries  $\Delta_{ij} = d_{ij}^{-\zeta}$ , with  $D = [d_{ij}]$  a known matrix of bilateral travel times, and the elasticity  $\zeta$  unknown.

---

<sup>8</sup>We used the support of Gemini 3.0 to derive this proof, in particular the formulation and solution of the fixed point problem in theorem 1 in step 2.

- $B(s)$  is an unknown diagonal matrix of seller terms,  $(B(s))_{ii} = \tilde{\beta}_i$ . We impose the normalization constraint  $(B(s))_{11} = 1$ .
- $A(s)$  is the unknown diagonal normalization matrix of buyer terms,  $A(s)_{ii} = \tilde{\alpha}_i$ , defined uniquely by the fact that trade shares sum to one  $\Pi(s)\mathbf{1} = \mathbf{1}$ .

**Observations.** We observe the column-normalized matrices of coin shares within hoards,  $H(t, s)$ , with the share of coins minted in region  $m$  in period  $t$  among coins in a hoard buried in region  $h$  in period  $s$  corresponding to element  $(H(t, s))_{m,h}$  defined as in section E.1.1. Sections E.1.1 and E.1.2 show that knowledge on empirical coin hoards is asymptotically sufficient to recover true shares of coins within coin stocks, which we now take as given:  $(H(t, s))^{true} = (H(t, s))^{pred.} = (H(t, s))$ .

Let  $\boldsymbol{\sigma}(s) = S(s)^T \mathbf{1}$  be the vector of column sums of the cumulative matrix of coin types in circulation at time  $s$ ,  $S(s) = \sum_{t=1}^{s-1} S(t, s)$ . Let  $\Sigma(s) = \text{diag}(\boldsymbol{\sigma}(s))$ .

$$H(t, s) = S(t, s)\Sigma(s)^{-1} \quad (\text{E.3})$$

Note that we only use information on shares of coins types within a hoard (summing up to one).

Our goal is to recover  $\zeta$  (travel time elasticity),  $M(t)$  (minting output), and  $B(t)$  (seller terms).

### Step 1: Recovery of the elasticity parameter $\zeta$

We first recover the elasticity  $\zeta$  using ratios of observations. This is possible because the ratios collect the diagonal matrices  $M(t)$ ,  $A(t)$  and  $B(t)$  into separate coin origin and destination fixed effects via the properties of logarithms.

Construct the observation ratio matrix  $Y$  between period 2 and period 3:

$$Y = H(1, 2)^{-1}H(1, 3) = (1 - \lambda)\Sigma(2)\Pi(3)\Sigma(3)^{-1} \quad (\text{E.4})$$

Substituting the structure of  $\Pi(3)$ :

$$Y_{ij} = (1 - \lambda)\sigma_i(2)A_i(3)d_{ij}^{-\zeta}B_j(3)\sigma_j(3)^{-1} \quad (\text{E.5})$$

Take the natural logarithm:

$$\ln(Y_{ij}) = \underbrace{\ln((1 - \lambda)\sigma_i(2)A_i(3))}_{u_i} + \underbrace{\ln(B_j(3)\sigma_j(3)^{-1})}_{v_j} - \zeta \ln(d_{ij}) \quad (\text{E.6})$$

We apply the Double Centering Operator (2-way fixed effect)  $J = I - \frac{1}{N}\mathbb{J}$ , where  $\mathbb{J}$  is the matrix of ones, to annihilate the row and column terms:

$$J \ln(Y) J = -\zeta [J \ln(D) J] \quad (\text{E.7})$$

The parameter  $\zeta$  is uniquely recovered via Frobenius norm minimization:

$$\zeta = -\frac{\text{tr}((J \ln(D) J)^T (J \ln(Y) J))}{\text{tr}((J \ln(D) J)^T (J \ln(D) J))} \quad (\text{E.8})$$

### Step 2: Recovery of Relative Hoard Sizes via Fixed Point Theory

With  $\zeta$  known, we compute the bilateral terms matrix  $\hat{\Delta} = D^{-\zeta}$ . We now seek to recover the mass vector  $\sigma(3)$  (number of coins within hoards) up to a global scalar  $\kappa$ .

**Structural Decomposition.** We remove the bilateral terms from the ratio matrix using Hadamard (element-wise) division:

$$Z = Y \oslash \hat{\Delta} \quad (\text{E.9})$$

Analytically,  $Z_{ij} = (1 - \lambda)\sigma_i(2)A_i(3)B_j(3)\sigma_j(3)^{-1}$ . This is a Rank-1 matrix. Compute the singular value decomposition:  $Z = \mathbf{u}\mathbf{v}^T$ . This establishes the functional dependency of the unknown  $B(3)$  (seller terms) on the unknown  $\sigma(3)$ :

$$\mathbf{v}_j \propto B_j(3)\sigma_j(3)^{-1} \implies B(\sigma(3)) = \text{diag}(\mathbf{v} \circ \sigma(3)) \quad (\text{E.10})$$

Consequently, the normalization matrix  $A(3)$  (buyer terms) is also a function of  $\sigma(3)$ :

$$A(\sigma(3)) = \text{diag}(\hat{\Delta}B(\sigma(3))\mathbf{1})^{-1} \quad (\text{E.11})$$

**The Fixed Point Equation.** We derive the coin mass conservation for  $\sigma(3)$ .

1. **Coin flows from  $t = 1$ :** Since  $Y = (1 - \lambda)\Sigma(2)\Pi(3)\Sigma(3)^{-1}$ , we have:

$$Y\boldsymbol{\sigma}(3) = (1 - \lambda)\Sigma(2)\Pi(3)\mathbf{1} = (1 - \lambda)\boldsymbol{\sigma}(2) \quad (\text{E.12})$$

Thus, the mass from the previous period is  $\boldsymbol{\sigma}(2) = \frac{1}{1-\lambda}Y\boldsymbol{\sigma}(3)$ .

2. **Minting injection at  $t = 2$ :** From  $H(2, 3)$ , we have  $(1 - \lambda)M(2)\mathbf{1} = H(2, 3)\boldsymbol{\sigma}(3)$ .

Total Coin Mass Equation:

$$\boldsymbol{\sigma}(3) = \Pi(3)^T[(1 - \lambda)\boldsymbol{\sigma}(2) + (1 - \lambda)M(2)\mathbf{1}] \quad (\text{E.13})$$

Substituting the components:

$$\boldsymbol{\sigma}(3) = \Pi(3)^T[Y\boldsymbol{\sigma}(3) + H(2, 3)\boldsymbol{\sigma}(3)] \quad (\text{E.14})$$

This yields the mapping  $\mathcal{T} : \mathbb{R}_{++}^N \rightarrow \mathbb{R}_{++}^N$  for any candidate  $\boldsymbol{\xi}$  for  $\boldsymbol{\sigma}(3)$ :

$$\boldsymbol{\xi} = \mathcal{T}(\boldsymbol{\xi}) \equiv \Pi(\boldsymbol{\xi})^T[Y + H(2, 3)]\boldsymbol{\xi} \quad (\text{E.15})$$

where  $\Pi(\boldsymbol{\xi})$  is defined from (E.10) and (E.11) as  $\Pi(\boldsymbol{\xi}) = A(\boldsymbol{\xi})\hat{\Delta}B(\boldsymbol{\xi})$ .

### Existence and Uniqueness Proof.

**Theorem 1** *The mapping  $\mathcal{T}$  admits a unique solution in the projective space of positive rays.*

**Proof.** We utilize the **Hilbert Projective Metric**  $d_H(\mathbf{x}, \mathbf{y}) = \ln \frac{\max(x_i/y_i)}{\min(x_i/y_i)}$ .

1. **Positivity:** Since  $d_{ij}$  is finite,  $\hat{\Delta}$  is strictly positive. For  $\boldsymbol{\xi} > 0$ ,  $\Pi(\boldsymbol{\xi})$  is strictly positive.  $K = Y + H(2, 3)$  is non-negative and non-zero. Thus  $\mathcal{T}$  maps the interior of the positive cone to itself.
2. **Homogeneity:** Consider a scalar  $c > 0$ .

$$B(c\boldsymbol{\xi}) = cB(\boldsymbol{\xi})$$

$$A(c\boldsymbol{\xi}) = \text{diag}(\hat{\Delta}(cB(\boldsymbol{\xi})\mathbf{1}))^{-1} = c^{-1}A(\boldsymbol{\xi})$$

$$\Pi(c\boldsymbol{\xi}) = (c^{-1}A)\hat{\Delta}(cB) = \Pi(\boldsymbol{\xi}) \quad (\text{Scale Invariant})$$

Therefore,  $\mathcal{T}(c\boldsymbol{\xi}) = \Pi(\boldsymbol{\xi})^T K(c\boldsymbol{\xi}) = c\mathcal{T}(\boldsymbol{\xi})$ . The map is homogeneous of degree 1.

3. **Contraction:** By Birkhoff's Theorem (Birkhoff, 1957, 1965), any strictly positive, homogeneous map is a strict contraction under  $d_H$ .

By the Banach Fixed Point theorem, there exists a unique fixed point ray. Let  $\boldsymbol{\xi}^*$  be the unit-norm solution. The true mass vector is  $\boldsymbol{\sigma}(3) = \kappa\boldsymbol{\xi}^*$ , where  $\kappa$  is the **unknown global scaling factor for minting** (the reason why we need to normalize minting in one, single, region  $\times$  period). ■

### Step 3: Exact Recovery of $B(3)$ and Scaled Recovery of $M(1)$ and $M(2)$

**Exact Recovery of  $B(3)$ .** Using the recovered direction  $\boldsymbol{\xi}^*$ , we calculate the candidate buyer terms diagonal:

$$\tilde{\mathbf{b}} = \mathbf{v} \circ \boldsymbol{\xi}^* \quad (\text{E.16})$$

From Eq. (E.10), the true diagonal is  $\mathbf{b}(3) \propto \tilde{\mathbf{b}}$ . Unlike the mass vector,  $B(3)$  is constrained.

$$(B(3))_{11} = 1 \quad (\text{E.17})$$

This allows us to solve for the exact proportionality constant. Let  $\alpha = 1/(\tilde{b})_1$ .

$$B(3) = \alpha \cdot \text{diag}(\tilde{\mathbf{b}}) \quad (\text{E.18})$$

This matrix of seller terms is **exactly recovered** (no  $\kappa$  ambiguity), under the normalization of the seller term for region 1. Consequently,  $A(3)$  and  $\Pi(3)$  are exactly recovered.

**Explicit Recovery of  $M(1)$  and  $M(2)$ .** The minting matrices  $M(t)$  can only be recovered up to the global scalar  $\kappa$ . From the row sums of the unnormalized observations:

$$M(2) = \frac{1}{1-\lambda} \text{diag}(H(2,3)\boldsymbol{\sigma}(3)) = \kappa \left[ \frac{1}{1-\lambda} \text{diag}(H(2,3)\boldsymbol{\xi}^*) \right] \quad (\text{E.19})$$

$$M(1) = \frac{1}{1-\lambda} \text{diag}(H(1,2)Y\boldsymbol{\sigma}(3)) = \kappa \left[ \frac{1}{1-\lambda} \text{diag}(H(1,2)Y\boldsymbol{\xi}^*) \right] \quad (\text{E.20})$$

### Step 4: Recursive Recovery of $M(s-1)$ and $B(s)$ for $s > 3$

Assume  $\boldsymbol{\sigma}(s-1)$  is known (up to the scalar  $\kappa$ ).

1. **Recover  $\sigma(s)$ :** Summing the columns of the observation  $H(s-1, s)$ :

$$\sigma(s) = \sigma(s-1) + H(s-1, s)\sigma(s) \quad (\text{E.21})$$

This is a linear system:

$$(I - H(s-1, s))\sigma(s) = \sigma(s-1) \quad (\text{E.22})$$

Solve for  $\sigma(s)$ .

2. **Recover  $M(s-1)$ :**

$$M(s-1) = \frac{1}{1-\lambda} \text{diag}(H(s-1, s)\sigma(s)) \quad (\text{E.23})$$

3. **Recover  $B(s)$ :** Isolate the trade share matrix:

$$\Pi(s) = \frac{1}{1-\lambda} M(s-1)^{-1} H(s-1, s) \Sigma(s) \quad (\text{E.24})$$

Compute  $K_s = \Pi(s) \oslash \hat{\Delta}$ . Singular value decomposition yields the right singular vector  $\mathbf{q}$ .

$$B(s) = \frac{1}{q_1} \text{diag}(\mathbf{q}) \quad (\text{Exact Recovery}) \quad (\text{E.25})$$

### Step 5: Uniqueness of the Solution Sequence

We have established a constructive solution. We must now verify that no alternative sequence of matrices exists that generates the same data. The system possesses a gauge freedom if there exists a vector sequence  $u(t)$  such that  $u(t) = \Pi(t)u(t+1)$  with  $u_1(t) = 1$  and  $u(t) \neq \mathbf{1}$ .

**Theorem 2** *If  $N \leq T$  and the matrix  $D$  is generic, the solution is unique up to the global scalar  $\kappa$ .*

**Proof.** Let  $\mathbf{z} \in \mathbb{R}^N$  be a perturbation of the final gauge vector  $u(T+1) = \mathbf{1} + \mathbf{z}$ . For the normalization  $(B)_{11} = 1$  to hold at all previous time steps,  $\mathbf{z}$  must satisfy:

$$e_1^T \Pi(t) \Pi(t+1) \dots \Pi(T) \mathbf{z} = 0 \quad \forall t \in \{1, \dots, T\} \quad (\text{E.26})$$

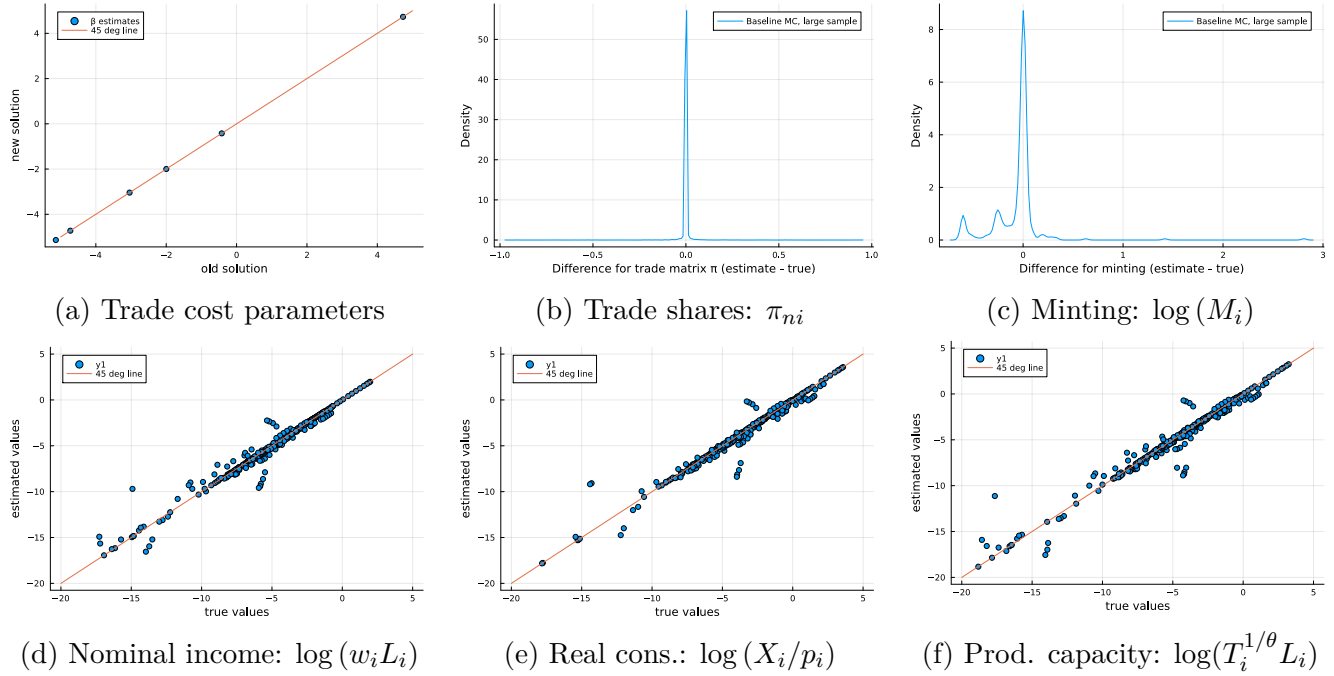
where  $e_1 = [1, 0, \dots, 0]^T$ . Let  $\mathcal{O}$  be the Observability Matrix where row  $k$  is  $e_1^T \Pi(T-k+1) \dots \Pi(T)$ . Since the matrices  $\Pi(t)$  are strictly positive (due to  $A, B, D > 0$ ), they are irreducible. For generic parameters, the directions of the first rows of cumulative products span  $\mathbb{R}^N$ . Thus,  $\text{rank}(\mathcal{O}) = N$ .

The only solution to  $\mathcal{O}\mathbf{z} = \mathbf{0}$  is  $\mathbf{z} = \mathbf{0}$ . Therefore,  $u(t) = \mathbf{1}$  is the only valid gauge, and the recovered parameter matrices are unique. ■

## E.2 Numerical identification with sparse data and finite sample

**Identification with sparse data.** We first show that our estimator is successful at recovering known (true) parameters even with extremely sparse data as in our millennia old dataset on coin hoards. We treat the estimated parameters from section 3, using the specification in column 2 of table 3 with multiple religious border effects, as known (true) parameters. We use those parameters to simulate the entire sequence of coin stocks and coin flows using our full structural model in section 2. We then collapse our simulated dataset of coin stocks into hoards of sizes normalized to 1 (so that we only have information on shares of coin types within each hoard). Finally, we estimate all parameters using this simulated dataset.

Figure E.1 presents the results. Panel (a) shows that we are able to recover, up to machine



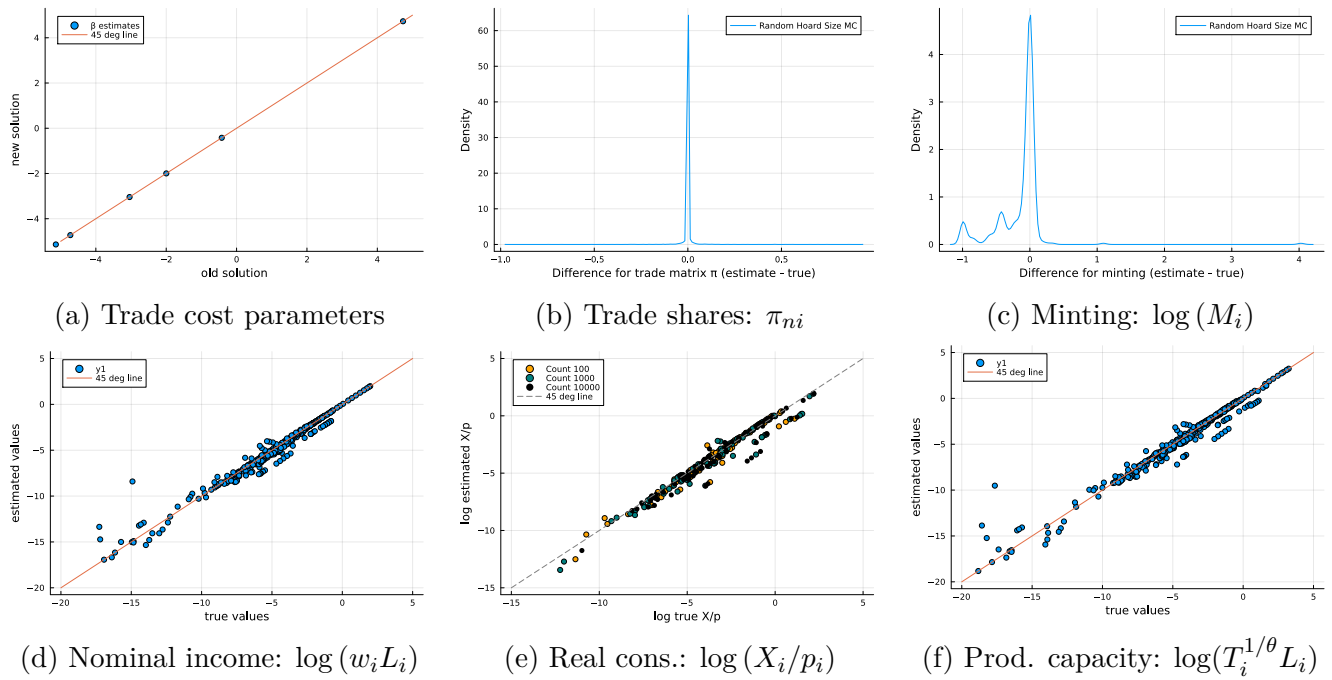
Appendix Figure E.1: Monte Carlo Simulation with Equal Sized Hoards

precision, the known (true) parameter vector  $(\zeta, \kappa)$  governing bilateral trade costs. Panels (b) and (c) also show that we are able to precisely recover true trade shares and true minting output. More importantly, panels (d)-(f) show that we recover equilibrium variables—nominal incomes,

real consumption, and production capacity—with a high degree of accuracy. There are small discrepancy between known (true) values and estimated values due to numerical imprecisions.

**Identification with random-sized hoards.** We confirm our formal identification result that differences in hoard sizes have no impact on our ability to recover parameters. As for figure E.1, we start from the same estimated parameters, simulate our structural model, and simulate a coin hoard dataset. But unlike in figure E.1, instead of normalizing all hoard sizes to one, we randomly assign small (100 coins), medium (1,000 coins), and large (10,000 coins) sizes to hoards. This random re-sizing mimics a possible selection bias, where it may be more likely to discover hoards in specific regions and for specific time periods. We then estimate all parameters using this simulated dataset of random-sized hoard, and confront them to the known (true) parameters.

Figure E.2 presents the results. As with equal-sized hoards, we recover all parameters with



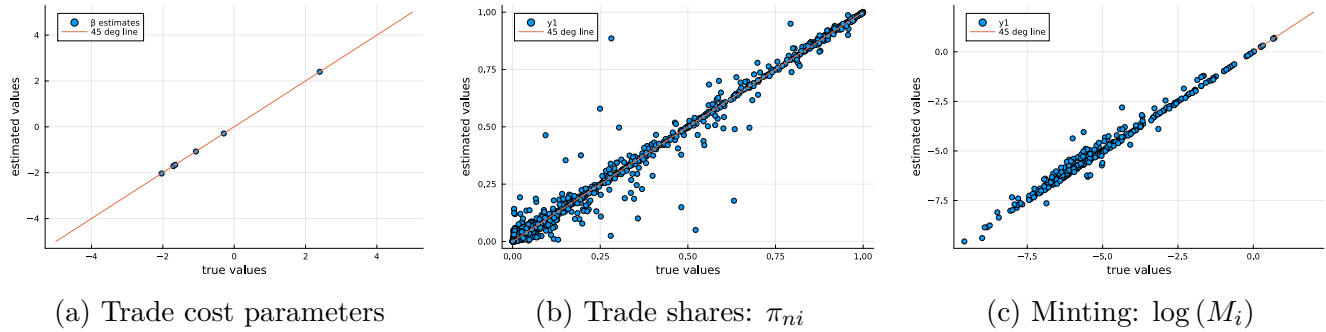
Appendix Figure E.2: Monte Carlo Simulation with Small/Medium/Large Hoards

a high degree of accuracy. More importantly, panel (e) shows that our estimated parameters do not have any systematic tendency to estimate larger (or smaller) economic sizes for larger hoards: we use three different colors for estimated parameters corresponding to small, medium, and large hoards; for a given size (e.g. small hoards shown in yellow), small discrepancies between true and estimated parameters are equally likely to be above or below the 45 degree line. This means, e.g.,

that we are not naively inferring that regions which are wealthy today, and therefore more likely to fund archaeological research and discover ancient coin hoards, were wealthy in the past.

**Estimation with young coins only.** Step 5 in our formal identification proof in section E.1 states that we may need as many generations of coins as regions for identification ( $T \geq N = 13$ ) to guarantee the uniqueness of our solution. It does not however specify how severe the problem of underidentification would be with too few generations of coins. We explore this question numerically.

We simulate a dataset of coin stocks using known parameters. Unlike our estimated parameters, we choose positive minting parameters ( $M_n[t] > 0, \forall n, t$ ) to ensure that our results are not driven by sparsity. We first draw randomly 100,000 coins from the simulated model, using *coins of all ages*. We collect them into a simulated dataset of coin hoards (as before, we normalize all hoard sizes to 1) and estimate all parameters using this simulated dataset. Figure E.3 confirms that with

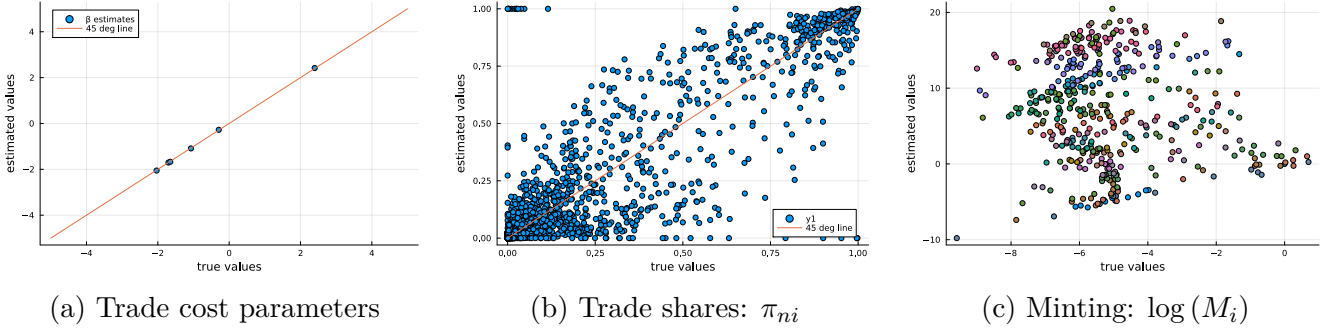


Appendix Figure E.3: Monte Carlo simulation with coins of all ages

data on coins of all ages, our estimator recovers the true parameters with a high level of accuracy.

We then draw randomly 100,000 coins from the simulated model, using *young coins only*, i.e. coins of age 1 and 2 only. We collect those young coins into a simulated dataset of coin hoards (each normalized to size 1) and estimate all parameters using this simulated dataset. Figure E.4 shows that with information on *young coins only*, our estimator is unable to recover all true parameters.

As expected from our asymptotic identification proof, panel (a) shows that our ability to recover the parameters governing bilateral trade flows is not deteriorated by the loss of information on older coins: this step in the identification is performed using only two consecutive generations of coins (see equation E.8 in step 1 of the proof in section E.1), and uses logs to control for *any* seller terms and minting parameters with two-way fixed effects.



Appendix Figure E.4: Monte Carlo simulation with young coins only

But the estimator fails at systematically disentangling seller terms from minting. A closer inspection of our (underidentified) estimates for minting in panel (c) reveals that while we are able to approximately recover the relative sizes of minting output within a period, we are unable to identify the levels of minting across periods. We use different colors for different periods. For each period, estimated versus true minting are approximately aligned along lines with slopes equal to one; but the levels (intercepts) of those lines differ across periods. This inability to recover the correct scale across periods is to be expected from theorem 2 in step 5 of the proof in section E.1.

### E.3 Numerical identification with misspecified model

**Bias against old and distant coins (temporal and geographic ‘home bias’).** To assess the degree to which our estimates may be biased because we mistakenly ignore a bias against old and distant coins, we proceed as follows. We simulate a synthetic dataset using a (known) model where the coin loss rate is systematically different for coins minted recently and close by (low  $\lambda$ ) and for coins minted long ago and far away (high  $\lambda$ ). We then estimate on this synthetic dataset the parameter of a misspecified model which *incorrectly* assumes a constant  $\lambda$  for all coins irrespective of where and when they were minted.

Formally, we make the following assumption for the “true” (known)  $\lambda$  process for coin losses:

- coins minted in location  $m$  depreciate at a high rate ( $\lambda_{high} = 0.35$ ) when they are in distant locations, i.e. locations at a distance larger than the median pairwise distance between regions;
- coins minted more than 2 periods in the past depreciate at a high rate ( $\lambda_{high} = 0.35$ );
- otherwise, coins depreciate at a low rate ( $\lambda_{low} = 0.25$ )

We purposefully choose a very large 40% difference between the fast and slow depreciation rates, so that we can gauge how sensitive our estimation is to misspecification biases.

We use our baseline dynamic model of coin diffusion, equation (10), except for the coin loss rate which varies between  $\lambda_{high}$  and  $\lambda_{low}$  depending on where and when a coin is used, to simulate a dynamic of coin stocks. From this simulated model, we draw, with replacement, 100,000 synthetic coins, which we combine into a synthetic dataset of coin hoards. We then use this synthetic dataset to estimate the parameter of our *misspecified* model, incorrectly assuming a constant  $\lambda = 0.3$ .

The results are presented in table E.1. Our misspecified model leads us to incorrectly estimate

Coefficient on	True Value	Estimate
Log Travel Time	-3.04	-3.13
Political Border	-0.42	-0.43
Religious Border: East	-2.0	-2.0
Religious Border: West	-4.73	-4.76
Religious Border: Mediterranean	-5.14	-5.18

Appendix Table E.1: Comparison of  $\Theta^{true}$  vs  $\hat{\Theta}$ , Old-distant vs young-proximate coins

a distance elasticity larger than the true (known) elasticity: 3.13 versus 3.04. However, despite the substantial misspecification of the coin loss rate, the difference between the estimated and true distance elasticity remains small. Importantly, all other parameters governing bilateral trade flows are equal or almost equal to their true (known) value.

**Pro- and anti-Islamic biases (religious ‘home bias’).** To quantify the extent to which our estimate of the religious border effect may be biased if we mistakenly ignore a home bias against Islamic coins in non-Islamic regions, and against non-Islamic coins in Islamic regions, we perform a similar exercise. We simulate a synthetic dataset using a (known) model where the coin loss rate is systematically different for coins minted in a region with the same or a different religion. Formally, we assume that if a coin was minted in a non-Islamic (respectively Islamic) region, it is more 33% more likely to be reminted when used in an Islamic (resp. non-Islamic) region ( $\lambda_{high} = 0.4$ ) than when used in a non-Islamic (resp. Islamic) region ( $\lambda_{baseline} = 0.3$ ). We use our baseline dynamic model of coin diffusion, equation (10), except for the coin loss rate which varies between  $\lambda_{high}$  and  $\lambda_{baseline}$  depending on where and when a coin is used, to simulate a dynamic of coin stocks. From this simulated model, we draw, with replacement, 100,000 synthetic coins, which we combine into

a synthetic dataset of coin hoards. We then use this synthetic dataset to estimate the parameter of our *misspecified* model, incorrectly assuming a constant  $\lambda = 0.3$ .

The results are presented in table E.2. Again, misspecifying the process for reminting, and

Coefficient on	True Value	Estimate
Log Travel Time	-3.04	-3.04
Political Border	-0.42	-0.42
Religious Border: East	-2.0	-2.16
Religious Border: West	-4.73	-4.88
Religious Border: Mediterranean	-5.14	-5.29

Appendix Table E.2: Comparison of  $\Theta^{true}$  vs  $\widehat{\Theta}$ , Islamic vs non-Islamic coins

ignoring a systematic religious bias in reminting, induces a bias in our estimates for the border effect. However, as earlier, despite introducing a large misspecification for the reminting process, the bias in our border estimates remains relatively small. Those biases are small in comparison, for instance, to the very large fluctuations in the geographic composition of Mediterranean trade we document in section 4.2. We also note that, as earlier, the other parameters governing bilateral trade (distance elasticity and political border effect) are unaffected by this religious misspecification bias.

To conclude, we confirm that a violation of our fungibility assumption leads to biased estimates, but we also confirm that those biases are likely to be quantitatively small.

## References

- BIRKHOFF, G. (1957): “Extensions of Jentzsch’s Theorem,” *Transactions of the American Mathematical Society*, 85, 219–227.
- (1965): “Uniformly Semi-Primitive Multiplicative Processes. II,” *Journal of Mathematics and Mechanics*, 14, 507–512.